Valorization of Bio-derived Lactic Acid to Acrylic Acid and Other Value Added Products

Thesis Submitted to AcSIR for the Award of
the Degree of
DOCTOR OF PHILOSOPHY
In Chemical Sciences

By

Vidhya Changadev Ghantani

Registration Number- 10CC11J26051

Under the guidance of

Dr. Shubhangi B. Umbarkar

Catalysis & Inorganic Chemistry Division

CSIR - National Chemical Laboratory

Pune - 411 008, India

राष्ट्रीय रासायनिक प्रयोगशाला
(वैज्ञानिक तथा औद्योगिक अनुसंधान परिषद)
डॉ. होमी भाभा मार्ग पुणे - 411 008. भारत
NATIONAL CHEMICAL LABORATORY
(Council of Scientific & Industrial Research)
Dr. Homi Bhabha Road, Pune - 411 008. India.

Certificate of the Guide

This is to certify that the work incorporated in this Ph. D. thesis entitled, **"Valorization of bio-derived lactic acid to acrylic acid and other value added products"** submitted by **Ms. Vidhya C. Ghantani,** to Academy of Scientific and Innovative Research (AcSIR) in fulfillment of the requirements for the award of the Degree of ***Doctor of Philosophy,*** embodies original research work under my supervision. I further certify that this work has not been submitted to any other University or Institution in part or full for the award of any degree or diploma. Research material obtained from other sources has been duly acknowledged in the thesis. Any text, illustration, table *etc.*, used in the thesis from other sources, have been duly cited and acknowledged.

Vidhya C. Ghantani
Student

Dr. Shubhangi B. Umbarkar
Supervisor

Date: November 9th, 2015
Place: Pune, INDIA

Communication Channels
NCL Level DID : 2590
NCL Board No. : +91-20-25902000
EPABX : +91-20-25893300
+91-20-25893400
FAX
Director's Office : +91-20-25893355
COA's Office : +91-20-25893619
COS&P's Office : +91-20-25893008
WEBSITE
www.ncl-india.org

Declaration by the Candidate

I, hereby declare that the thesis entitled **"Valorization of bio-derived lactic acid to acrylic acid and other value added products"** submitted by me for the degree of **Doctor of Philosophy** to the **Academy of Scientific and Innovative Research (AcSIR)**, is the record of work carried out by me at **Catalysis & Inorganic Chemistry Division, National Chemical Laboratory** under the guidance of **Dr. Shubhangi B. Umbarkar** and has not formed the basis for the award of any degree or diploma to this or any other University. I further declare that the material obtained from other sources has been duly acknowledged in the thesis.

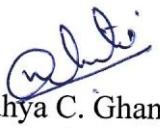

Vidhya C. Ghantani

Student

Date: November 9th, 2015

Place: Pune, INDIA

Dedicated to…

My beloved late father and my mother who have been my inspiration and motivation to overcome hardships and strive for higher goals in life.

My beloved husband for his constant support and encouragement for my work.

My daughter, Nidhi, the little angel who has been the source of liveliness and motivation.

Acknowledgement

I take this opportunity to thank the people whose support has made it possible to complete my doctoral dissertation work. It is a genuine pleasure to express my deep sense of gratitude to my mentor and guide Dr. Shubhangi B. Umbarkar. Her dedication and keen interest towards the research work and her encouraging attitude to her students has been the impetus for completing my work. Her timely advice, meticulous scrutiny, scholarly advice and consistent encouragement have facilitated me to a great extent to realize my thesis. I could not have imagined having a better advisor and mentor for my Ph. D study. Her guidance and advice shall help me in shaping my future professional career.

I owe a deep sense of gratitude to Dr. M. K. Dongare for his keen interest in my work at every stage of research. His prompt inspirations, timely suggestions with kindness, enthusiasm and dynamism have enabled me to complete my thesis. He has been a guiding light during my research work. He was always made himself available to clarify doubts despite his busy schedule which helped me overcome bottlenecks during the research. It has been a great opportunity to work with him and receive his guidance and support

My sincere thanks to **Director**, CSIR-NCL, Pune - 411008, for providing facilities to carry out the research work. I am grateful to the institute for providing an amicable ideal research environment and friendly atmosphere to work with. None the less I appreciate the financial support provided by CSIR for my Ph.D. work.

I would like to thank my DAC committee members Dr. A. T. Biju (Chairman), Dr. S A R Mulla and Dr. A. A. Kelkar, for their constant assessment and their insightful suggestions and comments and encouragement. It was their critics during assessment which provided insights that helped me explore and widen my research from various perspectives.

I specially thank the UCCS Lille team- **Prof. Pascal Granger** and **Dr. Christine LANCELOT** for giving me an opportunity to work with them under UCCS *(CNRS)-CSIR-NCL (CSIR) collaborative project.* I sincerely thank my lab-mates and friends- **Trupti, Swati, Vaibhav, Rajesh, Samadhan, Pavan, Atul, Macchindra, Ashwini, Sumeet, Reshma, Dhananjay, Sonali and Tanushree.** The stimulating discussions and the fun we had in the last four years always kept a fresh and healthy atmosphere in the lab. I wish to

thank my all Divisional and NCL friends. I would like to thank specially to my friends **Dr. Ravi, Dr. Prasad and Sana** for their inspiration and support during my Ph.D. tenure. All my colleagues and friends been a great support both in my professional as well as personal life

I am very grateful to my mother, inspite of the various hardships in life in raising us, she always encouraged us to carry on our studies and strive for higher goals in life. It was because of her belief in me that I could reach this level. My gratitude to my late father whose love and values help me sail through life. Thanks to my family members for their support, encouragement and all of the sacrifices that you've made on my behalf. Your prayer for me was what sustained me this far. At the end I would like to express appreciation to my beloved husband Mr. Narayan Ashtekar who was always my support in these moments. Special thanks to my little princess my daughter Nidhi, for being good and tolerant inspite of me not being able to devote much time to her during my research work. Her smile and joyfulness turned to be my source of energy.

I thank God for all the blessings and for being there for me always.

CONTENTS

LIST OF TABLES

LIST OF FIGURES

LIST OF SCHEMES

LIST OF SYMBOLS

°C	-Celsius
w/w	-weight/weight
rpm	-revolutions per minute
$m^2 g^{-1}$	-square meter per gram
µmol g^{-1}	-micromole per gram
mL min^{-1}	-milliliter / minute
N_2	-nitrogen gas
WHSV	-weight hourly space velocity

LIST OF ABBREVIATION

GHG	- Greenhouse gases
XRD	- X- ray diffraction
BET	-Brunauer–Emmett–Teller
SEM	-Scanning electron microscopy
EDAX	-Energy dispersive X- ray spectroscopy
TPD	- Temperature programmed desorption
FTIR	- Fourier transform infrared spectroscopy
^{31}P MAS NMR	-^{31}P magic angle spinning nuclear magnetic resonance spectroscopy
HDO	-Hydrodeoxygenation
HAP	-Hydroxyapatite
CP	-Calcium pyrophosphate
Ca/P	-Calcium to phosphorous
FFAP	-Free Fatty Acid Phase
FID detector	-Flame Ionized Detector
$Ca(NO_3)_2$	-Calcium nitrate
$(NH_3)_2HPO_4$	-Diammonium hydrogen phosphate
$NaH_2PO_4.2H_2O$	-Sodium dihydrogen phosphate
$Na_2HPO_4.2H_2O$	-Disodium dihydrogen phosphate
$Na_3PO_4.12H_2O$	-Trisodium dihydrogen phosphate
NH_4OH	-Ammonium hydroxide
KBr	-Potassium Bromate

Chapter 1

Introduction

1.1 Dependency on petrochemicals

Increased demands for energy and chemicals, stringent environmental regulations, and unrelenting depletion of fossil fuel sources led an interest in recent research for alternative and renewable energy resources. Biomass has been recognized as one of the most feasible resources to produce energy and chemicals. In 1850, main source of energy was biomass. During this period, need for new chemicals and new materials to meet growing demands of industry and consumer, drove an industrial revolution. At the turn of 20th century, the main sources for C-based feedstock were primarily derived from coal. Over the years, due to global politics and economical forces, chemical enterprises moved farther away from renewable sources and became heavily dependent on fossil fuels (crude oil and natural gas), both as a feedstock for commodity chemical and as an energy source.[1] The world consumes 4.4 billion tonnes of petroleum per year. The majority of fossil fuels are used to generate energy. More specifically, 86% of crude oil is used for heating (44%) and transport (42%) and remaining 14% is utilized by the chemicals industry and its derivatives, which includes 4% for plastics. The rise in population has increased the demand for more energy and consumer products hence; demand for fossil fuels is predicted to increase by more than 50% by 2025. The vast use of fossil fuel has also led to the problem of Greenhouse Gas (GHG) emissions.[2]

The depletion of fossil fuel reserves and the problem of GHG are shifting society's dependence to renewable biomass resources. This dependency shift is generally contributing towards the development of a sustainable industrial society and effective management of greenhouse gas emissions. During production of energy from biomass, CO_2 released during energy conversion is utilized in subsequent biomass regrowth. Hence, biomass has the potential to generate lower greenhouse gas emissions as compared to the combustion of fossil fuels. The shift from petroleum hydrocarbons to highly oxygenated bio-based feedstock will create remarkable opportunities for the chemical processing industry. Biomass can provide sources for both energy and carbon, and being renewable it is the only sustainable source for the industrial community.[3] The three main aspects necessary for a biomass economy are: (1) growth of the biomass feedstock, (2) biomass conversion into a fuel, and (3) fuel utilization.

In this respect, the "Roadmap for Biomass Technologies", a report has predicted that by 2030, 20% of transportation fuel and 25% of chemicals will be manufactured from biomass.[4] To achieve these goals, the US Department of Energy (US DOE) and the US Department of

Agriculture (USDA) has estimated that the US could produce 1.3 billion dry tons of biomass per year without any major changes in agricultural practices and can still meet its food, feed and export demands.[5]

1.2 Bio-refinery concept

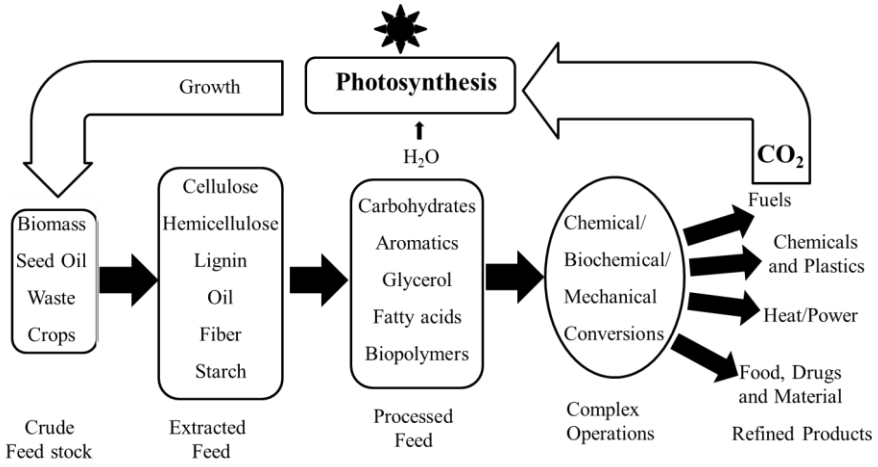

Fig. 1.1 Overview: Processing of crude feedstock's to refined products in a sustainable bio refinery.

The conversion of biomass by various pathways into energy and chemicals led to the concept of a bio-refinery, as shown in Fig 1.1. The development of a bio-based industry involves the appraisal of a broad range of conversion technologies including enzymatic, catalytic and thermochemical processes. The US DOE has commissioned a study to identify the top 30 value-added chemicals (shown in Table 1.1) that can be produced from carbohydrates and synthesis gas.[6] Petroleum feeds usually have a low extent of functionality (e.g., -OH, -C=O, -COOH) and thus suitable for use as fuels after appropriate catalytic treating (e.g., cracking to control molecular weight, isomerization to control octane number). Unlike petroleum, biomass-derived molecules contain excess functionality and the challenge in this field is to develop methods to control this functionality in the final product; fuels and chemicals. Carbohydrates represent the largest fraction of the annual biomass production and they are therefore proposed to be the major starting input in the upcoming bio-refineries.[7-10] Due to high extent of functionality, carbohydrate feeds have low volatility and high reactivity and must be processed by liquid-phase technologies. In general, a variety of fuels and chemical intermediates can be produced from carbohydrates by employing various types of reactions including hydrolysis, dehydration, isomerization, aldol

condensation, reforming, hydrogenation, and oxidation *etc*. The heterogeneous catalysts used for these reactions can include acids, bases, metals, and metal oxides. Several types of reactions typically occur during a given process, allowing use of multifunctional catalysts. Thermochemical processing, such as gasification, liquefaction, pyrolysis, and supercritical treatments of biomass-derived feedstock's, involves high-temperature treatment of biomass. Reactions such as hydrolysis, dehydration, isomerization, oxidation, aldol condensation, and hydrogenation are often carried out at temperatures near or below 400 K. Hydrogenolysis and hydrogenation reactions are usually carried out at higher temperatures (*e.g.,* 470 K), and aqueous-phase reforming is carried out at slightly higher temperatures (*e.g.,* 500 K) and at higher pressures (>50 atm) in order to maintain the water in the liquid state. Vapour-phase reforming of oxygenated hydrocarbons can be carried out over a wide range of temperatures and at modest pressures (*e.g.,* 10 atm).[11] Among these processes, pyrolysis process has received special consideration since it directly converts the biomass into solid, liquid and gaseous products by thermal decomposition in the absence of oxygen. Liquid produced after pyrolysis of biomass is termed as pyrolysis oil or bio-oil. Bio-oils are dark brown liquids composed of a mixture of various chemicals such as organic acids, aldehydes, furfurals, ketones, alcohols, carbohydrates, phenolics, water insoluble lignin fragments and water. Due to high oxygen and water content and low carbon density, bio oils have a low energy density compared to fossil fuels. Upgrading of these bio oils is necessary as the oxygen containing compounds easily polymerize and cause instability to the oil which causes poor performance during combustion. But during hydroprocessing of these oils, oxygen containing compounds cause catalyst deactivation. There are several technologies available such as zeolite cracking and hydrodeoxygenation (HDO) to upgrade bio oil to fuel, which can be used appropriately, transported and stored. It is reported that upgraded bio oil obtained from HDO process contains higher H/C content as compared to zeolite cracking.[12] HDO process is carried out at elevated pressure in hydrogen atmosphere and at temperature from 300-600 °C. HDO process removes oxygen as water, converting oxygenated chemicals to hydrocarbons.

Bio-based feedstock already has an impact on some practical applications, such as solvents, plastics, lubricants, and fragrances. One of such bio derived bulk chemical is lactic acid. It is a bi-functional compound bearing a hydroxyl group and an acid function, being

responsive to numerous chemical conversions to useful products. Lactic acid is utilized in the chemical, food, pharmaceutical and cosmetic industries. It has applications in food and beverages as preservative and pH adjusting agent. It is also used in pharmaceutical and chemical industries as a solvent, as a starting material in the synthesis of lactate esters. A bio-derived plastic such as polylactic acid polymers could be an environment friendly alternative to plastics derived from petrochemical materials. Their biological compatibility and hydrolytic degradation enables them to develop new applications. Hence lactic acid has been identified as one of the chemicals among top 30 value-added chemicals. In April 2002, Cargill Dow started their first large-scale polylactic acid plant in Blair, Nebraska. The plant has 140,000 t/year capacity and Cargill Dow projects a possible market of 8 billion pounds by 2020.[13]

Table 1.1 Top 30 bulk chemicals obtained from biomass

Carbon Number	Potential Top 30 candidates
1	Carbon monoxide & hydrogen (syngas)
2	None
3	Glycerol, 3 hydroxypropionic acid, lactic acid, malonic acid, propionic acid, serine
4	Acetoin, aspartic acid, fumaric acid, 3-hydroxybutyrolactone, malic acid, succinic acid, threonine
5	Arabinitol, furfural, glutamic acid, itaconic acid, levulinic acid, proline, xylitol, xylonic acid
6	Aconitic acid, citric acid, 2,5 furan dicarboxylic acid, glucaric acid, lysine, levoglucosan, sorbitol

1.3 Lactic acid background

Lactic acid was first identified as an acidic constituent of food nearly 250 years ago. It has been shown to be widespread in nature and has been prepared industrially by fermentation since 1881 (Fieser & Fieser, 1950). The acid occurs in two stereo-isomeric forms and these have been named as d- and 1-lactic acid or D (-) and L (+) lactic acid (Scheme 1.1). The pure isomers form colorless monoclinic crystals having a melting point of 54 °C. Chemical and physical

properties of lactic acid are given in Table 1.2. A synthetic racemic lactic acid prepared by mixing equal quantities of the D (-) and L (+) isomers melts in the range of 28 to 33 °C.

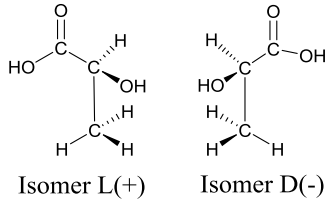

Scheme 1.1: Isomers of lactic acid.

Commercially lactic acid is present in aqueous solutions of 20 to 90 wt%. As lactic acid is prone to esterification, the solutions at equilibrium always contain a fraction of oligomers, the amount of which depends on the total concentration of lactoyl units (as shown in scheme 1.2).[14] Because of the reversibility of the esterification, lactoyl unit is readily hydrolyzed into lactic acid. Depending on the water content, the dimer may also condensate with another lactic acid molecule forming a linear trimer and water, and so on. As an example, due to the esterification tendency, a 90 wt% solution in equilibrium only contains 65.9% free lactic acid, while rest 24.1% is encountered in the dimer form. Pure lactic acid is a white crystalline solid not a liquid. Due to condensation and its high hygroscopicity, pure lactic acid production restricts to laborious crystallization.[15] Lactide, cyclic ester of two lactic acid molecules (cyclic dimer) is the important building block in producing polylactic acid. As lactide is less stable in water, only small traces of it are found in aqueous lactic acid solutions.[16]

Table 1.2 Chemical and physical properties of lactic acid[17-20]

Physical Properties	**Unit**	**Isomer/ concentration**	**Reported Range**
Melting point	°C	L or D racemic	52.7 - 53.0 16.4 - 18.0
Boiling point	°C (at 1.87 kPa)	L or D racemic	103 122
Solid density	g/mL (at 20 °C)	--	1.33
Liquid density of aq. Solution	g/mL (at 25 °C)	20 wt% 88.6 wt%	1.057 1.201
pKa	n/a	L or D racemic	3.79 - 3.86 3.73

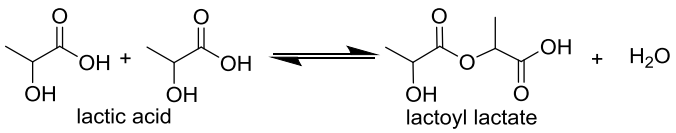

Scheme 1.2 Isomerization of lactic acid.

Lactic acid is industrially produced from sugars on a medium sized scale. Its production capacity is over 500,000 tons while the actual production is nearing 260,000 tons per year.[21] Lactic acid (2-hydroxypropionic acid) can be produced by chemical synthesis or by fermentation. Lactic acid is synthesized chemically by reacting, acetaldehyde with hydrogen cyanide in liquid phase under high pressure in presence of a base to produce lactonitrile. After its recovery and purification by distillation, hydrochloric acid or sulfuric acid is added to hydrolyze lactonitrile to lactic acid. The formed lactic acid is esterified with methanol to produce methyl lactate, which is purified by distillation. The purified methyl lactate is finally hydrolyzed in acidic aqueous solution to lactic acid and methanol, the latter being recycled in the same process.[22] In fermentation pathway, lactic acid is synthesized by fermentation of different carbohydrates such as glucose (from starch), maltose (produced by specific enzymatic starch conversion), sucrose (from syrups, juices, and molasses), lactose (from whey) *etc.*[23]

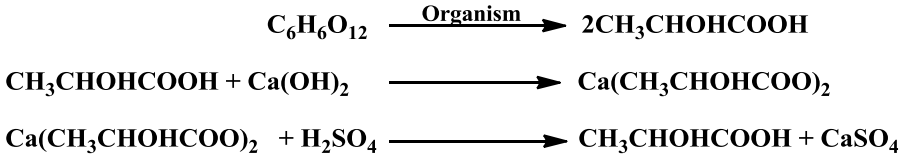

Scheme 1.3 Hexose sugars conversion to lactic acid.

On the basis of the nature of fermentation, Lactic Acid Bacteria (LAB) is classified into (1) homofermentative and (2) heterofermentative. Homofermentative LAB produces virtually a single product, *i.e.,* lactic acid, whereas the heterofermentative LAB produces lactic acid along with other products such as ethanol, diacetyl, formate, acetoin or acetic acid, and carbon dioxide.[24] The main drawback of fermentation process is its low productivity and tedious recovery procedure, which generates 1 ton of calcium sulfate per ton of lactic acid, accounting for up to 50% of the production cost (Scheme 1.3). Thus, more efficient processes for lactic acid production are desired. Recent advances in membrane-based separation and purification

technologies, in particular micro- and ultrafiltration and electrodialysis, have led to the beginning of new processes which should lead to low-cost production.[25]

Currently, the 'green chemistry' philosophy is being increasingly adopted by the chemical industry; hence new production procedures of valuable chemicals from biomass-derived raw materials are being sought. Lactic acid can be synthesised from glucose which includes base-catalyzed degradation of sugars as shown in scheme 1.4.

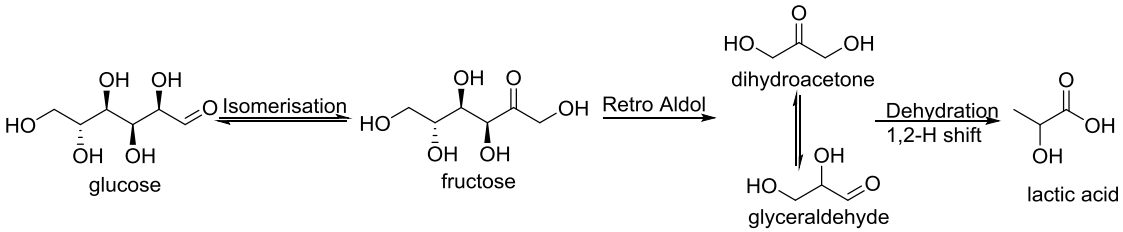

Scheme 1.4: Possible pathways for the conversion of glucose to lactic acid.

Zhou *et al*.[26] have shown 25.6% yield of lactic acid from a C_6-polyol, mannitol, under alkaline hydrothermal condition at 300 °C. Glycerol, being a byproduct from biodiesel production with currently low value as compared to other biomass derived chemical is an interesting feedstock for valorization. Kishida *et al.*[27] reported lactic acid synthesis from glycerol following hydrothermal reaction pathway in the presence of NaOH at 300 °C. Recently, a tandem reaction pathway has been developed to transform glycerol into lactic acid selectively.[28, 29] However synthesis of lactic acid from biomass is still at bench level due to its low productivity and harsh reaction conditions.

In early 1990s, a new manufacturer, Archer Daniels Midland (ADM), entered the business using carbohydrate fermentation technology. In late 1997, Cargill joined forces with Dow Chemical and established a Cargill–Dow polylactic acid (PLA) polymer venture based on carbohydrate fermentation technology. Currently, NatureWorks LLC (http://www.natureworksllc .com) is the leader in lactic polymer technology and markets. Over the past 10 years, this company has carried out voluminous work on the development of lactic acid based products such as: the polydilactide-based resins (Nature-Works PLA®), used in plastics and packaging applications, and the Ingeo™ polydilactide-based fibers that are used in specialty textiles and fiber applications.[30]

1.4 Valorization of lactic acid

Chemically, lactic acid is a highly functional molecule. Being renewable feedstock molecule with a high reactivity and a low energy density, making it less suitable as a fuel but excellent as an active precursor for different chemicals. Scheme 1.5 shows the valorization pathways for lactic acid. Various transformations revealed two major reaction pathways, dehydration and esterification. Dehydration (combined with other reactions) results in molecules like acetaldehyde, acrylic acid, 2,3-pentanedione and propionic acid, whereas esterification provides the synthesis of alkyl lactates, lactide and PLA. Two other possibilities are reduction and oxidation, yielding 1,2-propanediol and pyruvic acid, respectively.

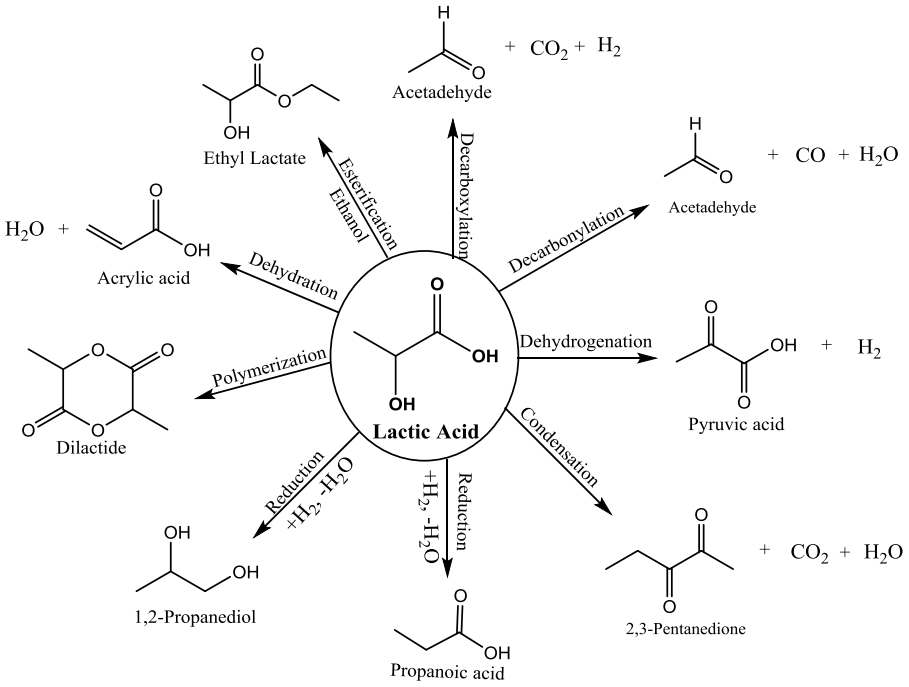

Scheme 1.5 Lactic acid possible reaction pathways.

Lactic acid can be converted to 1,2-propanediol by hydrogenation of carboxylic C=O group. The main application of 1,2-propanediol is its use as a building block of unsaturated polyester resins, which are combined with polystyrene and a filler into thermoset composite materials.[31] Also it has wide application range such as; an antifreeze for food processing to a softening agent in skin care products. 1,2-propanediol is a precursor for polyethers used in urethane foams. Currently, 1,2-propanediol is produced from hydrolysis of propylene oxide, therefore dependent on nonrenewable propylene.[32] An alternative production based on renewable

feedstock could release the 1,2-propanediol production from its non-renewable source. Glycerol and lactic acid can be alternative renewable sources. The first propanediol formation from lactate was shown in the 1930s and 1940s, where pure ethyl lactate was converted to 1,2-propanediol over Raney Ni with yield exceeding 80% at very high pressures (>25 MPa). Luo *et al*.[33] have shown the first catalytic hydrogenation of free lactic acid using unsupported rhenium black as a catalyst.

Lactic acid undergoes deoxygenation and forms propionic acid. Propionic acid is one of the important commodity chemical used in production of cellulose plastics, herbicides, and perfumes. As a strong mold inhibitor, calcium, sodium, and potassium salts of propionate are also widely used as food and feed preservatives. Currently, almost all propionic acid is produced by petrochemical processes, at an annual production rate of about 400 million pounds in USA.[34] $PtH(PEt_3)_3$ has shown 50% yield of propionic acid from lactic acid at a moderate temperature.[35] Molybdenum based catalysts has shown that propionic acid is the dominant product in lactic acid dehydration reaction.[36-39]

Pyruvic acid is one of the important chemical intermediate which can be synthesized by oxidative hydrogenation of lactic acid.[40-47] Vanadium and molybdenum based catalysts have shown promising activity for oxidative dehydrogenation of lactic acid to pyruvic acid. Pyruvic acid and its derivatives are used as an intermediate in perfume, food additives, and electronic materials. They are also used as raw material for many bioactive substances. Pyruvic acid is produced by dehydrative decarboxylation of tartaric acid. Compared to the conventional steam-cracking method of dehydrogenation, oxidative dehydrogenation is more favorable since the reaction is exothermic and avoids the thermodynamic constraints of non-oxidative routes by forming water as a by-product. Also, carbon deposition during oxidative dehydrogenation is eliminated, leading to stable catalytic activity.

The 2,3-pentanedione is another product obtained by the lactic acid following condensation pathway. It is used as a flavoring agent, a biodegradable solvent, a photoinitiator, and an intermediate for other high-value compounds. Dehydration of lactic acid at elevated pressures (0.5 MPa) over sodium phosphate catalysts led to the discovery of 2,3-pentanedione formation.[48] Different types of catalysts were screened for lactic acid condensation to 2,3-pentanedione.[49,50]

Lactic acid is prone to undergo decarboxylation/ decarbonylation to acetaldehyde at higher temperature. Acetaldehyde is a useful precursor in the chemical industry used in different types of condensation and addition reactions; it also serves for the production of acetic acid. Acetaldehyde is a byproduct in acrylic acid or 2,3-pentanedione process and it can be avoided by decreasing acidity and introducing basicity to the catalyst. Due to the lower price of acetaldehyde compared to lactic acid (about 35% lower), the formation of this product in gas phase conversions is usually not desired.[51] Mainly acidic catalysts showed more formation of acetaldehyde from lactic acid. [38, 52-57]

Due to high content of oxygen (C:O atomic ratio 1), lactic acid may be considered as a model compound of highly functionalized biomass-derived molecules in reactivity studies. Ruiz and Dumesic[58] have demonstrated the use of a Pt(0.1%)/Nb_2O_5 catalyst at 5.7 MPa with hydrogen in the gas phase at temperatures between 300-350 °C for the efficient conversion of lactic acid to various valuable chemicals (propionic acid and C_4–C_7 ketones). These chemicals can be used for the production of high energy-density liquid fuels (C_4–C_7 alcohols) as shown in scheme 1.6. Rennard *et al.*[59] reported a catalytic oxidative reforming of ethyl lactate and lactic acid. Auto-thermal reforming by partial oxidation was carried out over platinum and rhodium based catalysts supported on alumina foam monoliths. Products were varying between synthesis gas (CO and H_2) and olefins by variation of the feed: O_2 (C:O) ratio. The selectivity to synthesis gas was high at C:O ratios below 1.3, especially for the ester, which was active in reforming reaction than the free acid. The addition of cerium or lanthanum to the catalytic system was also found to enhance the selectivity to synthesis gas. Non-equilibrium products such as ethylene and acetaldehyde were observed at ratios of C:O > 1.3.

Synthesis of propionic acid, acetaldehyde, 2,3-pentanedione, 1,2-propanediol and pyruvic acid from lactic acid is still at bench level. Only production of ethyl lactate and polylactates from lactic acid has been commercialized by number of industries. Along with lactic acid, its esters also have many applications in chemical industry as a solvent. Esterification of lactic acid was performed using either homogeneous or heterogeneous catalysts as well as using enzymes.[60] The most prominent lactic acid ester is ethyl lactate. Ethyl lactate, due to its many solvent properties is an interesting alternative green solvent to replace existing hazardous solvents. It has excellent solvating ability for many resins, pigments, gums, greases *etc.* It is very effective against variety

of contaminants. It is used as raw material for the skin care industry. Ethanol is derived from biomass; hence ethyl lactate is completely renewable and biodegradable. Polymerization of lactic acid to high molecular weight polylactates can be achieved in two ways: i) Direct condensation - involves solvents under high vacuum; and ii) Formation of the cyclic dimer intermediate (lactide) - solvent free.

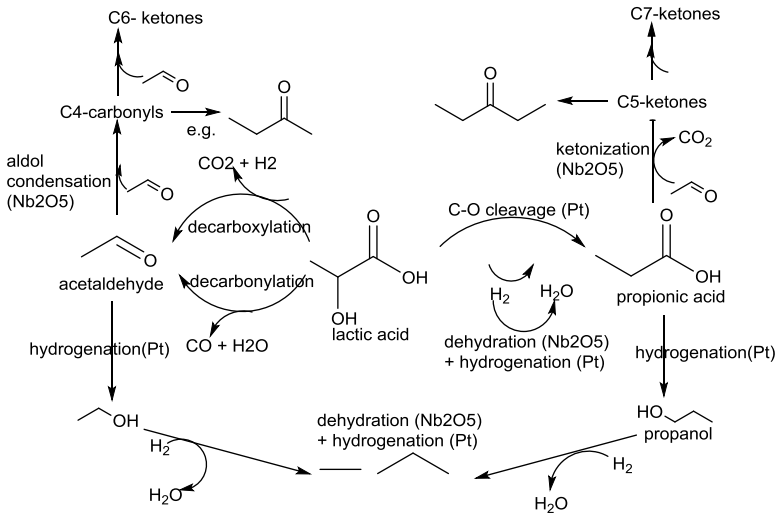

Scheme 1.6 Possible pathways for conversion of lactic acid to various valuable chemicals.

Polylactic acid is currently manufactured on a million-kilogram scale.[61] The global PLA market was estimated to be 360.8 kilo tons in 2013, which is expected to reach 1,205.3 kilo tons by 2020. PLA has several advantages: it is biocompatible and biodegradable, and can be readily broken down thermally by hydrolysis. The polylactic acid is relatively hard, with the glass transition temperature in the range 60-70 °C and melting at 170-180 °C. Polylactic acid shows unique features such as biodegradability, thermoplastic processibility and ecofriendliness that offer uses as commodity plastic, as in packaging, agricultural products and disposable materials. It is used in food packaging, such as rigid containers, shrink wraps and short (shelf)-life trays as well as mulch film and rubbish bags.[62]

1.5 Lactic acid dehydration to acrylic Acid

Acrylic acid is another lactic acid derivative produced by dehydration pathway. It is a commodity chemical of considerable value with an estimated annual production capacity of 4.2 million metric tons.[63] It is utilized in organic synthesis as a raw material. Polymers produced from acrylic acid can be used in synthetic resins, synthetic fibers and absorbent resins. Also

numerous applications of acrylic acid in surface coatings, textiles, adhesives, paper treatment, leather, fibers, detergents, *etc*. are known. The acrylic market stood at 3.3 million in 2006 and the global petroleum based market was US $ 8 billion in 2011 and expected growth of 3-4% per year. Currently, 100% of acrylic acid is produced out of fossil oil, mostly via direct oxidation of propene. Therefore, the production of acrylic acid via dehydration of lactic acid is an attractive target for new bio-based compound, and most lactic acid conversion studies have focused on this reaction. Table 1.3 shows the market analysis of acrylic acid and its derivatives. Researchers are trying to develop new green routes to produce acrylic acid from renewables. Beyond the inherent benefit of being a green process, bio based routes have potential to offer protection against petrochemicals market volatility and it will also produce acrylic acid in a more ecofriendly and economically comparable manner. Lactic acid is one of such renewable precursor for acrylic acid synthesis.

Table 1.3 Acrylic acid and its derivatives market analysis[64]

Entry no.	Product	Classification	Market opportunity	Market size
1	Acrylic acid	Adhesive, polymers	Acrylates (adhesive, coating) superabsorbent polymers, detergent polymers	2 billion pounds per year and $0.48 per pound
2	Acrylonitrile	Polymers	Acrylic fibers (carpets, clothing) acrylonitrile -butadiene-styrene and styrene-acrylonitrile (pipes, fitting automobiles, furniture packaging) nitrile rubber, copolymer, adiponitrile, acrylamide.	3.13 billion pounds per year and $0.31 -0.33 per pound
3	Acrylamide	Resins	Polyacrylamide, styrene butadiene latex, acrylic resins	206 billion pounds per year and $1.76-1.86 per pound

First acrylic acid synthesis from lactic acid was reported by Holmen *et al*.[65] in 1958 by dehydration using mixtures of Na_2SO_4 and $CaSO_4$, CaSO4 and $Na_4P_2O_7$, $Ba_3(PO_4)_2$, $BaSO_4$ as a

catalyst. Modified sodium dihydrogen phosphate on silica buffered with sodium bicarbonate used by Sawicki, showed 89% lactic acid conversion with 49% selectivity for acrylic acid (42% yield).[66] A series of catalysts such as sulphate and phosphate metal salts, different zeolites, and different calcium phosphates were reported later for lactic acid dehydration as shown in Table 1.4. Alkali salts were employed as supported on silica whereas alkaline metal salts were employed as such in lactic acid dehydration reaction. Less concentration of lactic acid was employed in the range of 20-30 wt% and with less flow 1 mL h^{-1} in these studies. Selectivity was less for sodium salts as compared to alkaline salts such as barium strontium. Alkali/alkaline-metal lactate salt was formed between the free lactic acid and the alkali/alkaline-metal salt. It was the predominant and active species on the catalyst support surface which was shown by MAS ^{31}P NMR and FTIR spectroscopy. [67-73] Deactivation occurring for alkaline earth phosphates during lactic acid and ester dehydration reactions was investigated. Polymerization of ethyl acrylate at the surface of the catalysts led to a strong deactivation of catalysts. Due to high stability of ethyl lactate, its conversion was lower than that of lactic acid. Here water vapour pressure plays important role in product selectivity. Large amount of water to the feed limits ethyl acrylate formation, which improves the catalyst stability. This favors the formation of acetaldehyde and reduces the selectivity to dehydration product acrylic acid. Hence the mechanistic study showed that acrylic acid was not formed by hydrolysis of ethyl acrylate or dehydration of lactic acid but by an independent dehydration/hydrolysis route.[74]

Modified zeolites have shown improved catalytic performances due to the tuned acidity/basicity and doped metal electronic promoter effect; which influenced the chemical adsorption of reactant/product molecules and inhibited the proceeding of side-reactions and deactivation. The conversion as well as selectivity was affected by the structure, type of alkali-metal and the acidic/basic nature of the zeolite. Y zeolite, having well-developed and organized three-dimensional channels of 0.74 nm aperture, which provide easy access to small molecules such as lactic acid, acrylic acid, *etc.* while diffusion of large-sized molecules such as 2,3-pentanedione, polylactate, *etc.* is hindered. Thus, NaY-supported catalyst may suppress the formation of 2,3-pentanedione while enhancing the production of acrylic acid. Deactivation for zeolites occurs due to blockage of the active sites by the formation of the deposits of clusters containing carboxyl groups.[75] New flow apparatus was proposed by G. Nafe *et al.*[76] for the

conversion of lactic acid to acrylic acid in the gas phase. Evaporator was spatially separated from the reactor by using high-temperature stable plastics. This modified setup avoids formation of deposits on the catalyst bed.

Acrylic acid can be synthesized from other renewable chemicals such as 3-hydroxypropionic acid, glycerol *etc.* The 3-hydroxypropionic acid was converted to acrylic acid with 97% selectivity using high surface area γ-alumina dehydration catalyst.[77] Glycerol was converted into acrylic acid (59.2%) on wt%$PO_4/W_{2.2}V_{0.4}Nb_{2.4}O_{14}$ catalyst directly under oxidative condition.[78] Acrylic acid synthesis from other nonrenewable sources is also reported.[79] The PEG-derived VPO catalysts were tested for aldol condensation of acetic acid/ methyl acetate with formaldehyde to give acrylic acid and methyl acrylate as a product.[80] Acrylic acid synthesis from acetic acid and formalin following condensation pathway was proposed. Similarly vanadium-phosphate oxides prepared by ultrasonic impregnation method were tested for acrylic acid synthesis using a fixed-bed tubular micro reactor from CH_3COOH and HCHO. The $V{-}P/SiO_2$ binary oxide catalyst with a bulk density ratio of 1:2 showed yield and selectivity of acrylic acid as 21.9% and 97.8% respectively. Influences of acidic and alkaline sites, as well as ratio of V^{4+} and V^{5+}, on catalyst activity were further studied.[81]

Lactic acid conversions were studied in supercritical water. Lactic acid undergoes three primary reaction pathways. First one is the acid-catalyzed heterolytic decarbonylation pathway where carbon monoxide, water, and acetaldehyde are the products. Second one is homolytic decarboxylation pathway where carbon dioxide, hydrogen, and acetaldehyde are the products. Third one is heterolytic dehydration pathway where acrylic acid and water are the products.[82] The dehydration of lactic acid was conducted in a Hastelloy C-276 annular reactor in near-critical water. The presence of phosphate salts and/or base suppresses the competing pathways which in turn increases the yields of acrylic acid.[83] Lactic acid dehydration was studied with a flow apparatus in supercritical water at high temperatures (450 °C) and high pressures (40–100MPa). The maximum selectivity of acrylic acid was 44% at 23% lactic acid conversion over silica supported sodium polyphosphates catalyst.[84]

Generally feedstock characteristics play an important role in the lactic acid dehydration process. Usually, diluted aqueous solutions with different concentrations of lactic acid in water such as 0.05 M, 26 wt%, 29 wt%, 34 wt%, 38 wt%, 50 wt% as well as lactates solution in water

such as 50 wt%, 60 wt% were used for their dehydration to acrylic acid or to corresponding acrylates. Zhang *et al.*[85] proposed that, moderate amount of water could prevent hydrolysis of methyl lactate to lactic acid followed by deposition and decomposition of lactic acid polymers on the catalyst surface, thus inhibiting coke formation. Traditionally dehydration reaction was carried out in presence of N_2 gas, but Zhang *et al.* have shown that activity for acrylic acid in lactic acid dehydration is more when CO_2 is the carrier gas. Due to excess CO_2 there is inhibition of decarbonylation/decarboxylation, thus improving dehydration selectivity.[85,86]

Table 1.4 Dehydration of lactic acid/esters to acrylic acid on various catalysts

Type of catalyst		**Reaction conditions* A, B, C**	**Catalytic activity# D, E**	**Ref.**
Alkali/ alkaline sulphates and phosphates	Na_2HPO_4 on silica	A- 20% B- 20 mL h^{-1}, C- 350 °C	D- 42%	87
	Na_3PO_4 on silica-alumina	C- 350 °C contact time- 0.6 s	E- 36%	88
	20% $NaNO_3$/SBA15	A- 34%, B-5 mL h^{-1}, C-370 °C	D- 43%	69
	NH_3 treated $AlPO_4$	C- 340 °C contact time- 4.2 s	E- 43%	89
	m($CaSO_4$)/*m*($CuSO_4$)/ *m*(Na_2HPO_4)/*m*(KH_2PO_4) ::150.0/ 13.8/2.5/1.2	A- 26 wt%, C-330 °C, contact time- 88 s	D-63.7%	86
	m($CaSO_4$):*m*($CuSO_4$) :(Na_2HPO_4):*m*(KH_2PO_4) ::150.0:13.8:2.5:1.2	ML -60%, C- 400°C , contact time- 7.7 s	E- 63.9%	85
	$Ba_3(PO_4)_2$	A- 20%, GHSV-3438 h^{-1}, C-350 °C	D- 85%	90
	$Ba_3(PO_4)_2$	GHSV- 1750 h^{-1}, C- 385 °C	E- 49%	73
	$Ba_2P_2O_7$	A- 20%, B-1 mL h^{-1}, C-400 °C	LA conv.- 99.7%, E- 76%	91

	$BaSO_4$	A- 20%, B- 1 mL h^{-1}, C- 400 °C	LA conv.- 99.8%, E- 74.0%	92
	$Sr_2P_2O_7$ (0.10wt% H_3PO_4)	A- 20%, B-1 mL h^{-1}, C- 400 °C	D- 72 %	93
	Sodium arsenate	C- 300 °C, 0.5 MPa	E- 58%	94
	$Sr_{10}(PO_4)_6(OH)_2$	A- 38%, B- 1.2 mL h^{-1}, C- 350 °C	D- 45%	95
Modified zeolites	2wt% La/NaY	A- 38%, LHSV- 3 h^{-1}, C- 350 °C	D- 56%	96
	2.8K/NaY	A- 29%, B- 4.5 mL h^{-1}, C- 325 °C	LA conv.- 98.8%, E- 50%	97
	KI-modified NaY	A- 29%, B- 4.5 mL h^{-1}, C- 375 °C	LA conv.- 97.6%, E- 67.9%	98
	2% Ba/NaY	A- 38% solution, LHSV - 3 h^{-1}, C- 325 °C	D- 44.6%	99
	14 wt%Na_2HPO_4/NaY	A- 34%, B- 6 mL h^{-1}, C- 340 °C	D- 58.4%	100
	12 wt%Na_2HPO_4/modified NaY nanocrystallites	A- 34%, B- 6 mL h^{-1} C- 340 °C	D- 74.3%	101
	K_xNa_{1-x} β where x= 0.94 ($K_{0.94}Na_{0.06}$ β)	A- 10%, WHSV-2.1 h^{-1}, C-360 °C	D- 61%	102
	45 wt% K_2HPO_4:$Al_2(SO_4)_3$(6:4)/MCM-41	A(ML)- 60%, B-1.2 mL h^{-1}, C- 410 °C	ML conv. 90%, E-70%	103
	ZSM-5 treated 0.5 NaOH : 0.5 Na_2HPO_4 (mol/L)	LHSV- 4 h^{-1} C- 350 °C	LA conv. 96.9% E-77.9%	104
Calcium phosphate	$Ca_3(PO_4)_2$-SiO_2 (80:20 wt%)	A(ML) – 50%, B- 0.7 mL h^{-1} , C- 370 °C	Con. 73.6% E- 70%	105
	$Ca_3(PO_4)_2$-$Ca_2(P_2O_7)$ of 50:50 wt%	A(ML)- 50% B- 2.1 mL h^{-1} , C- 390 °C	ML con. 91% E- 75%	106
	$Ca_{10}(PO_4)_6(OH)$ (Ca/P of	A- 38%, B- 1.2 mL h^{-1},	LA con. 91.4%,	107

	1.67)	C- 350 °C	D- 72%	
	$Ca_{10}(PO_4)_6(OH)$ (Ca/P-1.55)+NaOH	A- 38%, B- 1.2 mL h^{-1}, C- 350 °C	LA conv. 90%, E-78%	108
	Hydroxyapatite (Ca/P ratio of 1.62)	A-7.4 kPa in H_2O,C-360 °C, WHSV-2.1 h^{-1}	LA conv.- 70%, E-71%	109
	$Ca_3(PO_4)_2$ and $Na_4P_2O_7$	A: 50% B: 31 mL h^{-1} and C: 425 °C	D- 50%	65

*A-lactic acid solution, B- feed flow and C- temperature, # D-yield, E- selectivity

As seen from the above literature survey several types of catalysts have been reported for lactic acid valorization to acrylic acid. Most of the studies reported mainly alkali and alkaline earth metal salts, especially sulfates and phosphates, are more effective catalysts for lactic acid dehydration. However, these studies suffer few drawbacks such as lower selectivity to acrylic acid, use of very low WHSV, low lactic acid concentration, deactivation of catalyst and more number of side products. Hence, there is still a need to design active catalyst for lactic acid dehydration which will offer high selectivity for acrylic acid using high concentration of lactic acid and high thermal stability to catalyst without undergoing deactivation. This can be attempted by fundamental understanding of roles of the catalyst in lactic acid dehydration. In literature, acidic catalysts mainly shows acetaldehyde but as the acidity is lowered the selectivity for other products such as acrylic acid increases. Especially alkali and alkaline earth metals form alkali lactate and inhibit decarboxylation/decarbonylation during lactic acid dehydration process. Phosphate based catalysts (alkali/alkaline) whether supported or as such have shown better activity for lactic acid dehydration reaction. Hence, catalysts such as calcium phosphates which show less acidity were selected for these studies.

1.6 Calcium phosphate catalysts for lactic acid dehydration

Most of the previous studies illustrated that metal phosphates, mainly alkali and alkaline earth metals, were effective catalyst for the dehydration of lactic acid to acrylic acid. Mainly different forms of calcium phosphate like calcium hydroxyapatite, tricalcium phosphate and calcium pyrophosphates have shown good activity for lactic acid dehydration. Catalysts with mild acidity or mild basicity have been used for lactic acid dehydration in earlier work. Surprisingly, calcium hydroxyapatite (HAP) and calcium pyrophosphate (CP) contains both

weak acidic and weak basic sites in a single crystal and hence it is expected to be an efficient catalyst for dehydration reaction.[110-112]

In the biomaterial research field, a great attention was given on calcium phosphates synthesis that can be used in orthopedics and dentistry, in the form of coatings, granules, porous or solid blocks, also in the form of various composite materials. The most frequently studied, clinically tested and used synthetic materials of calcium phosphate (CaP) are hydroxyapatite [HAP -$Ca_{10}(PO_4)_6(OH)_2$], β-tricalcium phosphate [β -TCP - $Ca_3(PO_4)_2$] and biphasic HAP/ β-TCP mixture.

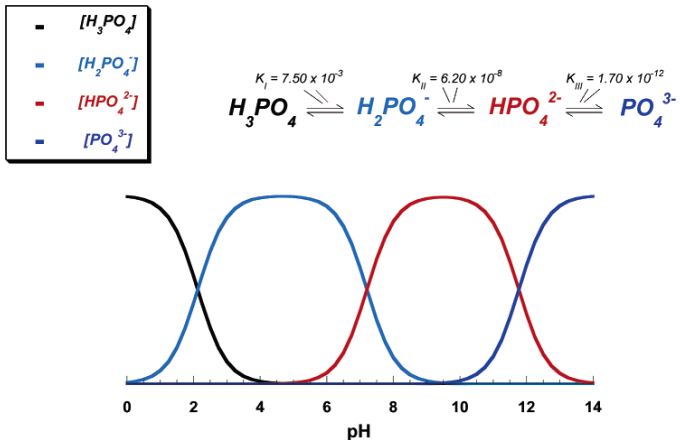

Fig. 1.2 pH variation of ionic concentrations in tripotic equilibrium for phosphoric acid solutions.[113]

Calcium phosphates are formed by three main elements: calcium (oxidation state +2), phosphorus (oxidation state +5) and oxygen (oxidation state -2). Many calcium phosphates also contain hydrogen in different conditions such as an acidic phosphate anion (for example, HPO_4^{2-}), hydroxyl group (for example, $Ca_{10}(PO_4)_6(OH)_2$) or in a form of bonded water (for example, $CaHPO_4 \cdot 2H_2O$). Majority of compounds of this class are poorly soluble in water and non-soluble in alkaline solutions, but all of them easily dissolve in acids. There are a large variety of calcium phosphates present (as given in Table 1.5), which are differentiated by the type of the phosphate anion: ortho- (PO_4^{3-}), meta- (PO_3^-) or pyro- ($P_2O_7^{4-}$) and poly- ($(PO_3)_n^{n-}$).[114] The effect of pH on the synthesis of calcium phosphates is integrally linked to the properties of phosphate-containing solutions. Due to the tripotic equilibrium that exists within these systems, variations in pH alter the relative concentrations of the four polymorphs of phosphoric acid (Fig. 1.2). These

polymorphs determine the chemical composition and Ca/P ratio of resulted calcium phosphate precipitate at that pH.[115]

Table 1.5 Properties of different type's calcium phosphate

Phases	**Chemical Formula**	**Ca/P ratio**	**Mol. Wt. (g)**	**Density (g/cc)**	**Solubility at 25 °C -log(Ksp)**	**pH stability range in aq.**	**Mineral**
Tetracalcium phosphate	$Ca_4P_2O_9$	2.0	366	3.05	38-44	can not be precipitated	Hilgenstockite
Hydroxyapatite	$Ca_{10}(PO_4)_6(OH)_2$	1.67	1004	3.16	116.80	9.5-12	Hydroxyapatite
Ca-deficient hydroxyapatite	$Ca_{10-x}(HPO_4)_x$ $(PO_4)_{6-x}$ $(OH)_{2-x}$ $0<x<1$	<1.67	966-1004	--	85.10	6.5-9.5	--
β-Tricalcium phosphate	$Ca_3(PO_4)_2$	1.50	310	3.07	28.90	can not be precipitated	--
α-Tricalcium phosphate	$Ca_3(PO_4)_2$	1.50	310	2.86	25.50	can not be precipitated	--
Amorphous calcium phosphate	$Ca_3(PO_4)_2.nH_2O$ n=3-4.5	1.50	364-391	--	25.70	Metastable (6.0-12)	--
Whitlockite	$Ca_{10}(HPO_4)(PO_4)_6$	1.43	1071	3.13	81.70	Metastable	Whitlockite
Octocalcium phosphate	$Ca_8(HPO_4)_2$ $(PO_4)_4.5H_2O$	1.33	982	--	96.6	Metastable (6.0-7.0)	--
Dicalcium phosphate dehydrate	$CaHPO_4.2H_2O$	1.00	172	2.34	6.59	2.0-6.5	Brushite
Dicalcium phosphate anhydrate	$CaHPO_4$	1.00	136	2.93	6.90	2.0-6.0	Monetite
Calcium pyrophosphate	$Ca_2P_2O_7$	1.00	254	3.09	--	Can not be precipitated	--
Monocalcium phosphate	$Ca(H_2PO_4)_2.H_2O$	0.50	252	2.22	Highly soluble	Metastable (0.1-2.0)	--

monohydrate							
Calcium oxide	CaO	--	56	3.35	Reactive	--	Lime
Calcium hydroxide	$Ca(OH)_2$	--	74	2.24	5.10	--	Portlandite
Calcium carbonate	$CaCO_3$	--	100	2.71	8.32	--	Calcite

1.7 Different types of calcium phosphates

1.7 a) Monocalcium phosphate (monohydrate and anhydrous)

Monocalcium phosphate exists in the monohydrate (MCPM, $Ca(H_2PO_4)_2.H_2O$) or anhydrous salt (MCPA, $Ca(H_2PO_4)_2$). For both MCPM and MCPA, Ca/P ratio is 0.5, and both are most acidic and water soluble with solubility of 1.14 at 25 °C for both. Both have the triclinic space group crystallographic structure.

1.7 b) Dicalcium phosphate (dihydrate - brushite and anhydrate - monetite)

Dicalcium phosphate dihydrate (DCPD, $CaHPO_4.2H_2O$) known as the mineral brushite can easily be crystallised from aqueous solution of calcium phosphate at pH <6.5. DCPD crystals consist of $CaHPO_4$ chains arranged parallel to each other, while lattice water molecules are interlayered between them. It transforms into dicalcium phosphate anhydrous (DCPA, $CaHPO_4$) known as monetite at temperatures above 80 °C. DCPD has monoclinic space group and DCPA triclinic space group. DCPA is less soluble in water than DCPD due to the absence of water inclusions.

1.7 c) Octacalcium phosphate

Octacalcium phosphate (OCP) with chemical formula $Ca_8(HPO_4)_2(PO_4)_4.5H_2O$ is found as an unstable transient intermediate during the precipitation of the thermodynamically more stable HAP in aqueous solutions (given by equation 1.1). OCP has the crystallographic structure of triclinic space group.

$$Ca_8H_2(PO_4)_{6.5}H_2O + 2Ca_2^{+} \longrightarrow Ca_{10}(PO_4)_6(OH)_2 + 3H_2O + 4H^{+} \quad \text{Eqn. 1.1}$$

1.7 d) Tricalcium phosphates and whitlockite

Tricalcium phosphates (TCPs) can exist in either α-TCP or β-TCP crystal form. β-TCP cannot be precipitated from aqueous solutions but can be prepared by thermal decomposition (> 800 °C) of calcium deficient HAP (CDHAP). α-TCP is stable at temperatures between 1180-1400 °C and is formed by the phase transformation of β-TCP. Whitlockite is the Mg-substituted form of β-TCP. Although α-TCP and β-TCP have exactly the same chemical composition, they differ in their crystallographic structure and their solubility. α-TCP exists in monoclinic space group, while, β-TCP in rhombohedral space group. α-TCP is more reactive than β-TCP in aqueous systems and has higher specific energy which can be hydrolysed to a mixture of other calcium phosphates. At different pH α-TCP transform into different forms of calcium phosphate as shown in equation 1.2.

$$\alpha Ca_3(PO_4)_2 + 6H_2O \longrightarrow 2CaHPO_4.2H_2O + Ca(OH)_2 \text{ (in acidic region)}$$

$$3\alpha Ca_3(PO_4)_2 + 7H_2O \longrightarrow Ca_8H_2(PO_4)_6.5H_2O + Ca(OH)_2 \text{ (in neutral region)}$$

$$(10\text{-}x)\alpha Ca_3(PO_4)_2 + 3(2+n\text{-}x)H_2O \longrightarrow 3Ca_{10}\text{-}x(HPO_4)_x(PO_4)_{6\text{-}x}(OH)_{2\text{-}x}.nH_2O + 2(1\text{-}x)H_3PO_4 \text{ (in basic region)}$$

---------- Eqn. 1.2

1.7 e) Hydroxyapatite

Hydroxyapatite (HAP) has the chemical formula $Ca_{10}(PO_4)_6(OH)_2$ as to denote the crystal unit cell comprises of two molecules. HAP is the second most stable and least soluble calcium orthophosphate in water (*Ks* of -log 116.8) after fluoroapatite (FAP; *Ks* of -log 120.0). The crystallographic structure of HAP is hexagonal space group.

1.7 f) Tetracalcium phosphate (Hilgenstockite)

Tetracalcium phosphate (TTCP or TetCP, $Ca_4(PO_4)_2O$) has a Ca/P ratio of 2.0 and is the most basic among all of the existing calcium phosphate orthophosphates. TTCP cannot be synthesised in an aqueous environment. Mixtures of calcium carbonate ($CaCO_3$) and dicalcium

phosphate anhydrate ($CaHPO_4$) are heated to 1400-1500 °C for 6-12 h. TTCP has the monoclinic space group. The reaction is given in equation 1.3.

$$2CaHPO_4 + 2CaCO_3 \longrightarrow Ca_4(PO_4)_2O + 2CO_2 + H_2O \qquad \text{Eqn. 1.3}$$

1.7 g) Calcium pyrophosphate

The crystals exist in at least two polymorphs, one triclinic (denoted t-CPPD) with known structure and the other monoclinic (denoted m-CPPD). Calcium pyrophosphate hydrates (CPP, $Ca_2P_2O_7{\cdot}nH_2O$) are involved in several forms of arthritis, including calcium pyrophosphate crystal deposition disease, also known as pseudogout, and osteoarthritis (OA), the most frequent form of rheumatic disease.[116]

1.8 OBJECTIVES OF THE THESIS

Diminution of fossil fuels and the increasing demands for energy and consumer end products requires alternative renewable source. Owing to this, researchers are trying to develop new alternative sources for energy and chemicals. Lactic acid is one such chemical which is obtained from renewable resources. Dehydration of lactic acid to acrylic acid is being considered as one of the attractive alternate route for the manufacture of acrylic acid from renewable raw materials. Acrylic acid is of significant value for consumer end products industry. Currently acrylic acid is produced from nonrenewable source, propylene. Researchers are trying to develop new green routes to produce acrylic acid from renewables. Bio based routes will offer less dependency on petrochemicals and promotes ecofriendly synthesis of acrylic acid. Lactic acid is one of such renewable precursor for acrylic acid synthesis.

As seen from the above literature survey several types of catalysts have been reported for lactic acid valorization to acrylic acid. However, there are some shortcomings such as lower selectivity to acrylic acid, very high selectivity for gaseous products like CO, CO_2, H_2 along with acetaldehyde, use of very less WHSV, low lactic acid concentration, deactivation of catalyst and more number of side products. Hence, there is necessity to design active catalyst for lactic acid dehydration, which will offer high selectivity for acrylic acid using high concentration of lactic acid and reduces gaseous products. Also active catalysts should show high per pass yield with more life for catalyst activity. In literature, phosphate based catalysts have shown better activity

for lactic acid dehydration reaction. Alkali phosphates due to their water solubility can leach out from the support and which may lead to decrease in activity, on the other hand alkaline phosphates due to water insolubility shows stable catalytic activity. Calcium phosphates which are insoluble in water have previously shown good activity for dehydration reactions with their less acidity. Therefore calcium phosphates were selected for these studies. In the present study we have tried to develop different calcium phosphate based catalysts by varying synthesis parameters and its evaluation for vapour phase dehydration of lactic acid to acrylic acid. Different types of calcium phosphates were prepared by precipitation method, and characterized by several techniques in this Ph.D. work. Due to high oxygen and water content and low carbon density, biomass has a low energy density compared to fossil fuels. To increase the energy density and reduce transportation costs of biomass, there are several technologies available; one of them is hydrodeoxygenation (HDO) to remove oxygen. Lactic acid was considered as a model substrate for HDO in present studies. The detailed objectives are given as follows.

1. Preparation of different types of calcium phosphates such as hydroxyapatite (HAP), calcium pyrophosphate (CP) with varying Ca/P ratio by precipitation method.
2. Study the influence of various parameters such as pH and Ca/P ratio on both composition and physico-chemical properties of the catalyst.
3. Characterisation of synthesised catalysts using XRD, SEM, BET surface area and CO_2 and NH_3-TPD, RAMAN, ^{31}P MAS NMR *etc.* techniques.
4. Screening of the prepared catalysts for vapour phase lactic acid conversion to acrylic acid and propionic acid in a fixed bed continuous down flow reactor.
5. Optimization of the reaction parameters such as temperature, WHSV and lactic acid concentration to achieve highest acrylic acid yield.
6. Time on stream activity measurement in a continuous operation on active catalyst.
7. Use of *in situ* FTIR spectroscopy to study *in situ* formed species during reaction, catalyst interaction with the substrate and factors affecting the selectivity for acrylic acid.
8. Study the effect of dopant such as molybdenum oxide on calcium phosphate for HDO process considering lactic acid as a model substrate.
9. Investigation of the pathway for propionic acid formation from lactic acid.

1.9 Outline of the thesis

Chapter wise work distribution during the Ph.D. tenure.

Chapter 1:

An outlook on fast depleting fossil fuels and emerging renewable resources as an alternative energy and commodity chemical sources has been discussed in detail. This chapter describes different resources available for lactic acid production by using different routes such as biological and chemical. Availability of different route for lactic acid valorization has been discussed in detail. Lactic acid can be converted to acrylic acid following dehydration route. Chapter also gives an overview of the application of heterogeneous catalysis for valorization of lactic acid. This chapter gives an overview about different types of calcium phosphates available in nature. These phosphate based heterogeneous catalysts were active for lactic acid dehydration, specifically $Ca_3(PO_4)_2$, HAP, $Ca_2P_2O_7$.

Chapter 2:

Preparation of hydroxyapatite (HAP) with varying Ca/P ratio by precipitation method has been explained. The Ca/P ratio was maintained by adjusting pH and prepared catalysts were calcined at 600 °C. The detailed characterization using XRD, BET-surface area, NH_3-CO_2 TPD, FTIR, EDAX and SEM has been discussed in this chapter. Prepared catalysts were screened for vapour phase dehydration of lactic acid to acrylic acid using a quartz fixed bed down flow reactor at atmospheric pressure. Reaction parameters were optimised for best catalytic activity. Mechanistic studies were carried out using *in situ* FTIR spectroscopy. A possible reaction pathway for lactic acid dehydration and decarbonylation of lactic acid has been proposed using *in situ* FTIR spectroscopy studies.

Chapter 3:

Preparation of calcium pyrophosphate (CP) with varying Ca/P ratio by precipitation method has been explained. Different types of sodium phosphates were used to vary Ca/P ratio without maintaining pH and prepared catalysts were calcined at 600 °C. Similar to the previous chapter, the detailed characterization using XRD, BET-surface area, NH_3-CO_2 TPD, FTIR, EDAX, ^{31}P MAS NMR, RAMAN spectroscopy and SEM has been discussed in this chapter.

Prepared catalysts were screened for vapour phase dehydration of lactic acid to acrylic acid using a quartz fixed bed down flow reactor at atmospheric pressure. Reaction parameters were optimised for best catalytic activity. Mechanistic studies were carried out using *in situ FTIR* spectroscopy.

Chapter 4:

The fourth chapter deals with hydrodeoxygenation of lactic acid. Here MoO_3 supported on CP catalyst for lactic acid hydrodeoxygenation reaction was used. MoO_3 supported on CP, SiO_2, Al_2O_3 catalysts were prepared by wet impregnation method. SiO_2, Al_2O_3 supports were taken for comparison. The effect of MoO_3 on catalytic activity has been studied. Prepared catalysts were screened for vapour phase hydrodeoxygenation of lactic acid to propionic acid without using external H_2 source in a quartz fixed bed down flow reactor at atmospheric pressure. Possible pathway for the formation of propionic acid from lactic acid has been investigated by carrying hydrogenation of acrylic acid.

Chapter 5:

This chapter is the summary and conclusions of the thesis work. Summary includes the conclusion of the present study with respect to catalyst synthesis, characterisation, and catalytic activity for lactic acid dehydration with different Ca/P ratio.

1.10 References

[1] J. P. van Wyk, *Trends Biotechnol.* 2001, **19**, 172-177.

[2] A. J. Ragauskas, C. K. Williams, B. H. Davison, G. Britovsek, J. Cairney, C. A. Eckert, W. J. Frederick Jr., J. P. Hallett, D. J. Leak, C. L. Liotta, J. R. Mielenz, R. Murphy, R. Templer, and T. Tschaplinski, *Science*, 2006, **311,** 484-489.

[3] a)A. B. Lovins, in *Winning the Oil Endgame: Innovation for Profits, Jobs, and Security*, B. T. Aranow, Ed. (Rocky Mountain Institute, Snowmass, CO, 2004), 1-122.; b) H. L. Chum, and R. P. Overend, *Adv. Solar Energy*, 2003, **15**, 83-89.

[4] The Roadmap for Biomass Technologies in the U.S., Biomass R&D Technical Advisory Committee, US Department of Energy, Accession No. ADA 436527, 2002.

[5] R. D. Perlack, L. L. Wright, A. Turhollow, R. L. Graham, B. Stokes, and D. C. Erbach, Biomass as Feedstock for a Bioenergy and Bioproducts Industry: The Technical Feasibility of a Billion-Ton Annual Supply, Report No. DOE/GO-102995-2135; Oak Ridge National Laboratory, Oak Ridge, TN, 2005. Available electronically at http://www.osti.gov/bridge.

[6] T. Werpy, G. Petersen, "Top Value Added Chemicals from Biomass: Vol. 1—Results of Screening for Potential Candidates from Sugars and Synthesis Gas", Report No. NREL/TP-510– 35523; National Renewable Energy Laboratory, Golden, CO, 2004. Available electronically at http://www.osti.gov/bridge.

[7] S. Van de Vyver, J. Geboers, P. A. Jacobs and B. F. Sels, *ChemCatChem*, 2011, **3**, 82-94.

[8] J. A. Geboers, S. Van de Vyver, R. Ooms, B. Op de Beeck, P. A. Jacobs and B. F. Sels, *Catal. Sci. Technol.*, 2011, **1**, 714-726.

[9] R. Rinaldi and F. Schuth, *ChemSusChem*, 2009, **2**, 1096-1107.

[10] B. Kamm, M. Kamm, P. R. Gruber and S. Kromus, *Biorefineries*-15 *Industrial Processes and Products*, Wiley-VCH Verlag GmbH, 2008, 1-40.

[11] J. N. Chheda, G. W. Huber, and J. A. Dumesic, *Angew. Chem. Int. Ed*. 2007, **46,** 7164-7183

[12] M. Yasir, S. Chowdhury, N. Mansor, N. M. Mohammad, and Y. Uemura, *Appl. Mech.*

and Materi., 2014, **625**, 357-360.

[13] a) Fahey, J. Shucking Petroleum. *Forbes Magazine* 2001, Nov 26, 206. b) Mccoy, M. *Chem. Eng. News*, 2003, **81**, 17-18.

[14] a)Annals of the New York Academy of Sciences, 1965, **119**, 854-867; b) M. Brin, *Ann. NY Acad. Sci.*, 1965, **119**, 942-956, c) M. Brin, *Ann. NY Acad. Sci.*, 1965, **119**, 1084-1090.

[15] R. Auras, L.-T. Lim, S. E. M. Selke, H. Tsuji and Editors, Poly (Lactic Acid): Synthesis, Structures, Properties, Processing, And Applications, *John Wiley & Sons, Inc*., 2010.

[16] S. Inkinen, M. Hakkarainen, A.-C. Albertsson and A. Sodergard, *Biomacromolecules*, 2011, **12,** 523-532.

[17] *Galactic*, 2012, available online at: http://www.lactic.com., R. Datta, in *Kirk-Othmer Encyclopedia of Chemical Technology*, John Wiley & Sons, Inc., 2000. 42.

[18] W. Groot, J. van Krieken, O. Sliekersl and S. de Vos, in *Poly(Lactic Acid)*, John Wiley & Sons, Inc., 2010, pp. 1-18.

[19] Z. Jin, Y. Tian and J. Wang, in *Poly(Lactic Acid)*, John Wiley & Sons, Inc., 2010, 19-25.

[20] S. P. Chahal and J. N. Starr, in *Ullmann's Encyclopedia of Industrial Chemistry*, Wiley-VCH Verlag GmbH & Co. KGaA, 2000.

[21] Nattrass and A. Higson, *National Non-Food Crops Centre, 'Renewable Chemicals Factsheet: Lactic Acid'* 2010, available online at: http://www.nnfcc.co.uk/publications/nnfcc-renewable-chemicalsfactsheet-lactic-acid

[22] P. Dey, P. Pal, *J. Membrane Science*, 2012, **389**, 355-362.

[23] N. Narayanan, P.K. Roychoudhury, and A. Srivastava, *Electr.J. Biotech.* 2004, 7, 15-19.

[24] R. P. John, K. M. Nampoothiri and A. Pandey, *Appl. Microbiol. Biotechnol.*, 2007, **74,** 524-534.

[25] A. Corma, S. Iborra and A. Velty, *Chem. Rev.*, 2007**, 107**, 2411-2502.

[26] H. Zhou, F. Jin, B. Wu, J. Cao, X. Duan and A. Kishita, *J Phys: Conf Series*, 2010, **215,** 012125-012129.

[27] H. Kishida, F. M. Jin, Z. Y. Zhou, T. Moriya and H. Enomoto, *Chem. Lett.*, 2005**, 34**,

1560-1561.

[28] Y. H. Shen, S. H. Zhang, H. J. Li, Y. Ren and H. C. Liu, *Chem. Eur. J.*, 2010, **16**, 7368-7371

[29] H. J. Cho, C-C. Chang and W. Fan, *Green Chem.*, 2014, **16**, 3428-3433.

[30] R. P. John, K. M. Nampoothiri and A. Pandey, *Appl. Microbiol.Biotechnol.*, 2007**, 74**, 524-534.

[31] E. DHondt, S. Van de Vyver, B. F. Sels and P. A. Jacobs, *Chem. Commun. (Cambridge, U. K.)*, 2008, **7**, 6011-6012.

[32] C. J. Sullivan, in *Ullmann's Encyclopedia of Industrial Chemistry*, Wiley-VCH Verlag GmbH & Co. KGaA, 2000.

[33] G. Luo, S. Yan, M. Qiao, J. Zhuang, and K. Fan, *Appl. Catal. A-Gen.*, 2004, **275**, 95-102.

[34] Y. Fan, C. Zhou and X. Zhu, *Catal. Rev. Sci. Eng.*, 2009, **51,** 293-324.

[35] B. Odell, G. Earlam, and D.J. Cole-Hamilton, *J. Organomet. Chem.* 1985, **290**, 241-248.

[36] G.C. Gunter, R.H. Langford, J.E. Jackson and D.J. Miller, *Ind. Eng. Chem. Res.*,1995, **34**, 974-980.

[37] L. J. Velenyi, Lyndhurst, and S. R. Dolhyj, **Us Patent 4,663,479.**

[38] B. Katryniok, S. Paul and F. Dumeignil, *Green Chem.*, 2010, **12**, 1910-1913.

[39] Ties J. Korstanje, Hendrik Kleijn, Johann T. B. H. Jastrzebski and Robertus J. M. Klein Gebbink, *Green Chem.,* 2013, 15, 982-985.

[40] T. Tsujino, Yokoyama and K. Matsuoka, ***Jpn. Patent* 56-19854**, 1981.

[41] T. Tsujino, S. Ohigashi, S. Sugiyama, K. Kawashiro, and H. Hayashi *J. of Mol. Catal.*, 1992, **71,** 25-35.

[42] M. Ai, *App. Catal. A: Gen.* 1997, **165**, 461-465.

[43] M. Ai and K. Ohdanr, *J. Mol.r Catal. A*: *Chem.*, 2000, **159**, 19-24.

[44] J. C. Vtdrine, J. M. M. Millet, and J. C. Volta, *Catal. Today,* 1996, **32,** 115-119.

[45] S. Sugiyama, N. Shigemoto, N. Masaoka, S. Suetoh, H. Kavami, K. Miyaura, H. Hayashi, *Bull. chem. Soc. Jpn.* 1993, **66**, 1542-1547.

[46] E. V. Ramos-Fernandez, N. J. Geels, N. R. Shiju and G. Rothenberg, *Green Chem.*, 2014, **16,** 3358-3363.

[47] T. Yasukawa, W. Ninomiya, K. Ooyachi, N. Aoki, and K. Mae, *Ind. Eng. Chem. Res*. 2011, **50,** 3858-3863.

[48] G. C. Gunter, D. J. Miller, and J. E. Jackson, *J. Catal*. 1994, **148**, 252-258.

[49] M. S. Tam, R. Craciun, D. J. Miller and J. E. Jackson, *Ind. Eng. Chem. Res*. 1998, **37,** 2360-2364.

[50] Fan, M. L.; Chao, Z. S.; Li, L. J.; Xie, S. J.; Qin, H. W.; Chen, J. W. Hunan Daxue Xuebao (J. Hunan Univ., Nat. Sci.) 2011, **38**, 58-61.

[51] M. Dusselier, P. V. Wouwe, A. Dewaele, E. Makshina, and B. F. Sels, *Energy Environ. Sci.***,** 2013, **6**, 1415-1442.

[52] C. Hammaecher, J. Paul, *J. Catal*., 2013, **300**, 174-182.

[53] C. Tang, Z. Zhai, X. Li, L. Sun, and W. Bai, *J. of Catal.* 2015, **329**, 206-217.

[54] C. Tang, J. Peng, X. Li, Z. Zhai, W. Bai, N. Jiang,H. Gao and Y. Liao, *Green Chem.*, 2015, **17,** 1159-1166.

[55] Z. Zhai, X. Li, C. Tang, J. Peng, N. Jiang, W. Bai, H. Gao and Y. Liao, *Ind. Eng. Chem. Res*., 2014, **53**, 10318-10327.

[56] C. Tanga, Z. Zhai, X. Li, L. Sun, and W. Bai, *J. of the Taiwan Inst. of Chem. Eng.*, 2015, **000**, 1-10.

[57] C. Tang, J. Peng, X. Li, Z. Zhai, H. Gao, W. Bai, N. Jiang, and Y. Liao, *Korean J. Chem. Eng*., 2015 DOI: 10.1007/s11814-015-0094-y.

[58] J. C. S. Ruiz and J. A. Dumesic, *Green Chem.*, 2009, **11,** 1101-1104.

[59] D. C. Rennard, P. J. Dauenhauer, S. A. Tupy and L. D. Schmidt, *Energy Fuels*, 2008, **22**, 1318-1327.

[60] P. Maki-Arvela, I. L. Simakova, T. Salmi and D. Y. Murzin, *Chem. Rev.*, 2014, **114**, 1909-1971.

[61] R. Auras, B. Harte, and S. Selke, *Macromol. Biosci.* 2004, **4**, 835-839.

[62] F. A. C. Martinez, E. M. Balciunas, J. M. Salgado, J. M. D. Gonzalez, A. Converti, R. P. de Souza Oliveira, *Trends in Food Science & Technology*, 2013, 30, 70-83.

[63] K. Weissermel, H. J. Arpe, *Industrial Organic Chemistry*; Wiley-VCH: Weinheim, 2003.

[64] Iea,bioenergy.task42-biorefineries.com

[65] Holmen, R. E. **US Patent 2859240**, 1958.

[66] R. A. Sawicki, **U.S. Pat. 4729978**, 1988.

[67] G. C. Gunter, R. Craciun, M. S. Tam, J. E. Jackson, and D. J. Miller *J. Catal*. 1996, **164**, 207-212.

[68] J. Zhang, Y. Zhao, M. Pan, X. Feng, W. Ji, and C.-T. Au, *ACS Catal*. 2011, **1,** 32-37.

[69] J. Zhang, Y. Zhao, X. Feng, M. Pan, J. Zhao, W. Ji, and C-T Au, *Catal. Sci. Technol.***,** 2014, **4**, 1376-1385.

[70] M. S. Tam, R. Craciun, J. E. Jackson, and D. J. Miller, *Ind. Eng. Chem. Res*. 1998, **37,** 2360-2365.

[71] D. C. Wadley, M. S. Tam, P. B. Kokitkar, J. E. Jackson and D. J. Miller, *J. Catal.* 1997, **165,** 162-171.

[72] M. S. Tam, R. Craciun, D. J. Miller and J. E. Jackson, *Ind. Eng. Chem. Res*., 1998, **37,** 2360-2366.

[73] E. Blanco, P. Delichere, J.M.M. Millet, and S. Loridant, *Catal. Today,* 2014, **226,** 185-192.

[74] E. Blanco, C. Lorentz, P. Delichere, L. Burel, M. Vrinat, J.M.M. Millet, and S. Loridant, *App. Catal. B: Env.l,* 2016, **18**, 596-606.

[75] G. Nafe, M.-A. Lopez-Martinez , M. Dyballa , M. Hunger , Y. Traa, Th. Hirth, and E. Klemm, *J. Catal.* 2015, **329,** 413-424.

[76] G. Nafe, Y. Traa, Th. Hirth, and E. Klemm, *Catal. Lett.* 2014, **144**, 1144-1150.

[77] L. Craciun, G. P. Benn, J. Dewing, G. W. Schriver, W. J. Peer, B. Siebenhaar and U. Siegrist, **US2010/0113822A1,** 2010.

[78] K. Omata, K. Matsumoto, T. Murayama, and W. Ueda, *Catal. Today*, 2015, **259**, 205-212.

[79] M. A. Lilga T. A. Werpy and J. E. Holladay, ***US patent* 2004/0110974A1**, 2004.

[80] X. Feng, B. Sun, Y. Yao, Q. Su, W. Ji, and C-T Au, *J. Catal*. 2014, **314,** 132-141.

[81] D. Yang, D. Li, H. Yao, G. Zhang, T. Jiao, Z. Li, C. Li, and S. Zhang, *Ind. Eng. Chem. Res.* 2015, **54**, 6865-6873.

[82] W-L Mok and M. J. Antal, *J. Org. Chem.* 1989**, 54,** 4596-4602.

[83] C. T.Lira and P. J. McCrackin, *J. Ind. Eng. Chem. Res.* 1993,**32**, 2608-2613.

[84] T. M. Aida, A. Ikarashi, Y. Saito, M.Watanabe, R. L. Smith Jr. and K. Arai, *J. Supercrit. Fluids*, 2009, **50,** 257-264.

[85] J. Zhang, J. Lin, X. Xu and P. Cen, *Chin. J. Chem. Eng*. 2008, **16,** 263-269.

[86] J. Zhang, J. Lin, P. Cen, *Can. J. Chem. Eng*. 2008, **86**, 1047-1053.

[87] Z. Zhang, Y. Qu, S. Wang, and J. Wang, *Ind. Eng. Chem. Res.* 2009, **48**, 9083-9089.

[88] G. Gunter, D.J. Miller and J.E. Jackson, *J. Catal.*, 1994, **148**, 252-260.

[89] C. Paparizos, S. R. Dolhyj, and W. G. Shaw, ***U.S. Pat.* 4786756**, 1988.

[90] J. V. Lingoes and D. I. Collias, **US 2013/0274514 A1.**

[91] C. Tang, J. Pen, G. Fan, X. Li, X. Pu and W. Bai, *Catal. Commun.*2014, **43,** 231-234.

[92] J. Peng, X. Li, C. Tang and W. Bai, *Green Chem*., 2014, **16**, 108-111.

[93] C. Tang, J. Peng, X. Li, Z. Zhai, N. Jiang, W. Bai, H. Gao and Y. Liao. *RSC Adv.*, 2014, **4**, 28875-28882.

[94] G. C. Gunter, R. H. Langford, J. E. Jackson and D. J. Miller, *Ind. Eng. Chem. Res.* 1995, **34**, 974-980.

[95] Y. Matsuura, A. Onda, S. Ogo, and K. Yanagisawa, *Catal. Today*, 2014, **226**, 192-197.

[96] H. J. Wang, D. H. Yu, P. Sun, J. Yan, Y. Wang, and H. Huang, *Catal. Commun*., 2008, **9**, 1799-1803.

[97] P. Sun, D. H. Yu, K. Fu, M. Gu, Y. Wang, H. Huang and H. Ying, *Catal. Commun.*, 2009, **10**, 1345-1349.

[98] P. Sun, D. Yu, Z. Tang, H. Li and H. Huang, *Ind. Eng. Chem. Res.* 2010**, 49**, 9082-9087.

[99] Y. Jie, Y. Dinghua, S. Peng, and H. He, *Chin. J. Catal.*, 2011, **32**, 405-411.

[100] J. Zhang, Y. Zhao, M. Pan, X. Feng, W. Ji, and C.-T. Au, *ACS Catal*. 2011, **1,** 32-37.

[101] J. Zhang, Y. Zhao, X. Feng, M. Pan, J. Zhao, W. Ji, and C-T Au, *Catal. Sci. Technol.***,** 2014, **4**, 1376-1385.

[102] B. Yan, L-Z. Tao, Y. Liang and B-Q. Xu, 2014, *Chem. Sus. Chem*, 2014, 7, 1568-1578.

[103] B. Wang, C. li, Q. Zhu and T. Tan, *RSC Adv.*, 2014, **4**, 45679-45686.

[104] X. Zhang, L. Lin, T. Zhang, H. Liu, and X. Zhang, *Chem. Eng. J.*, , 2015, http://dx.doi.org/10.1016/j.cej.2015.09.039.

[105] J-M Lee, D-W Hwang, Y. K. Hwang, S. B. Halligudi, J.-S. Chang, and Y-H Han, *Catal. Comm.*, 2010, **11,** 1176-1180.

[106] J. H. Hong, J-M Lee, H. Kim, Y. K. Hwang, J-S Chang, S. B. Halligudi, and Y-H Han, *App. Catal. A: Gen.*, 2011, **396,** 194-200.

[107] A. Onda, Y. Mastuura, and K. Yanagisawa, **US2012/0277467 A1**, 2012.

[108] Y. Matsuura, A. Onda, and K. Yanagisawa, *Catal. Comm.*, 2014, **48,** 5-10.

[109] B. Yan, L-Z. Tao, Y. Liang, and B-Q Xu, *ACS Catal.* 2014, **4**, 1931-1943.

[110] T. Tsuchida, J. Kubo, T. Yoshioka, S. Sakuma, T. Takeguchi and W. Ueda, *J. Catal.*, 2008, **259**, 183-89.

[111] C. L. Kibby and W. K. Hall, *J. Catal.*, 1973, **31**, 65-73.

[112] J. A. S. Bett and W. K. Hall, *J. Catal.*, 1968, **10**, 105-113..

[113] A. K. Lynn and W. Bonfield, *Acc. Chem. Res*. 2005, **38**, 202-207.

[114] S. V. Dorozhkin, *J. Mater.* Sc. 1975**, 2**, 2045-2050.

[115] A. K. Lynn, R. E. Cameron, S. M. Best, R. A. Brooks, N. Rushton, and W. Bonfield, *Key Eng. Mater*. 2004, **254-256,** 593-596.

[116] a)H.-K. Ea, C. Nguyen, D. Bazin, A. Bianchi, J. Guicheux, P. Reboul, M. Daudon, and F. Liote, *Arthritis Rheum.* 2011, **63**, 10-15.; b) A. C. Jones, A. J. Chuck, E. A. Arie, D. J. Green, M. Doherty, *Semin. Arthritis Rheum.* 1992, ***22***, 188-202.

Chapter 2

Catalytic Dehydration of Lactic Acid to Acrylic Acid Using Calcium Hydroxyapatite Catalysts

Abstract

A series of calcium hydroxyapatite (HAP) catalysts were synthesised with a Ca/P ratio ranging from 1.3 to 1.89 by a co-precipitation method that involved changing the pH of the calcium and phosphorous precursors. The physicochemical characterization by XRD, SEM, BET surface area and CO_2 and NH_3-TPD techniques confirmed the hydroxyapatite formation. These HAP catalysts were used for the vapour phase dehydration of lactic acid to acrylic acid. The HAP catalyst with a Ca/P ratio of 1.3 was found to be the most efficient catalyst among the synthesised series, which gave 100% conversion of lactic acid and 60% selectivity towards acrylic acid at 375 °C when a 50% (w/w) aqueous solution of lactic acid was used. The higher selectivity towards acrylic acid has been correlated to the increased acidity and reduced basicity of the HAP catalyst with a Ca/P ratio of 1.3 compared to the other HAP catalysts. The catalyst was found to be very stable and no deactivation was observed even after 300 h of reaction time. *In situ* FTIR studies were performed for understanding the mechanistic aspects and showed the formation of calcium lactate as an intermediate species during the dehydration of lactic acid to acrylic acid.

2.1 Introduction

Utilization of renewable feedstock (biomass) as a raw material for synthesis of fine chemicals is of the utmost importance as the world is facing dual problems of depleting fossil fuel resources and environmental concerns about current processes.[1] The major advantages of using a biomass-derived feedstock is the high content of oxygenated groups (e.g., -OH, -C=O and -COOH) leading to high reactivity, low volatility and high solubility in water. Hence, aqueous phase processing of the feedstock is also a major/added advantage.

Lactic acid is one of the attractive renewable feedstocks obtained by biomass fermentation. It contains multiple reactive functionalities and is considered as one of the most promising building blocks for the future growth of chemical industry based on renewable raw materials. A number of value added commodity chemicals, like acrylic acid, 2,3-pentanedione, pyruvic acid, 1,2-propanediol and ethyl lactate, can be obtained from lactic acid.[2] Ruiz and Dumesic[3] have demonstrated the use of a Pt(0.1%)/Nb_2O_5 catalyst for the efficient conversion of lactic acid to various valuable chemicals (propionic acid and C_4-C_7 ketones), which can be used for the production of high energy-density liquid fuels (C_4-C_7 alcohols).

Acrylic acid, an important starting material for the polymer industry, can be produced by the dehydration of lactic acid. A major derivative of acrylic acid (2-propenoic acid) is used exclusively to make acrylates and other derivatives. Glacial acrylic acid is used in super absorbent polymers. Acrylic acid is conventionally produced from non-renewable sources, such as propane and propylene. Hence, the production of acrylic acid from bio-derived lactic acid, a renewable source, is highly desired.[2]

The conversion of lactic acid and lactates to acrylic acid, acrylates and other products over silica and aluminium salts (sulfate, nitrate, phosphate, *etc*.) and mixtures of inorganic salts has been reported by Holmen.[4] Various phosphate-based catalysts, like sodium dihydrogen phosphate (NaH_2PO_4), $Ca_3(PO_4)_2$ supported on silica, silica/alumina,[5] aluminium phosphate[6] and Na_2HPO_4 in supercritical water,[7] have been used for lactic acid dehydration. NaY modified with potassium nitrate, lanthanum oxide and alkali phosphates, as well as various alkali earth metals (Ca, Mg, Sr, Ba, *etc*.), have also been reported for lactic acid

dehydration.[8] Furthermore Miller *et al.*[9] have investigated the activity of alkali metal salts supported on low surface area silica–alumina for lactic acid dehydration. The use of supercritical water for the conversion of lactic acid to acrylic acid has been systematically studied in the literature and three primary reaction pathways were proposed in supercritical water: (i) decarbonylation to acetaldehyde, CO and water, (ii) decarboxylation to acetaldehyde, CO_2 and H_2, (iii) dehydration to acrylic acid.[10,11] Acrylic acid has also been synthesized from lactic acid and acetic acid with a high consumption of acetic acid.[12] Wadley and co-workers have shown, by experimental design, that the highest yield and selectivity for 2,3-pentanedione was favourable at low temperature, elevated pressure and long contact times, while the yield and selectivity to acrylic acid were most favourable at high temperature, low pressure and short contact times when sodium nitrate supported on porous silica was used as catalysts.[13] Lactic acid dehydration has been also reported using calcium sulphate with cupric sulphate and phosphate as the promoter and CO_2 as the carrier gas.[14] Acrylic acid has also been prepared from 3-hydroxypropanoic acid using metal oxides, such as Al_2O_3, SiO_2 and TiO_2.[15]

Most of the previous studies illustrated that metal phosphates, mainly with alkali and alkaline earth metals, were effective catalysts for the dehydration of lactic acid to acrylic acid. However, previously a lower concentration of lactic acid (20-30% aqueous solution) has been used, which led to lower conversions as well as lower acrylic acid selectivity and in turn a lower per pass yield of acrylic acid. Mainly catalysts with mild acidity or mild basicity have been used for lactic acid dehydration in earlier work. Calcium hydroxyapatite (HAP) contains both weak acidic and weak basic sites in a single crystal and hence it is expected to be an efficient catalyst for dehydration.[16] Our group has successfully prepared HAP previously and tested it for clinical applications in the human body as a submerged tooth root implant.[17] HAP has been used as a catalyst for the dehydrogenation reaction of alcohols, as well as for the hydrogen transfer reactions of alcohols to ketones.[16] In stoichiometric HAP, an oxygen atom of the free -OH group is coordinated to three calcium cations, which are connected to each other to form a triangle. In nonstoichiometric HAP, one -OH group is missing per cation, creating a defect in order to maintain an overall charge balance, leading to a negative charge deficiency in a triangle. Such negative charge deficiencies exhibit Lewis type acidity eqn (2.1). When a water molecule replaces the missing -OH group, as in eqn (2.2), the electron

pair of the water oxygen becomes delocalized to fill the orbitals of the cations in the triangles. This polarization leads to the generation of Bronsted acidity due to the protons of the water molecules.[18] We have made an effort to use these properties of HAP for the vapour phase dehydration of lactic acid to acrylic acid and the results are reported herein.

$$Ca_{10-z}(HPO_4)_z(PO_4)_{6-z}(OH)_{2-z} \quad (2.1)$$

$$Ca_{10-z}(HPO_4)_z(PO_4)_{6-z}(OH)_{2-z}(H_2O)_z \quad 0< z \leq 1 \quad (2.2)$$

2.2 Experimental section

2.2.1 Materials

Calcium nitrate, diammonium hydrogen phosphate and ammonia solution were obtained from Thomas Baker chemicals India Ltd. Lactic acid (89%) from our CSIR-National Chemical Laboratory (CSIR-NCL) Pune pilot plant was obtained from a sugarcane fermentation process (process developed by CSIR-NCL).

2.2.2 Catalyst preparation method

Hydroxyapatite (HAP) was synthesized by a co-precipitation method as reported by Dongare *et al.*[17] In a typical synthesis, the required amount of calcium nitrate tetrahydrate and diammonium hydrogen phosphate were separately dissolved in deionized water. Ammonium hydroxide solution (25%) was added to both the solutions until the required pH was achieved. The calcium nitrate solution was added drop wise to the diammonium hydrogen phosphate solution with constant stirring. A thick white precipitate was obtained, which was filtered, washed with sufficient amount of water and dried at 120 °C for 16 h. The oven dried solid was calcined in air in a muffle furnace at 600 °C for 4 h.

2.2.3 Catalyst characterization

The X-ray diffraction analysis was carried out using a Rigaku X-ray diffractometer (Model DMAX IIIVC) with Cu-Kα radiation.

FTIR measurements were carried out using Shimadzu 8300 with KBr pellets in the range of 4000-400 cm^{-1} with 4 cm^{-1} resolution.

The BET surface area was determined using a NOVA 1200 Quanta chrome instrument. Prior to N_2 adsorption, the sample was evacuated at 200 °C.

Temperature programmed desorption of ammonia (NH_3-TPD) and CO_2 (CO_2-TPD) was carried out using a Micromeritics Autocue 2910. For TPD measurements 0.1 g of the catalyst sample was used. The sample was dehydrated at 600 °C for 1 h in a 50 mL min^{-1} helium flow and then cooled to 100 °C. Probe gas (5% NH_3 in helium for acidic sites and 10% CO_2 in helium for basic sites) was then adsorbed for 1 h in a 50 mL min^{-1} flow. The temperature was raised to 750 °C at a rate of 10 °C min^{-1} in a 30 mL min^{-1} helium flow.

To study the morphological appearance of the samples, scanning electron microscopy (SEM) was performed on a Leica Stereoscan-440 instrument equipped with a Phoenix EDAX attachment operated at 20 kV.

2.2.4 Catalyst activity test

Vapour phase dehydration of lactic acid to acrylic acid was carried out using a quartz fixed bed down flow reactor (id-11 mm) at atmospheric pressure. In the experiment, the catalyst with a particle size 20-40 mesh was charged in the middle section of the reactor with quartz wool packed at both ends. Porcelain beads were placed above the catalyst bed in order to vaporize the feed. Before catalytic evaluation, the catalyst was pre-heated at the required reaction temperature for 30 min under a flow of nitrogen (15 mL min^{-1}). The reaction temperature was measured by a thermocouple inserted in the catalyst bed. Lactic acid, of the required concentration (typically 50% w/w in water), was pumped into the pre-heating zone of the reactor using a peristaltic pump and nitrogen gas as the carrier. The reaction products were collected in a cold trap at 8 °C. The reaction mixture was analyzed using gas chromatography (Perkin Elimer) equipped with a FFAP capillary column (50 M × 0.320 mM) and FID detector. The GC was calibrated by external standard method. The amount of CO_x (CO and CO_2) was estimated based on the yield of acetaldehyde and propionic acid. The mass balance for all the reaction was more than 95%.

2.3 Results and discussion

2.3.1 EDAX analysis for Ca/P

All the catalysts were prepared by a co-precipitation method (Table 2.1). The precursor quantities corresponding to the required Ca/P ratio (1.5, 1.65 and 1.9) were taken for synthesis. The formation of HAP is represented in eqn (2.3). Factors like pH, temperature and stirring time are known to influence the morphology, crystallinity and surface area of HAPs. In particular, the pH of the solution is a very important parameter for controlling the Ca/P ratio in the final HAP catalyst. However, after changing the pH (7, 10 and 12) the actual Ca/P ratio obtained was estimated by EDAX analysis (Table 2.1). In this case the pH of the solution was gradually decreased from 12 to 7. At pH 12 catalyst HAP-1 was obtained with a Ca/P ratio of 1.85, whereas at pH 10 and 7, HAP-2 and HAP-3 were obtained with Ca/P ratios of 1.56 and 1.3, respectively. The catalysts were characterized by various physicochemical methods.

$$10Ca(NO_3)_2.4H_2O + 6(NH_4)_2HPO_4 + 8NH_4OH \rightarrow Ca_{10}(PO_4)_6(OH)_2 + 20\ NH_4NO_3 + 20H_2O \quad \text{eq. (2.3)}$$

2.3.2 The powder X-ray diffraction studies

The powder X-ray diffraction (XRD) patterns of the synthesized catalysts are shown in Fig. 2.1. The XRD pattern showed that the synthesized catalysts are crystalline in nature. The three most intense peaks located at 2θ ≈ 31.7° (2 1 1) - 100%, 32.95° (3 0 0) - 62.8%, and 32.2° (1 1 2) - 51.3% and other low intensity reflections are in good agreement with the reference data for $Ca_{10}(PO_4)_6(OH)_2$ [PDF 34-0010]. Although the crystallinity of all the catalysts was similar, a change in the crystallite size was observed (Fig. 2.1)[19] as evident from the broadening of the XRD peaks (the intense peak at 2θ ≈ 32.9°). The smaller crystallite size of HAP-1 may be due to the decrease in the crystal growth with the increase in the pH and was confirmed using Scherrer's formula. The crystal size was calculated from Scherrer's formula (Table 2.1) and it showed the gradual increase in the crystallite size for HAP-1 to HAP-3 from 107 to 171 nm, respectively. Similar observations were also reported and explained in the literature, confirming that the synthesized powders were hydroxyapatite.[16a]

The XRD spectrum also contains a noisy background which could be due to the glassy phosphate matrix.[20]

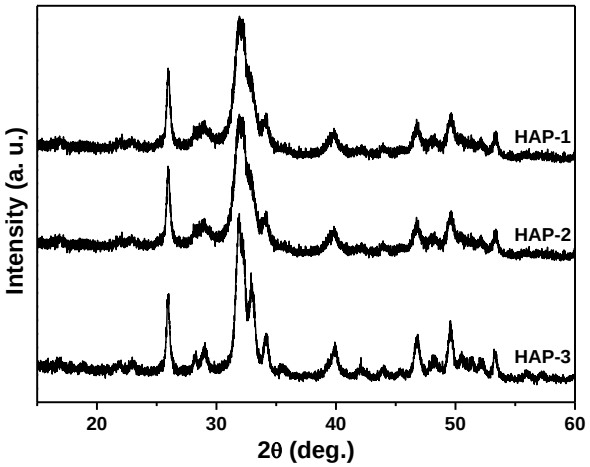

Fig. 2.1 X-Ray diffraction patterns of HAP with different Ca/P ratios.

2.3.3 FTIR spectroscopy studies

The synthesized catalysts were also characterized by FTIR spectroscopy (Fig. 2.2). The FTIR spectra showed a broad band at about 1000-1105 cm^{-1} indicating the formation of HAP. Bands at 1042 and 1094 cm^{-1} were observed due to the factor group splitting of the γ_3 fundamental vibrational mode of the tetrahedral PO_4^{3-}. The bands observed at 960 cm^{-1} and at 565 cm^{-1} correspond to the γ_1 and γ_4 symmetric P-O stretching vibrations of the PO_4^{3-} ion, respectively. The bands assigned to the stretching modes of the hydroxyl groups (-OH) in the HAP were observed in the spectra at 3570 cm^{-1} (strong) and 632 cm^{-1}. This confirms the formation of HAP.[21]

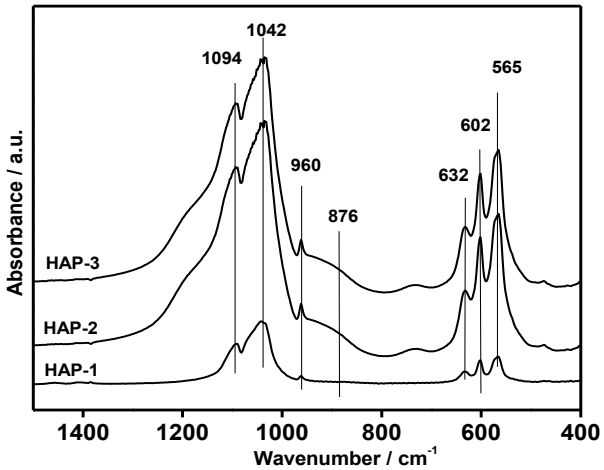

Fig. 2.2 FTIR spectra of HAP-1 HAP-2, HAP-3.

2.3.4 Scanning electron microscopy (SEM)

The catalyst morphology was studied using scanning electron microscopy (SEM) and the images are shown in Fig. 2.3. HAP-1 and HAP-2 (with Ca/P ratios ≥1.56) were prepared at higher pH and showed smaller particle sizes, whereas HAP-3, with a Ca/P ratio of 1.3, prepared at a lower pH showed an elongated rod-shaped highly crystalline material which is in agreement with the XRD pattern and particle size calculated using the Scherrer formula. The difference in shape may be due to precipitation of tabular brushite ($CaHPO_4 \cdot 2H_2O$) as a precursor at low pH, which gradually transformed to a HAP structure with an increase in pH.[16a]

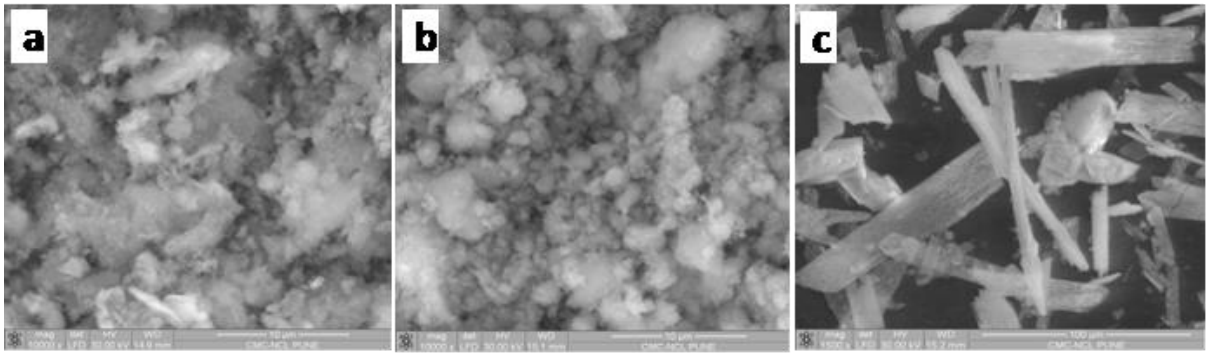

Fig. 2.3 SEM images of a) HAP-1, b) HAP-2, c) HAP-3.

2.3.5 Temperature programmed desorption studies

The temperature programmed desorption (TPD) of NH_3 and CO_2 was carried out to evaluate the total acidity and basicity of the synthesized hydroxyapatite (Table 2.1). Phosphate groups in HAP are responsible for the acidity of the catalyst, whereas the Ca^{2+} ions are responsible for the basicity. Hence an increase in the basicity and a decrease in the acidity was observed as expected, with an increase in the Ca/P ratio, as shown in Fig. 2.4.[16a,18] With a decrease in the Ca/P ratio from 1.85 (HAP-1) to 1.3 (HAP-3), an increase in the concentration as well as the strength of the acidity was observed.

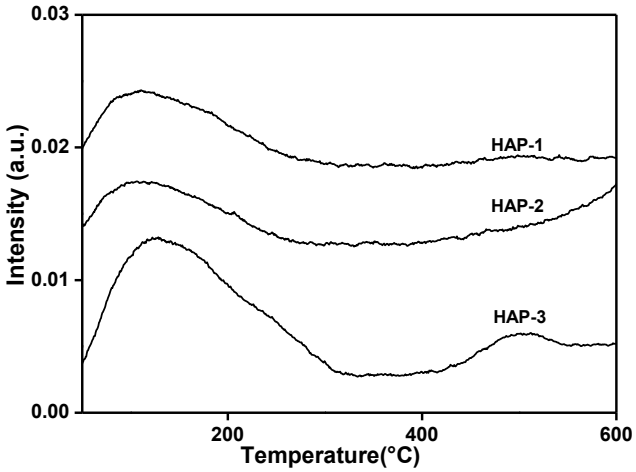

Fig. 2.4 NH3 TPD profiles for HAP-1, HAP-2 and HAP-3.

2.3.6 Textural characterization

The surface area of all the catalysts determined using the BET method showed an increase in surface area with an increase in the pH due to a decrease in crystal size (Table 2.1).

Table 2.1 Textural characterization, acidity and basicity of catalyst[a]

Catalyst Name	**Ca/P molar ratio**	**Crystal size[b] (nm)**	**pH of solution**	**Surface area, (m^2 g^{-1})**	**CO_2 desorbed, (µmol g^{-1})**	**NH_3 desorbed, (µmol g^{-1})**	**Selectivity toward acrylic acid (%)**
HAP-1	1.89	107	12	49	10.12	103	50
HAP-2	1.56	121	10	29	1.02	125	55
HAP-3	1.3	171	7	25	0.624	131	60

[a] Reaction conditions: lactic acid - 50% (w/w) in water, WHSV - 3 h^{-1}, temperature - 375 °C, carrier gas - N_2, carrier gas flow - 15 mL min^{-1}, Lactic acid conversion 100 %. [b] Crystal size calculated from Scherrer's formula.

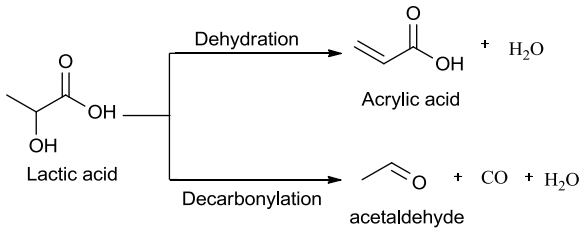

Scheme 2.1 General dehydration and decarbonylation scheme for lactic acid to acrylic acid.

2.4 Catalytic activity

2.4.1 Influence of Ca/P ratio on the dehydration of lactic acid to acrylic acid

The catalytic activities of the synthesized HAP's were tested for the vapour phase dehydration of lactic acid (Scheme 2.1) using a down flow reactor and the results are given in Table 2.1. The reaction was carried out at 375 °C using a 50% (w/w) aqueous solution of lactic acid and a WHSV of 3 h^{-1} using all the prepared catalysts. Surprisingly, 100% lactic acid conversion was obtained with all the HAP catalysts, though a difference in the acrylic acid selectivity was observed. With a decrease in the Ca/P ratio, an increase in the acrylic acid selectivity was observed, with a maximum 60% selectivity for acrylic acid when HAP-3 was used. This can be correlated to the acidic/basic properties of the catalysts. With an increase in the Ca/P ratio from 1.3 (HAP-3) to 1.85 (HAP-1) a decrease in the acidity was observed. Hence, the high selectivity for acrylic acid obtained with HAP-3 can be attributed to the higher acidity, which is in agreement with the literature reports.[22] The rate of dehydration can be correlated to the calcium deficiency and increasing concentration of surface P-OH groups.[16c]

2.4.2 Effect of temperature

The influence of the reaction temperature on lactic acid dehydration was studied in the range of 325-400 °C (Table 2.2, entry 1) using HAP-3, as it showed the maximum selectivity for acrylic acid. When the reaction temperature was gradually increased from 325 to 400 °C, the lactic acid conversion increased correspondingly from 60 to 100%, with a marginal increase in the acrylic acid selectivity from 57 to 60% up to 375 °C. However, the selectivity decreased to 54% with a further increase in the temperature to 400 °C, with a corresponding increase in the acetaldehyde selectivity (21.6%).

Table 2.2 Influence of reaction parameters on lactic acid dehydration[a]

Entry	Reaction parameters		Conversion (%)	% Selectivity		
				Acrylic acid	Acetaldehyde	Other products[e]
1	Temp.[b] (°C)	325	60	57	18.9	5.2
		350	90	59	18	5
		375	100	60	17.2	5.6
		400	100	54	21.6	2.6
2	WHSV[c] (h^{-1})	3	100	60	17.2	5.6
		4	85	56	19.2	5.6
		5	75	50	22	6
3	LA conc.[d]	50	100	60	17.2	5.6
	(w/w%)	60	91	59	18.8	3.4
		70	85	57	19.2	4.6
		80	70	57	19.2	4.6

Reaction conditions: [a] Catalyst- HAP-3, carrier gas- N_2, carrier gas flow-15 mL min^{-1} [b] WHSV- 3h^{-1}, Lactic acid conc.- 50%(w/w) [c] Lactic acid conc.- 50% (w/w), Temp- 375 °C [d] Temp- 375 °C and WHSV- 3h^{-1}, [e] Propionic acid, 2,3-pentanedione.

2.4.3 Effect of residence time on conversion and selectivity

The influence of the WHSV on reaction performance was studied under optimized reaction conditions using HAP-3 as the catalyst and the results are given in Table 2.2 (entry 2). The lactic acid feed was varied from 12 to 20 mL h^{-1} (corresponding to WHSV = 3-5 h^{-1} respectively) at 375 °C by keeping the other reaction conditions constant. When WHSV was gradually increased from 3 to 5 h^{-1}, a decrease in lactic acid conversion from 100 to 75% was observed, as expected, with a decrease in the acrylic acid selectivity from 60 to 50%, indicating that the WHSV of 3 h^{-1} with a corresponding contact time of 1.196 s provides the optimum residence time for dehydration, leading to minimum by-product formation.

2.4.4 Effect of lactic acid concentration

The effect of lactic acid concentration on reaction performance was studied using HAP-3 as catalyst and the results are presented in Table 2.2 (entry 3). With an increase in the lactic acid concentration from 50 to 80 wt% (wt/wt aqueous solution), a decrease in lactic acid conversion from 100 to 70% was observed; with a marginal decrease in acrylic acid selectivity from 60 to 57%. The rate of lactic acid self-polymerization is low at low lactic acid concentration and a better efficiency is expected for the target reaction. The sum of the selectivities in Table 2.2 are less than 100%, as the remaining selectivity is for gaseous product (CO/CO_2) formation as well as some escaped acetaldehyde in gaseous form. No other unknown products were observed in GC analysis.

The stability of the catalyst with time on stream was studied at 375 °C over HAP-3 (WHSV = 3 h^{-1} and lactic acid concentration = 50 wt%) for 300 h and there was no considerable decrease in the lactic acid conversion and acrylic acid selectivity. After 300 h, the conversion remained constant (100%) with a marginal decrease in acrylic acid selectivity from 60% to 57%. This proves the stability of hydroxyapatite catalyst under the reaction conditions.

The acrylic acid yield reported in the literature by lactic acid dehydration varies between 40-56%, with the main use of lower lactic acid concentrations (≤ 25% aqueous solution) in the range of 300-400 °C. Whereas, the results obtained in the present study, for lactic acid dehydration to acrylic acid, are better than the previously reported studies in the literature with 100% conversion and 60% acrylic acid selectivity. Especially the use of high concentration of lactic acid (≥50% aqueous solution) and very high WHSV as well as catalyst stability even up to 300 h are the major advantages of the present studies.

2.5 *In situ* FTIR studies

Zhang *et al*.[23] has studied the different pathways for lactic acid conversion to acrylic acid by dehydration, as well as decarbonylation and decarboxylation to acetaldehyde by DFT studies using sodium polyphosphate as catalyst. In the case of dehydration, the first step has been shown to be phosphate ester formation by elimination of protons from the hydroxyl group (-OH) of the lactic acid and the hydroxyl of phosphate group (-POH) of the catalyst,

which further led to the formation of acrylic acid by decomposition of the phosphate ester formed in the previous step. However, in the case of decarbonylation, the first step is the formation of a phosphate ester *via* elimination of the carboxylic -OH (-COOH) group of lactic acid and the proton of the -POH group of the catalyst. In the second step, acetaldehyde and CO are formed *via* decomposition of the phosphate ester. Though the formation of the phosphate ester is the first step and the decomposition of the phosphate ester is second step in dehydration, as well as decarbonylation, in the case of dehydration, the ester formation involves the hydroxyl group and decarbonylation involves the carboxylic group of lactic acid. To check the possibility of calcium lactate formation and, if the same mechanism holds true, for lactic acid dehydration using HAP catalysts, lactic acid was adsorbed on HAP-3 at room temperature and physisorbed lactic acid was removed by drying the catalyst at room temperature for 8 h and the FTIR spectrum was recorded. Further, the adsorbed lactic acid was desorbed at various temperatures from 50-200 °C. Fig. 2.5 shows the subtraction spectra of adsorbed lactic acid on HAP-3 and neat HAP-3. The spectrum was compared with authentic lactic acid and calcium lactate from the FTIR database. The spectrum clearly showed the formation of calcium lactate. The IR band for the carboxylic -OH group of lactic acid at 3373 cm^{-1} disappears and there is a considerable shift in the carbonyl (C=O) frequency of the carboxylic group from 1732 to 1604 cm^{-1}, indicating strong interaction of the carboxylic group with the calcium of HAP. The carbonyl stretching frequency of calcium lactate is observed at 1578 cm^{-1}. The presence of an additional carbonyl band at 1755 cm^{-1} matched well with the carbonyl frequency of free lactic acid (1754 cm^{-1}), suggesting that not all the lactic acid has formed calcium lactate. This indicates that due to calcium lactate formation, the carboxylic group of lactic acid is protected and hence decarbonylation is not possible as per the mechanism suggested by Zhang *et al*. by DFT studies, leading to very high selectivity for acrylic acid in the present case. Miller *et al*.[9] have also previously reported the formation of alkali lactates by interaction of lactic acid with the alkali metal of the catalysts when alkali metal salts supported on silica–alumina was used for lactic acid dehydration and concluded that the formation of alkali lactates was crucial for acrylic acid formation. The part of lactic acid which does not form calcium lactate on HAP may form acetaldehyde by the decarbonylation route. Hence, the mechanism of lactic acid dehydration on HAP can be explained as follows.

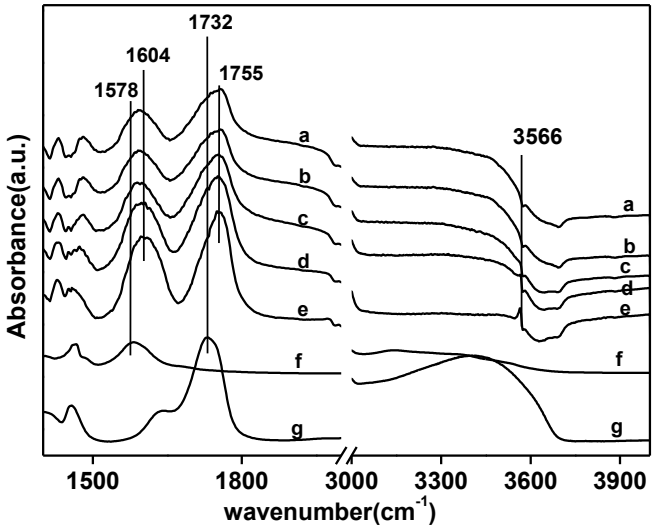

Fig. 2.5 FTIR difference spectra of lactic acid adsorbed on HAP-3 at room temperature and desorbed at (a) room temperature (b) 50 °C, (c) 100 °C, (d) 150 °C, (e) 200 °C. FTIR spectrum of (f) calcium lactate (g) lactic acid from FTIR database.

The lactic acid was dissociatively adsorbed on HAP as lactate on the Ca site and the carboxylic proton on phosphate oxygen (Scheme 2.2). Formation of lactate salt results in the protection of the carboxylic group avoiding decarbonylation and decarboxylation to acetaldehyde. Dissociative adsorption of lactic acid results in the formation of stable hydrogen phosphate groups which shows Bronsted acidity and forms phosphate ester with hydroxyl proton of lactic acid by dehydration. In next step this phosphate ester further decomposes to form acrylic acid. In HAP, the Ca-O distance is reported to be 0.239 and 0.240 nm due to this it can trap hydrogen. β-Tricalcium phosphate (TCP) has PO_4^{3-} ions, as in HAP; however, it cannot take a nonstoichiometric form and trap hydrogen as HPO_4^{2-}, hence TCP does not show good activity for lactic acid dehydration.[16a] However, *in situ* FTIR studies have shown the appearance of an -OH group at 3566 cm^{-1} during the reaction, which is assigned to the P-OH group. This clearly confirms the formation of phosphate -OH, leading to the generation of *in situ* Bronsted acidity. During decarbonylation, dissociative adsorption of lactic acid takes place on HAP (Scheme 2.3), where the hydroxyl group becomes adsorbed on calcium, forming a C-O-Ca bond and the hydroxyl proton gets abstracted by phosphate oxygen forming HPO_4^{2-}, which further reacts with the carboxylic -OH group to form the phosphate ester. This phosphate ester decomposed in the next step to give acetaldehyde and carbon monoxide.

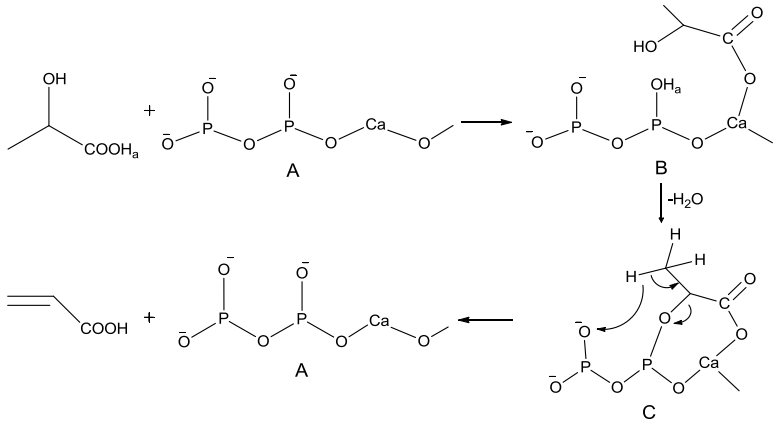

Scheme 2.2 Proposed mechanism for lactic acid dehydration using HAP

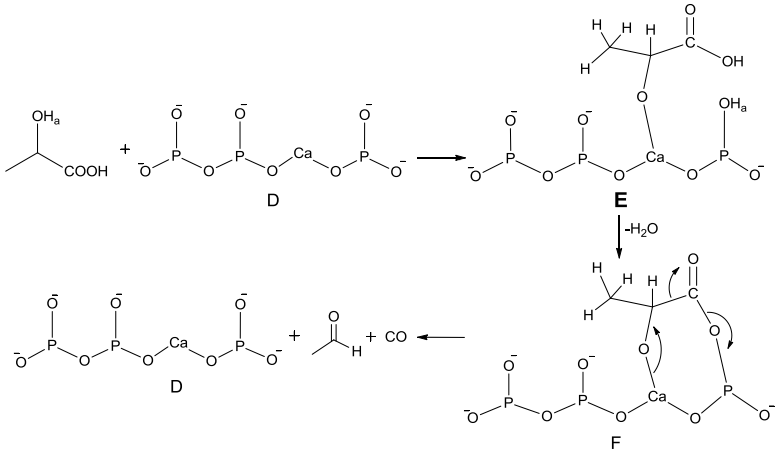

Scheme 2.3 Proposed mechanism for lactic acid decarbonylation using HAP

2.6 Conclusions

Calcium hydroxyapatites (HAP) with various Ca/P ratios, ranging from 1.3-1.85, could be synthesized by varying the pH of the reactants. The HAP with a Ca/P ratio of 1.3 has shown a very high efficiency for vapour phase dehydration of lactic acid to acrylic acid with 100% conversion and 60% selectivity for acrylic acid at 375 °C and 50% lactic acid concentration. The higher selectivity for acrylic acid may be correlated to the synergistic effect of the higher acid site density with the lower basic site density of HAP with a Ca/P ratio of 1.3. *In situ* FTIR studies showed the formation of calcium lactate as an intermediate species which favours the dehydration of lactic acid to acrylic acid, avoiding decarbonylation to acetaldehyde.

2.7 References

[1] A. Corma, S. Iborra and A. Velty, *Chem. Rev.,* 2007, **107**, 2411-2502.

[2] Y. Fan, C. Zhou and X. Zhu, *Catal. Rev. Sci. Eng.*, 2009, **51**,293-324.

[3] 3. J. C. S. Ruiz and J. A. Dumesic, *Green Chem.,* 2009, **11**, 1101-1104.

[4] R. E. Holmen, *U.S. Pat.,* **2859240**, 1958.

[5] (a) R. A. Sawicki, *U.S. Pat*., **4729978**, 1988; (b) J. Wang, Z. Zhang', Y. Qu and S. Wang, *Ind. Eng. Chem. Res.*, 2009, **48**, 9083-9089; (c) J.-M. Lee, D.-W. Hwang, Y. K. Hwang, S. B. Halligudi, J.-S. Chang and Y.-H. Han, *Catal. Commun.*, 2010, **11**, 1176-1180.

[6] C. Paparizos, S. R. Dolhyj, W. G. Shaw, *U.S. Pat.* **4786756**, 1988.

[7] C. T. Lira and P. J. McCrackin, *Ind. Eng. Chem. Res*., 1993, **32**, 2608-2613.

[8] (a) H. J. Wang, D. H. Yu, P. Sun, J. Yan, Y. Wang and H. Huang, *Catal. Commun.,* 2008, **9,** 1799-1803; (b) P. Sun, D. H. Yu, K. Fu, M. Gu, Y. Wang, H. Huang and H. Ying, *Catal. Commun.,* 2009, **10**, 1345-1349; (c) Y. Jie, Y. Dinghua, L. Heng, S. Peng and H. He, *J. Rare Earths,* 2010, **28**, 803-806; (d) Y. Jie, Y. Dinghua, S. Peng and H. He, *Chin. J. Catal.*, 2011, **32**, 405-411; (e) J. Zhang, Y. Zhao, M. Pan, X. Feng, W. Ji and C.-T. Au, *ACS Catal.*, 2011, **1**, 32-41.

[9] (a) G. C. Gunter, D. J. Miller and J. E. Jackson, *J. Catal.,* 1994, **148**, 252-260; (b) G. C. Gunter, R. H. Langford, J. E. Jackson and D. J. Miller, *Ind. Eng. Chem. Res.,* 1995, **34,** 974-980; (c) M. S. Tam, G. C. Gunter, R. Craciun, D. J. Miller and J. E. Jackson, *Ind. Eng. Chem. Res*., 1997**, 36,** 3505-3512; (d) M. S. Tam, R. Craciun, D. J. Miller and J. E. Jackson, *Ind. Eng. Chem. Res*., 1998, **37**, 2360-2366; (e) M. S. Tam, J. E. Jackson and D. J. Miller, *Ind. Eng. Chem. Res.*, 1999, **38,** 3873-3877.

[10] T. M. Aida, A. Ikarashi, Y. Saito, M. Watanabe, R. L. Smith Jr. and K. Arai, *J. Supercrit. Fluids,* 2009, **50**, 257-264.

[11] W. S. L. Mok and M. J. Antal Jr., *J. Org. Chem.,* 1989, **54**, 4596-4602.

[12] J. E. Holladay, M. A. Lilga and T. A. Werpy, *US Pat*., **0110974A1**, 2004.

[13] D. C. Wadley, M. S. Tam, P. B. Kokitkar, J. E. Jackson and D. J. Miller, *J. Catal*., 1997, **165**, 162-171.

[14] J. Zhang, J. Lin and P. *Cen, Can. J. Chem. Eng.*, 2008, **86**, 1047-1053.

[15] L. Craciun, G. P. Benn, J. Dewing, G. W. Schriver, W. J. Peer, B. Siebenhaar and U.

Siegrist, *US Pat.,* **2005222458**, 2005.

[16] (a) T. Tsuchida, J. Kubo, T. Yoshioka, S. Sakuma, T. Takeguchi and W. Ueda, *J. Catal.*, 2008, **259**, 183-189; (b) C. L. Kibby and W. K. Hall, *J. Catal.*, 1973, **31**, 65-73; (c) J. A. S. Bett and W. K. Hall, *J. Catal.*, 1968, **10**, 105-113.

[17] M. K. Dongare, A. P. B. Sinha and P. Singh, *T.I B. & A. O.*, 190, **4**, 69-73.

[18] S. J. Joris and C. H. Amberg, *J. Phys. Chem.*, 1971, **76**, 3171-3167.

[19] T. Tsuchida, J. Kubo, T. Yoshioka, S. Sakuma, T. Takeguchi and W. Ueda, *J. Jpn. Pet. Inst.*, 2009, **52**, 51-59.

[20] (a) A. R. Kmita, C. Paluszkiewicz, A. Slosarczyk and Z. Paszkiewicz, *J. Mol. Struct.*, 2005, **744-747**, 653-656; (b) A. Beganskiene, O. Dudko, R. Sirutkaitis and R. Giraitis, *Mater. Sci*., 2003, **9**, 383-386.

[21] I. Bogdanoviciene, A. Beganskiene, K. Tonsuaadu, J. Glaser, H.-J. Meyer and A. Kareiva, *Mater. Res. Bull.*, 2006, **41**, 1754-1762.

[22] T. Tsuchida, S. Sakuma, T. Takeguchi and W. Ueda, *Ind. Eng. Chem. Res*., 2006, **45**, 8634-8642.

[23] Z. Zhang, Y. Qu, S. Wang and J. Wang, *J. Mol. Catal. A: Chem*., 2010, **323,** 91-100.

Chapter 3

Nonstoichiometric Calcium Pyrophosphate: Highly Efficient and Selective Catalyst for Dehydration of Lactic Acid to Acrylic Acid

Abstract

Calcium phosphate catalysts were prepared by co-precipitation method using calcium nitrate and mixture of ammonium and different sodium phosphates as calcium and phosphate precursors respectively. Depending on the phosphate precursor the pH of the synthesis mixture changed during the catalyst precipitation. The catalysts characterisation by XRD and ICP revealed the formation of calcium pyrophosphate structure with varying Ca/P ratio from 1.02 to 0.76 which could be correlated to the different pH of the synthesis solution. Vapour phase dehydration of lactic acid to acrylic acid was carried out using these calcium pyrophosphate catalysts. Non-stoichiometric calcium pyrophosphate catalyst with Ca/P ratio 0.76 was found to be the most efficient catalyst among synthesized series with 100% lactic acid conversion and 78% acrylic acid selectivity at 375 °C. The higher selectivity for acrylic acid has been correlated to the increased acidity and reduced basicity of non-stoichiometric calcium pyrophosphate compared to other stoichiometric pyrophosphates. *In situ* FTIR studies showed the formation of higher amount of calcium lactate on non-stoichiometric compared to stoichiometric pyrophosphate leading to higher selectivity for acrylic acid.

3.1 Introduction

Depletion of fossil fuels and increasing pollution due to greenhouse gases emitted in the atmosphere has forced researchers worldwide to develop clean technologies based on renewable raw materials for sustainable development. Sustainable production of fuels and chemicals is possible using lignocellulosic biomass as an attractive raw material. Lactic acid derived from biomass fermentation has been identified as one of the high potential platform chemical in the biomass economy.[1,2] Lactic acid is very reactive molecule due to the presence of active functional groups, -OH and -COOH, which can be used to convert lactic acid to many value added products such as acrylic acid, propionic acid[3], 2,3-pantanedione[4], acetaldehyde[5], pyruvic acid[6], 1,2-propanediol[7] by different pathways. Acrylic acid, its amides and esters find wide applications in surface coatings, textiles, adhesives, paper treatment, leather, fibres, detergents, polymeric flocculants, dispersants, paints, adhesives, binders for leather, and in acrylate polymers *etc*. Dehydration of lactic acid to acrylic acid is being considered as one of the attractive alternate route for the manufacture of acrylic acid from renewable raw materials.

Catalytic dehydration of lactic acid/lactates to acrylic acid/acrylates has been reported previously using inorganic salts such as phosphates, silicates, carbonates, nitrates and sulphates as catalysts.[8-12] Catalysts having strong acidity mainly show decarbonylation/decarboxylation of lactic acid to acetaldehyde.[5] Hence for zeolites, modifiers such as potassium nitrate, lanthanum oxide and alkali phosphates as well as various alkaline earth metals like Ca, Mg, Sr, Ba *etc.* were used to change the surface acidity to achieve high efficiency for selective dehydration of lactic acid to acrylic acid.[13] Previously various phosphate based catalysts like sodium dihydrogen phosphate (NaH_2PO_4), $Ca_3(PO_4)_2$ supported on silica, silica/alumina, aluminium phosphate and Na_2HPO_4 in supercritical water, were used for lactic acid dehydration.[14] However some of the modifiers leach out easily from the support during reaction leading to catalyst deactivation. Hence water insoluble salts with desirable acidity were employed in the dehydration of lactic acid. Various alkali phosphates (ortho and pyro) such as calcium, strontium and barium phosphates were used for lactic acid dehydration by Blanco *et al*.,[15] with maximum acrylic acid selectivity of only 49% using $Ba_3(PO_4)_2$. Peng and co-workers investigated the effect of acidity of various metal sulfates on lactic acid dehydration, and $BaSO_4$ showed 74% selectivity for acrylic acid due to moderate

acidity.[16] When mixture of $Ca_3(PO_4)_2$ and $Ca_2P_2O_7$ (50/50 wt%) was tested for dehydration of ethyl lactate, methyl lactate and lactic acid, the conversion increased in the order ethyl lactate <methyl lactate < lactic acid, however the selectivity for acrylic acid was observed in the reverse order.[17] Matsuura and co-workers studied hydroxyapatite with different cations and anions for lactic acid dehydration and results showed calcium and strontium hydroxyapatite with moderate acidity to give highest acrylic acid yield. The same group studied addition of different bases like NaOH and ammonia for adjusting the pH and formation of non-stoichiometric calcium hydroxyapatite with incorporation of sodium which resulted in 78% yield for acrylic acid using 38% lactic acid solution with very low WHSV.[18] Similarly hydroxyapatite with Ca/P ratio of 1.62, calcined at 360 °C has shown 71% acrylic acid selectivity with 70% lactic acid conversion.[19] Normally different lactic acid concentrations ranging from 20wt% to 40wt% were used for lactic acid dehydration with lower WHSV leading to low space time yield.

Lactic acid dehydration requires catalysts with weak acidity and weak basicity, however fine tuning of surface acidity and basicity is very important for achieving maximum selectivity for acrylic acid. Recently we have reported lactic acid dehydration using series of hydroxyapatite with different Ca/P ratio as catalyst.[20] The catalyst with minimum Ca/P ratio of 1.3 showed maximum efficiency with 100% conversion and 60% acrylic acid selectivity along with the formation of acetaldehyde as the only byproduct. The catalyst with Ca/P ratio 1.3 showed the required acid base balances to achieve acrylic acid selectivity of 60%. As Ca/P ratio of hydroxyapatite was decreased from 1.67 (stoichiometric) to 1.3, considerable improvement in acrylic acid selectivity was observed. Hence to further increase the acrylic acid selectivity, the calcium phosphate catalysts were prepared using modified synthetic procedure to decrease the Ca/P ratio further using mixture of diammonium hydrogen phosphate and sodium phosphates as phosphate precursor and without maintaining constant pH throughout the catalyst preparation and the results are reported herein.

3.2 Experimental section

3.2.1 Materials

Calcium nitrate, di-ammonium hydrogen phosphate, ammonium hydroxide solution, sodium hydrogen phosphate ($NaH_2PO_4.2H_2O$), disodium hydrogen phosphate

($Na_2HPO_4.2H_2O$), and tri sodium phosphate ($Na_3PO_4.12H_2O$) were obtained from Thomas Baker chemicals India Ltd. Lactic acid (89%) was obtained from our CSIR-National Chemical Laboratory (CSIR-NCL) Pune pilot plant which is obtained from sugarcane fermentation process (process developed by CSIR-NCL).

3.2.2 Catalyst preparation method

Calcium phosphates catalysts using calcium nitrate, diammonium hydrogen phosphate and sodium phosphates were prepared by precipitation method. Typical sodium phosphate precursors like $NaH_2PO_4.2H_2O$, $Na_2HPO_4.2H_2O$ and $Na_3PO_4.12H_2O$ were used for the preparation and the final catalysts were denoted as CP-1, CP-2 and CP-3 respectively. In a typical synthesis of CP-1, calcium nitrate (36.95 g) and diammonium hydrogen phosphate (13.8 g) were dissolved separately in 125 mL deionized water each. Initially the pH of both the solutions was adjusted to 8 by addition of ammonium hydroxide solution (5% aqueous). $NaH_2PO_4.2H_2O$ (3.39 g) dissolved in 25 mL deionized water was added to the diammonium hydrogen phosphate solution. Calcium nitrate solution was added drop wise to the above mixture of phosphate precursors with constant stirring (700 rpm) at room temperature. As the precipitation proceeds decrease in pH was observed. A thick white precipitate formed was aged for 12 h then filtered, washed with water and dried in an oven at 120 °C for 12 h. The dried catalyst was calcined at 600 °C for 4 h. Catalysts CP-2 ($Na_2HPO_4.2H_2O$ 1.911 g) and CP-3 ($Na_3PO_4.12H_2O$ 2.7 g) were prepared following the similar procedure as mentioned above except the source of sodium phosphate.

Calcium phosphate catalyst without sodium phosphate was prepared for comparison, with Ca/P ratio 1.5 and denoted as CP. For preparation of CP calcium nitrate (38.9 g) and diammonium hydrogen phosphate (14.5 g) solutions were prepared separately in deionized water (125 mL each). Initially the pH of both the solutions was adjusted to 8 by adding ammonium hydroxide solution (5% aqueous). Calcium nitrate solution was added drop wise to the diammonium hydrogen phosphate solution with constant stirring (700 rpm) at room temperature. As the precipitation proceeds decrease in pH was observed. A thick white precipitate formed, was aged for 12 h then filtered, washed with water and dried in an oven at 120 °C for 12 h. The dried catalyst was calcined at 600 °C for 4 h.

3.2.3 Catalyst characterization

The X-ray diffraction analysis was carried out using a Rigaku X-ray diffractometer (Model DMAX IIIVC) with Cu-Ka radiation.

FTIR measurements were carried out using Shimadzu 8300 as KBr pellet in the range of 4000-400 cm^{-1} region with 4 cm^{-1} resolution averaged over 100 scans.

BET surface area was determined using NOVA 1200 Quanta chrome instrument. Prior to N_2 adsorption, the sample was evacuated at 250 °C.

To study Ca/P ratio, scanning electron microscopy EDAX was performed on a Leica Stereoscan-440 instrument equipped with a Phoenix EDAX attachment operated at 20 kV, ICP analysis was carried out on ICP AES SPECTRO ARCOS Germany FHS12 instrument.

Temperature programmed desorption of ammonia (NH_3-TPD) and CO_2 (CO_2-TPD) was carried out using a Micromeritics Autocue 2910. For TPD measurement 0.1 g of catalyst sample was used. Sample was dehydrated at 500 °C for 1 h in 50 mL min^{-1} helium flow and then cooled to 50 °C. Probe gas (5% NH_3 in helium for acidic sites and 10% CO_2 in helium for basic sites) was then adsorbed for 1 h in 50 mL min^{-1} flow. The temperature was raised up to 600 °C at a rate of 10 °C min^{-1} in 30 mL min^{-1} helium flow.

Raman spectra were recorded under ambient conditions on a Lab RAM infinity spectrometer (Horiba-Jobin-Yvon) equipped with a liquid nitrogen detector and a frequency doubled Nd-YAG laser supplying the excitation line at 532 nm with 1-10 mW power. The spectrometer was calibrated using the Si line at 521 cm^{-1} with a spectral resolution of 3 cm^{-1}.

Morphological appearance of the samples using scanning electron microscopy (SEM) was performed on a Leica Stereoscan-440 instrument equipped with a Phoenix EDAX attachment operated at 20 kV.

^{31}P MAS NMR analysis was carried out using Bruker 300 MHz, with resonance frequency of 121.49 MHz. The operating fields of 7.05 T, the spinning rates of 8 KHz, with 85% H_3PO_4 as reference material and recycle delay of 5.0 s were used during analysis.

3.2.4 Catalyst activity test

Vapour phase dehydration of lactic acid to acrylic acid was carried out using procedure reported previously.[20] In short quartz fixed bed down flow reactor (id-11 mm) was charged with catalyst (particle size 20-40 mesh) in the middle section with quartz wool packed in both the ends. Porcelain beads were placed above the catalyst bed in order to preheat the feed. Before catalytic evaluation, the catalyst was preheated at required reaction temperature for 0.5 h under flow of nitrogen (15 mL min^{-1}). The reaction temperature was measured by a thermocouple inserted in the catalyst bed. Lactic acid of required concentration (typically 50% w/w in water) was pumped in to the preheating zone of reactor using peristaltic pump and nitrogen gas as carrier. The reaction products were collected in a cold trap at 8 °C. The reaction mixture was analyzed using gas chromatograph (Perkin Elmer) equipped with a FFAP capillary column (50 M X 0.320 mM) and FID detector. The GC was calibrated by external standard method. The formation of CO and CO_2 was confirmed by GC, with molesieve and porapack Q column respectively using TCD detector. The amount of CO_x (CO and CO_2) was estimated based on the yield of acetaldehyde and propionic acid. The mass balance for all the reaction was more than 90%.

The *in situ* FTIR studies were carried out using previously reported procedure.[20] In a typical experiment lactic acid was adsorbed on CP and CP-3 catalyst at room temperature. The physisorbed lactic acid was removed by drying the catalyst at room temperature for 8 h and the FTIR spectrum was recorded. The adsorbed lactic acid was desorbed at various temperatures to detect the species formed *in situ* during the reaction. The spectrum of neat catalyst was subtracted to get the spectrum of adsorbed species.

3.3 Results and discussion

A series of calcium phosphate (CP) catalysts were prepared using calcium nitrate, diammonium hydrogen phosphate and additional phosphate precursors like $NaH_2PO_4.2H_2O$, $Na_2HPO_4.2H_2O$ and $Na_3PO_4.12H_2O$ to tune the Ca/P ratio by increasing the phosphate content. It is known that preparation of calcium phosphates is very sensitive to pH of the precursor solution and drastically affects the Ca/P ratio of the final catalyst composition. During the synthesis of catalysts using sodium phosphates, the pH of $Ca(NO_3)_2$ and $(NH_4)_2HPO_4$ was adjusted to 8. However due to difference in pH of the aqueous solution of

sodium phosphate precursors, the pH of the mixed phosphate solution was different (Table 3.1). Hence during addition of calcium nitrate solution to phosphate mixture and ultimately precipitation of calcium phosphate the pH of the mixture gradually decreased reaching 5 after complete addition of calcium nitrate. Hence the change in the pH of the solution during precipitation is expected to affect the catalyst structure, Ca/P ratio and in turn the catalytic activity. The pH of the sodium precursors are given in Table 3.1. Hence for comparison one catalyst was prepared without using any sodium phosphate and denoted as CP. For this catalyst also the pH of the synthesis mixture decreased from 8 to 5 after complete precipitation.

Table 3.1 pH of the phosphate solution during precipitation

Catalyst	**Phosphate precursor**	**pH of Na-phosphate solution**	**pH of combined phosphate solution**	**pH of solution after complete precipitation**
CP-1	$NaH_2PO_4.2H_2O$	4	7	5
CP-2	$Na_2HPO_4.2H_2O$	8.5	7.5	5
CP-3	$Na_3PO_4.12H_2O$	12	10	5
CP	-	-	-	5

3.3.1 ICP and EDAX analysis for Ca/P

The bulk and surface Ca/P ratio was determined by ICP and EDAX analysis and results are shown in Table 3.2. The Ca/P ratio for CP-1 and CP-2 were found to be 1.04 and 1.09 respectively which is in accordance with the almost similar pH of the combined phosphate solution. However for CP-3 the Ca/P ratio decreased considerably to 0.76. The catalyst prepared without sodium phosphate showed higher Ca/P ratio of 1.27.

At different pH different phosphate species exist, and at pH 8 predominantly HPO_4^{2-} exists.[21] HPO_4^{2-} species has very high affinity for calcium leading to precipitation of $CaHPO_4$. The precipitation of calcium phosphate from calcium and phosphate solutions is a

pH controlled process. At lower pH the solubility of calcium phosphate increased leading to the decrease in calcium incorporation, which in turn decreases the Ca/P ratio.[22] Addition of sodium phosphates led to increase in phosphate concentration thus resulting in decrease in Ca/P ratio. The additional phosphate alters the equilibrium between PO_4^{3-} to HPO_4^{2-} to $H_2PO_4^{1-}$ which leads to the further decrease in Ca/P ratio. It was reported that Ca/P ratio of the precipitate does not depend directly on the Ca/P ratio of initial reagents of calcium and phosphate but depends on pH and temperature during precipitation.

Table 3.2 Textural characterization, acidity and basicity of calcium pyrophosphates

Catalyst name	**Surface area, m^2/g**	**CO_2 desorbed, µmol/g**	**NH_3 desorbed, µmol/g**	**Acid base balance**	**Ca/P ratio by ICP**	**Ca/P ratio by EDAX**
CP-1	29	17.054	114	7	1.04	1.02
CP-2	21	16.094	128	8	1.09	1.03
CP-3	29	15.317	167	11	0.76	1.08
CP	28	34.907	071	2	1.27	1.10

3.3.2 Study of pH changes during catalyst precipitation

The change in pH during spontaneous precipitation of calcium phosphate from supersaturated solutions was studied at 30 °C, stirring speed 700 rpm and shown in Fig. 3.1. It showed decrease in pH during the first few minutes, followed by an irregular and slow decrease and finally became stable after 2 h.

3.3.3 Surface area determination

The surface area of all the catalysts determined using the BET method was found to be in the range 21–29 $m^2\ g^{-1}$ as shown in Table 3.2.

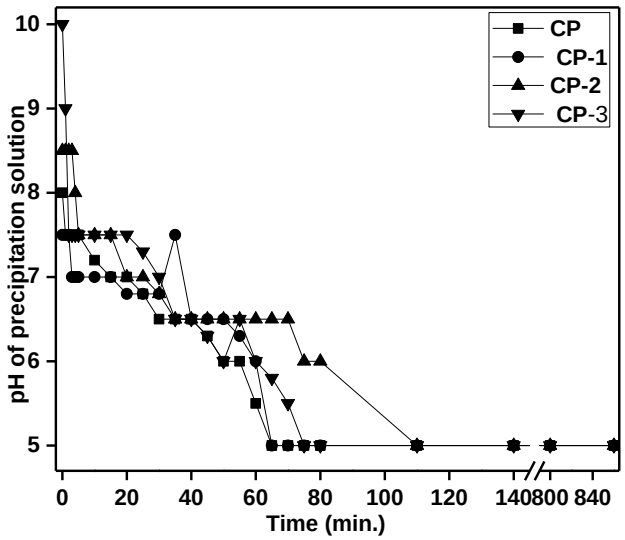

Fig. 3.1 Change in pH after addition of calcium solution to phosphate solution for CP (■), CP-1 (●), CP-2 (▲) and CP-3(▼). Measurements were carried out under continuous constant stirring (700rpm) and at constant temperature 30 °C.

3.3.4 The powder X-ray diffraction (XRD)

The powder X-ray diffraction (XRD) patterns of synthesized catalysts are shown in Fig. 3.2. The XRD pattern showed the crystalline nature for all the catalysts. The diffraction peaks at 26.7, 27.7, 28.9, 29.3, 30.69 and 32.37° match with the structure of β-calcium pyrophosphate (JCPDS-33-0297). The intensity of the peak at 29.3° considerably decreased in CP-3 compared to remaining catalysts indicating structural distortion which may be due to calcium deficiency as observed by EDAX and ICP analysis. However the overall XRD pattern retains the β-pyrophosphate structure. As the Ca/P ratio for CP-3 is considerably low compared to pyrophosphate structure (Ca/P = 1) the XRD of as synthesised catalyst was recorded (denoted as CP-3* in Fig. 3.2). The peaks at 26.38, 30.15, 32.52, 35.82, 49.26, 53.02° matched with monetite structure of $CaHPO_4$ (monetite JCPDS-04-0513) which transformed to pyrophosphate after calcination. Skinner[23] has studied the conversion of $CaHPO_4$ to different forms of calcium pyrophosphates at different temperatures and showed the formation of β-calcium pyrophosphate to be at the temperature below 800 °C. As all the catalysts in the present work were calcined at 600 °C the formation of stable β-pyrophosphate was observed in accordance with literature reports. In Ca-pyrophosphate or monetite structure the theoretical Ca/P ratio is 1 which is matching with Ca/P ratio in CP-1 and CP-2, however

for CP-3 the ratio is considerably low (0.76) indicating non-stoichiometric or Ca-deficient pyrophosphate structure. The only reported calcium phosphate with lower Ca/P ratio of 0.5 are $Ca(H_2PO_4)_2$, monocalcium phosphate monohydrated (MCPM) or anhydrous monocalcium phosphate (MCPA), which are water soluble and stable only in extremely acidic pH of 0-2. Hence in the present work we could precipitate the calcium phosphate with lower Ca/P ratio in basic medium as well as retain the pyrophosphate structure at high temperature with calcium deficiency.

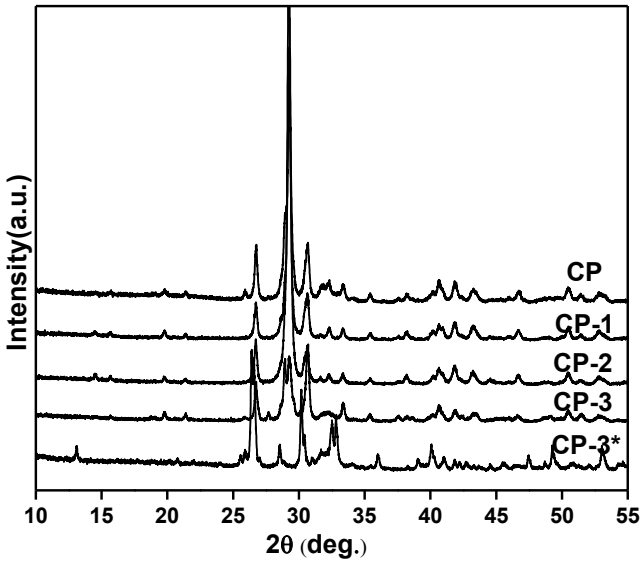

Fig. 3.2 The powder X-ray diffraction (XRD) patterns of synthesized catalysts, CP-3*- as synthesised CP-3 catalyst.

3.3.5 FTIR spectroscopy studies

Catalyst structure was further confirmed by FTIR spectroscopy (Fig. 3.3). Typical pyrophosphate stretching and bending vibrations were observed at 1215-941 and 723 cm^{-1} respectively.[24] Bands at 613-494 cm^{-1} are assigned to phosphate bending vibrations.[25] Thus the β-calcium pyrophosphate formation was confirmed by both XRD and FTIR studies. Likewise the formation of $CaHPO_4$ in as synthesised CP-3 catalyst (CP-3*) was also confirmed by FTIR from the characteristic band for HPO_4^{1-} at 898 cm^{-1}.

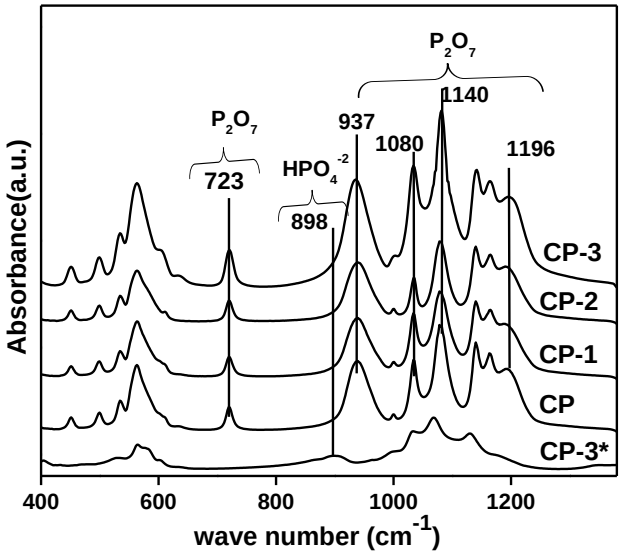

Fig. 3.3 FTIR spectra of synthesized CP catalysts and as synthesized CP-3 catalyst.

3.3.6 Temperature programmed desorption studies

The acid base properties of the catalysts were evaluated by temperatures programmed desorption (TPD) of CO_2 and NH_3 (Fig. 3.4) and the results are shown in Table 3.2. As the Ca/P ratio decreased from CP, CP-1 to CP-3, there is decrease in basicity and increase in the acidity. Phosphate groups in catalyst are responsible for acidity whereas Ca^{2+} ions are responsible for the basicity. Hence increase in the basicity and decrease in the acidity was observed as expected with increase in the Ca/P ratio.[20] CP-3 catalyst showed the highest acidity. The basicity of the reported CP catalyst was very weak (expressed in µmol g^{-1}) and the TPD profile is shown in Fig. 3.4a.

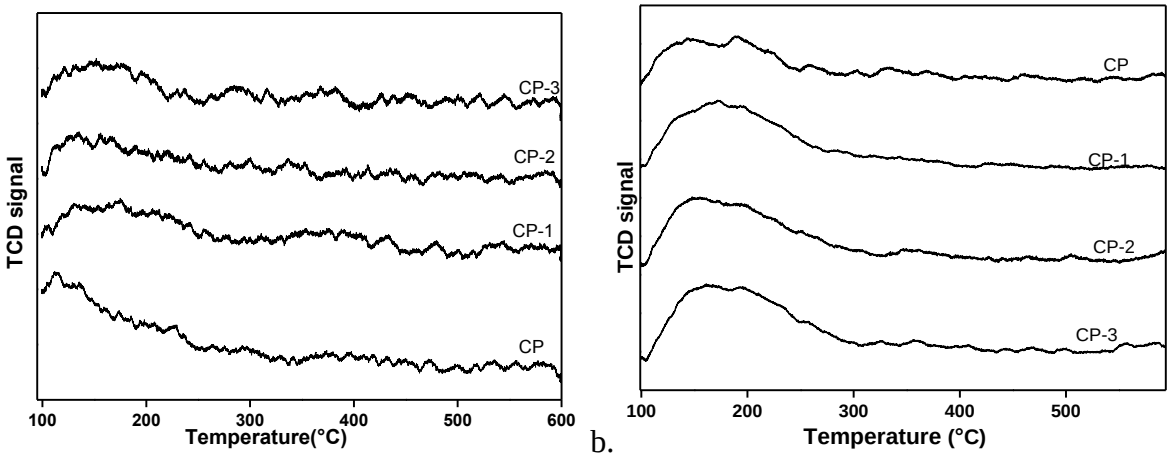

Fig. 3.4 a.CO_2 TPD profiles, b. NH_3 TPD profiles of CP, CP-1, CP-2, CP-3.

3.3.7 Raman spectroscopy studies

Raman analysis showed the presence of monoclinic β-calcium pyrophosphate (Fig. 3.5). The Raman peaks at 1159, 1115, 1049, 736, 524, 356 and 355 cm^{-1} matched with the Raman peaks reported for monoclinic calcium pyrophosphate.[26]

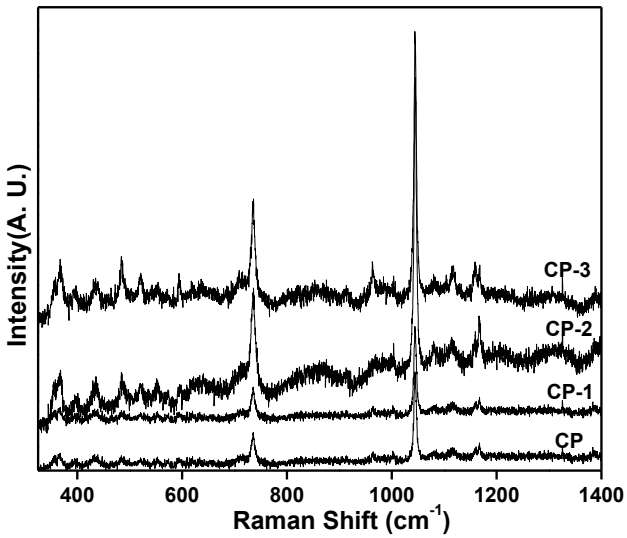

Fig. 3.5 Raman spectra of synthesized CP catalysts.

3.3.8 Scanning electron microscopy (SEM)

The particle size of all the CP catalyst was determined using SEM and the images are given in Fig. 3.6. However no considerable difference in particle size was observed.

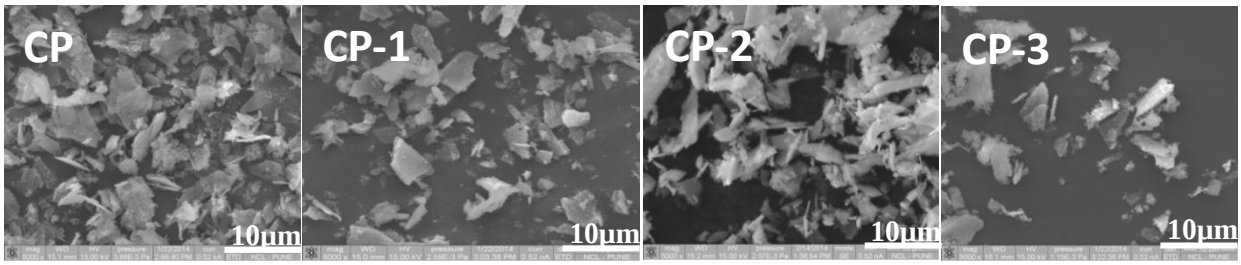

Fig. 3.6 SEM images for synthesized CP catalysts.

Thus the structure of all the synthesised catalysts was confirmed to be β-calcium pyrophosphate.

3.4 Catalytic activity

3.4.1 Influence of Ca/P ratio on the dehydration of lactic acid to acrylic acid

The synthesized calcium phosphate (CP) catalysts were tested for vapour phase dehydration of lactic acid (Scheme 3.1) and the results are shown in Table 3.3. The reaction was carried out with the previously reported optimised reaction conditions[20] *i.e.* using 50% (w/w) aqueous solution of lactic acid with WHSV of 3 h^{-1} at 375 °C. As expected, 100% lactic acid conversion was obtained with all CP catalysts at 375 °C using 50% lactic acid solution though with variable acrylic acid selectivity. CP-3 catalyst showed maximum selectivity of 74% for acrylic acid compared to CP-2 (70%), CP-1 (68%) and CP (55%). As CP-3 catalyst showed highest selectivity for acrylic acid, the effect of different reaction parameters such as temperature, residence time, concentration on lactic acid dehydration was studied using CP-3 catalyst and the results are given in Table 3.4.

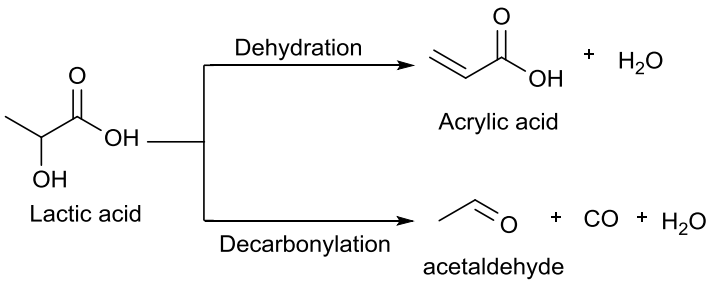

Scheme 3.1 General schematic for lactic acid conversion to acrylic acid and acetaldehyde.

3.4.2 Effect of temperature

The effect of temperature on lactic acid conversion and acrylic acid selectivity was studied by varying the temperature from 325 to 400 °C (Table 3.4, entry 1). Conversion of lactic acid increased from 75 to 100% with increase in reaction temperature from 325 to 400 °C with 50% lactic acid concentration and WHSV of 3 h^{-1}. Initially increase in the acrylic acid selectivity was observed from 32 to 74% with increase in the temperature from 325 to 375 °C, however further increase in the temperature to 400 °C led to decrease in the acrylic acid selectivity to 60% with corresponding increase in the formation of acetaldehyde and polylactates. At 325 °C lowest lactic acid conversion and acrylic acid selectivity was observed due to lactide formation.

Table 3.3 Dehydration of lactic acid to acrylic acid using calcium phosphate with different Ca/P ratio

Sl. No	Catalyst	Conversion	Acrylic Acid Selectivity	Acetaldehyde Selectivity	Other products Selectivity
1	CP	100	55	30	15
2	CP-1	100	68	15	17
3	CP-2	100	70	13	17
4	CP-3	100	74	10	16

Reaction condition: carrier gas- N_2, carrier gas flow-15 mL min^{-1}, WHSV 3 h^{-1}, lactic acid conc.- 50% (w/w), temperature- 375 °C, other products- propionic acid, 2,3-pentanedione, CO, CO_2.

3.4.3 Effect of residence time

The residence time of lactic acid on CP-3 was varied by progressively changing the WHSV from 1 to 4.5 h^{-1}. When WHSV was increased from 1 to 3 h^{-1}, the lactic acid conversion remained at 100% however with further increase in WHSV to 4 and 4.5 h^{-1}, the conversion decreased to 90 and 85% respectively due to decrease in residence time (Table 3.4, entry 2). Whereas volcano type trend was obtained for acrylic acid selectivity. The acrylic acid selectivity increased from 54 to 74% with increase in WHSV from 1 to 3 h^{-1} and then it decreased to 68 and 65% with further increase in WHSV to 4 and 4.5 h^{-1} respectively. As the residence time decreased there was increase in selectivity, though with 100% conversion for lactic acid. At very low residence time (WHSV-4, 4.5) there was decrease in conversion of lactic acid as well as selectivity for acrylic acid. WHSV-3 h^{-1} provides optimum residence time for maximum conversion as well as acrylic acid selectivity on CP-3 catalyst.

Table 3.4 Effect of various parameters on dehydration of lactic acid to acrylic acid using CP-3 catalyst[a]

Sl. no	Reaction parameters		Conv. (%)	Acrylic acid Selectivity (%)	Acetaldehyde selectivity (%)	Other products selectivity [e] (%)
1	Temp.[b] (°C)	325	75	32	15	53[f]
		350	90	45	15	40
		375	100	74	10	16
		400	100	60	20	20
2	WHSV[c] (h^{-1})	1	100	54	22	24
		2	100	62	16	22
		3	100	74	10	16
		4	90	68	12	20
		4.5	85	65	18	17
3	Lactic acid conc.[d] (w/w%)	25	100	78	8	14
		50	100	74	10	16
		60	96	60	20	20
		70	80	58	20	22
		80	70	53	23	24

Reaction conditions: [a] Catalyst- CP-3, carrier gas- N_2, carrier gas flow-15 mL min^{-1}. [b] WHSV- 3 h^{-1}, Lactic acid conc.- 50% (w/w). [c] Lactic acid conc.- 50% (w/w), Temp- 375 °C. [d] Temp- 375 °C, WHSV- 3 h^{-1}. [e] Other products- propionic acid, 2,3-pentanedione, CO, CO_2 . [f] lactide.

3.4.4 Effect of lactic acid concentration

The lactic acid concentration was gradually increased from 25 to 80 wt% (wt/wt aqueous solution) to study its effect especially on acrylic acid selectivity (Table 3.4, entry 3). Complete lactic acid conversion (100%) was obtained with 25 and 50% lactic acid concentration however gradual increase in the lactic acid concentration to 80% led to decrease in lactic acid conversion to 70%. Maximum selectivity (78%) for acrylic acid was obtained when 25% lactic acid was used which steadily decreased to 53% with increase in the lactic acid concentration to 80%. Acrylic acid yield of 78% is the highest yield reported so far in the literature for lactic acid dehydration at very high WHSV (3 h^{-1}). With increase in the lactic acid concentration residence time decreased which led to the decrease in Ca-lactate formation and consequently increase in the decarbonylation leading to more formation of acetaldehyde.

It is worth mentioning that mass balance for all the above mentioned reaction was 85-90%. Catalyst stability of CP-3 was tested under optimised reaction conditions and the catalytic activity was stable up to 20 h. The acetaldehyde formed in all the above mentioned reaction was predominantly due to decarbonylation of lactic acid as confirmed by GC analysis however formation of CO_2 was also observed with less selectivity indicating lesser extent of decarboxylation compared to decarbonylation. Decarboxylation of lactic acid is associated with formation of hydrogen which may be responsible for propionic acid formation by hydrogenation of acrylic acid. Alternate pathway for formation of propionic acid is deoxygenation of lactic acid. However hydrogenation of acrylic acid is more feasible path for formation of propionic acid as per previous studies.[27] Deoxygenation of lactic acid has been studied before in the literature. Previous studies have shown deoxygenation of lactic acid in presence of acidic catalysts like hydriodic acid,[28] supported heteropoly acids,[5] supported nitrates and phosphates,[4a.b.17,29] as well as doped zeolites[13a] or platinum based catalyst under high hydrogen pressure.[30] Various homogenous catalysts (Pd, Pt or Ir complexes) also have been used for deoxygenation of lactic acid in water at lower pH.[27,31] However in the present work the catalyst is very weakly acidic as well as reaction conditions are totally different than typically required for deoxygenation of lactic acid. Hence the formation of propionic acid in present work would be due to hydrogenation of acrylic acid and not by deoxygenation of lactic acid.

Recently many phosphate based catalysts such as $Ba_3(PO_4)_2$,[15] Na_2HPO_4 supported on NaY,[32] calcium and strontium hydroxyapatites[18a] as well as non-stoichiometric calcium hydroxyapatite modified with sodium[18b] have been used for lactic acid dehydration to acrylic acid. All the above mentioned phosphate based catalysts were operated in the temperature range of 340-400 °C with lactic acid concentration of 20-40%. Among the phosphate based catalysts Na_2HPO_4/NaY showed maximum lactic acid conversion of 93.5% with 79.5% selectivity for acrylic acid. Zhang *et al*.[33] have studied lactic acid dehydration using $NaNO_3$/SBA-15 catalyst with almost complete conversion, however with very poor (42%) acrylic acid selectivity. When $BaSO_4$ was used for lactic acid dehydration at 400 °C using 20% lactic acid solution, almost 100% lactic acid conversion is reported with 66% selectivity for acrylic acid.[16] Lactic acid dehydration on different barium phosphates was screened, however only barium pyrophosphate $Ba_2P_2O_7$ has shown very high acrylic acid selectivity (76%) with 20 wt% lactic acid concentration and with considerably lower WHSV (flow rate 1 mL h^{-1}) compared to present work.[34] Compared to previous reports on lactic acid dehydration to acrylic acid, the results obtained in the present study are better with 100% conversion and 78% acrylic acid selectivity. Especially the use of high concentration of lactic acid and very high WHSV leading to high per pass yield are the major advantages of the present catalysts.

3.5 ^{31}P MAS NMR spectroscopy

Though all the synthesised CP catalysts have shown β-calcium pyrophosphate structure, only CP-3 catalyst has shown maximum selectivity for acrylic acid whereas CP has shown lowest acrylic acid selectivity. Hence the structure of all CP catalysts was further studied by ^{31}P MAS NMR spectroscopy (Fig. 3.7 a and b). The NMR spectra showed three isotropic peaks at 0.2 (Q^0), -11.65 (Q^1) and -13.51 (Q^1) ppm. Q^0 represents the pyrophosphate species and Q^1 represents the metaphosphate species (as shown in Fig. 3.7).[35] The intensities of different species in CP showed the concentration of pyrophosphate species (Q^0 peak at 0.2 ppm) to be less than metaphosphate species (Q^1 peak at -11.65 and -13.51 ppm). In CP-3 the concentration of pyrophosphate species was considerably higher compared to metaphosphate species. The intensity of pyrophosphate peak gradually increased from CP to CP-3 which may be correlated to the acrylic acid selectivity which also gradually increased from CP to CP-3. The Ca/P ratio changed from 1.27 to 0.76 for CP and CP-3. More terminal P-OH

groups are present in pyrophosphate species compared to metaphosphate species as shown in the structure in Fig. 3.7, which is in accordance with higher acidity of CP-3 compared to CP.

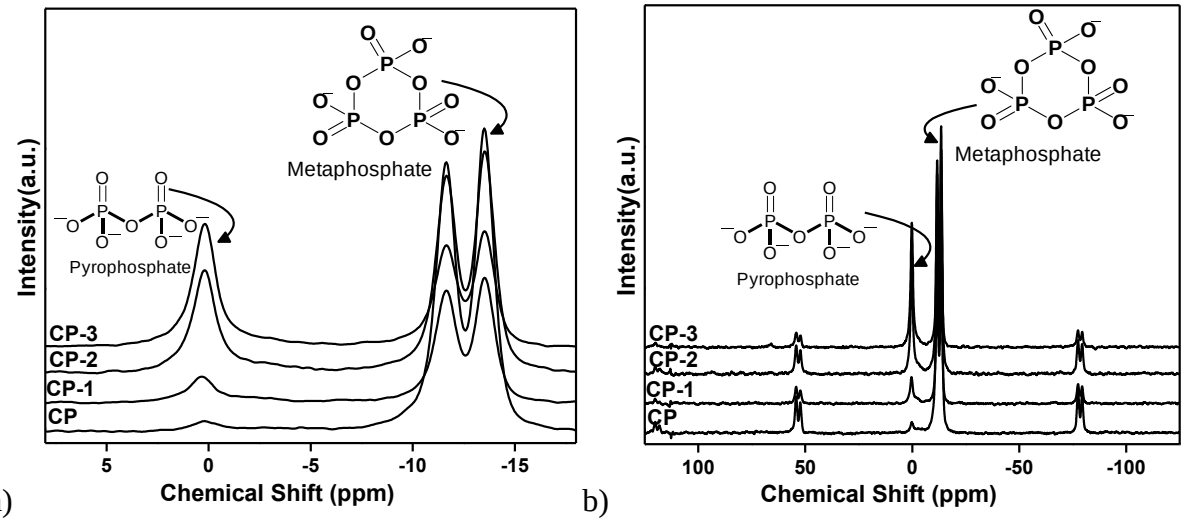

Fig. 3.7 ^{31}P MAS NMR spectra a. CP b. CP-1, c. CP-2 and d.CP-3.

3.6 *In situ* FTIR studies

As per the proposed mechanism in our previous work on lactic acid dehydration, calcium lactate formation is crucial for acrylic acid selectivity. To check the formation of calcium lactate species, *in situ* FTIR studies were carried out using previously reported experimental conditions[20] on catalysts which showed minimum (CP) and maximum (CP-3) selectivity for acrylic acid. Lactic acid was adsorbed on CP and CP-3 at room temperature and physisorbed lactic acid was removed by drying the catalyst at room temperature for 8 h and the FTIR spectrum was recorded. Further, the adsorbed lactic acid was desorbed at 50, 100 and 150 °C. The difference spectra of CP and CP-3 at 150 °C are shown in Fig. 3.8. Calcium lactate formation on both the catalysts CP and CP-3 was confirmed by carbonyl peak at 1600 cm^{-1} whereas free lactic acid adsorbed on catalyst was confirmed by presence of carbonyl peak at 1748 cm^{-1}. Carbonyl peaks of calcium lactate and lactic acid were used as measure of extent of calcium lactate formation which in turn can be correlated to the selectivity for acrylic acid observed on particular catalyst.

The ratio of area of the carbonyl peak at 1600 (for calcium lactate) and at 1748 cm^{-1} (for lactic acid) was calculated for CP and CP-3. The ratio was considerably higher for CP-3 (0.583) compared to CP (0.350) indicating higher extent of calcium lactate formation on CP-

3 compared to CP which can be directly correlated to higher selectivity for acrylic acid observed on CP-3 compared to CP. Though Ca/P ratio is less for CP-3 compared to CP the more formation of calcium lactate is observed on CP-3 which may indicate the more availability of calcium on the surface for formation of calcium lactate in CP-3 which may be due to the structural features of CP-3.

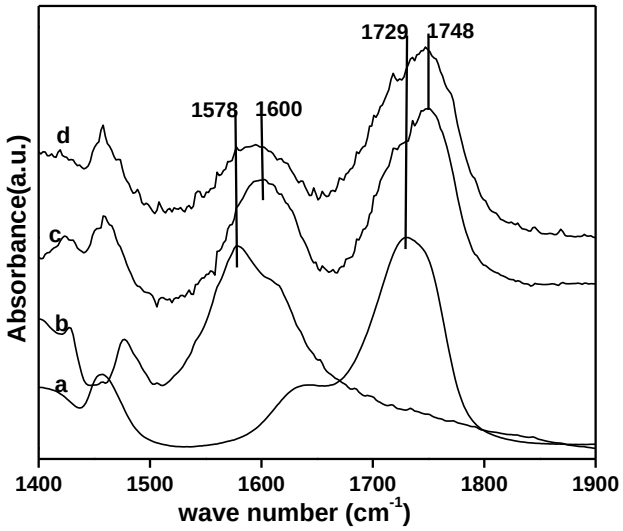

Fig. 3.8 FTIR spectrum of (a) lactic acid (b) calcium lactate from FTIR database, FTIR difference spectra of lactic acid adsorbed (c) CP-3, (d) CP at 150 °C.

3.7 Conclusions

Non stoichiometric calcium pyrophosphate catalyst prepared with Ca/P ratio 0.76 prepared by modifying synthetic procedure using mixture of diammonium hydrogen phosphate and sodium phosphates as phosphate precursors. This catalyst has shown very high efficiency for vapour phase dehydration of lactic acid to acrylic acid with 100% conversion and 74% acrylic acid selectivity at 375 °C with WHSV of 3 h^{-1} using 50% lactic acid concentration. The acrylic acid selectivity was further improved to 78% with 25% lactic acid concentration. The higher selectivity for acrylic acid was attributed to acid base balance at lower Ca/P ratio leading to formation of higher amount of calcium lactate as an intermediate compared to other stoichiometric calcium pyrophosphates as evidenced by *in situ* FTIR studies.

3.8 References

[1] M. Dusseleir, P. V. Wouwe, A. Dewaele, E. Makshina and B. F. Sels, *Energy Environ. Sci*., 2013, **6**, 1415-1442.

[2] P. Maki-Arvela, I. L. Simakova, T. Salmi and D. Y. Murzin, *Chem. Rev.,* 2014, **114,** 1909-1971.

[3] T. J. Korstanje, H. Kleijn, J. T. B. H. Jastrzebski and R. J. M. Klein Gebbink, *Green Chem.,* 2013, **15**, 982-988.

[4] (a) G. Gunter, D. J. Miller and J. E. Jackson, *J. Catal*., 1994, **148,** 252-260; (b) G. C. Gunter, R. H. Langford, J. E. Jackson and D. J. Miller, *Ind. Eng. Chem. Res*., 1995, **34,** 974-980; (c) M. S. Tam, G. C. Gunter, R. Craciun, D. J. Miller and J. E. Jackson, *Ind. Eng. Chem. Res*., 1997, **36**, 3505-3512; (d) M. S. Tam, R. Craciun, D. J. Miller and J. E. Jackson, *Ind. Eng. Chem. Res.,* 1998, **37**, 2360-2366.

[5] (a) B. Katryniok, S. Paul and F. Dumeignil, *Green Chem*., 2010, **12,** 1910-1913; (b) Z. Zhai, X. Li, C. Tang, J. Peng, N. Jiang, W. Bai, H. Gao and Y. Liao, *Ind. Eng. Chem. Res.,* 2014, **53**, 10318-10327.

[6] M. Ai and K. Ohdan, *Appl. Catal., A,* 1997, **165**, 461-465.

[7] R. D. Cortright, M. Sanchez-Castillo and J. A. Dumesic, *Appl. Catal., B,* 2002, **39**, 353-359.

[8] R. E. Holmen, *US Pat.,* 2859240, 1958.

[9] (a) R. A. Sawicki, *US Pat.,* **4729978**, 1988; (b) J. Wang, Z. Zhang, Y. Qu and S. Wang, *Ind. Eng. Chem. Res.,* 2009, **48**, 9083-9089; (c) J.-M. Lee, D.-W. Hwang, Y. K. Hwang, S. B. Halligudi, J.-S. Chang and Y.-H. Han, *Catal. Commun.,* 2010, **11,** 1176-1180.

[10] C. Paparizos, S. R. Dolhyj and W. G. Shaw, *US Pat.,* **4786756**, 1988.

[11] C. T. Lira and P. J. McCrackin, *Ind. Eng. Chem. Res.*, 1993, **32,** 2608-2613.

[12] J. Zhang, J. Lin and P. Cen, *Can. J. Chem. Eng*., 2008, **86**, 1047–1053.

[13] (a) H. J. Wang, D. H. Yu, P. Sun, J. Yan, Y. Wang and H. Huang, *Catal. Commun*., 2008, **9**, 1799-1803; (b) P. Sun, D. H. Yu, K. Fu, M. Gu, Y. Wang, H. Huang and H. Ying, *Catal. Commun*., 2009, **10,** 1345-1349; (c) Y. Jie, Y. Dinghua, L. Heng, S. Peng and H. He, *J. Rare Earths*, 2010, **28**, 803-806; (d) Y. Jie, Y. Dinghua, S. Peng and H. He, *Chin. J. Catal.*, 2011, **32**, 405-411; (e) J. Zhang, Y. Zhao, M. Pan, X. Feng, W. Ji

and C.-T. Au, *ACS Catal*., 2011, **1**, 32-41; (f) B. Yan, L.-Z. Tao, Y. Liang and B.-Q. Xu, *ChemSusChem*, 2014, **7,** 1568-1578.

[14] Y. Fan, C. Zhou and X. Zhu, *Catal. Rev.,* 2009, **51**, 293-324.

[15] E. Blanco, P. Delichere, J. M. M. Millet and S. Loridant, *Catal. Today*, 2014, **226,** 185-191.

[16] J. Peng, X. Li, C. Tang and W. Bai, *Green Chem.*, 2014, **16**, 108-111.

[17] J. H. Hong, J.-M. Lee, H. Kim, Y. K. Hwang, J.-S. Chang, S. B. Halligudi and Y.-H. Han, *Appl. Catal., A*, 2011, **396**, 194-200.

[18] (a) Y. Matsuura, A. Onda, S. Ogo and K. Yanagisawa, Catal. Today, 2014, **226(1),** 192-197; (b) Y. Matsuura, A. Onda and K. Yanagisawa, *Catal. Commun.*, 2014, 48, 5-10.

[19] B. Yan, L.-Z. Tao, Y. Liang and B.-Q. Xu, *ACS Catal*., 2014, **4**, 1931-1943.

[20] V. C. Ghantani, S. T. Lomate, M. K. Dongare and S. B. Umbarkar, *Green Chem*., 2013, **15**, 1211-1217.

[21] A. K. Lynn and W. Bonfield, *Acc. Chem. Res.*, 2005, **38,** 202-207.

[22] O. Mekmene, S. Quillard, T. Rouillon, J.-M. Bouler, M. Piot and F. Gaucheron, *Dairy Sci. Technol*., 2009, **89**, 301-316.

[23] H. C. W. Skinner, *Mater. Res. Bull.*, 1970, **5,** 437–448.

[24] S. Raynaud, E. Champion, D. Bernache-Assollant and P. Thomas, *Biomater.*, 2002, **23,** 1065-1072.

[25] A. M. El Kady, K. R. Mohamed and G. T. El-Bassyoun, *Ceram. Int*., 2009, **35,** 2933-2942.

[26] K.-H. Chen, M.-J. Li, W.-T. Cheng, T. Balic-Zunic and S.-Y. Lin, *Int. J. Exp. Pathol.*, 2009, **90**, 74-78.

[27] T. J. Korstanje, H. Kleijn, J. T. B. H. Jastrzebski and R. J. M. K. Gebbink, *Green Chem.*, 2013, **15**, 982-988.

[28] E. Lautemann, Justus Liebigs *Ann. Chem*., 1860, **113**, 217-220.

[29] D. Wadley, M. Tam, P. Kokitkar, J. Jackson and D. Miller, *J. Catal.*, 1997, **165**, 162-171.

[30] (a) J. C. Serrano-Ruiz and J. A. Dumesic, *ChemSusChem*, 2009, **2**, 581-586; (b) J. C. Serrano-Ruiz and J. A. Dumesic, *Green Chem*., 2009, **11**, 1101-1104.

[31] B. Odell, G. Earlam and D. J. Cole-Hamilton, *J. Organomet. Chem.*, 1985, **290**, 241-248.

[32] J. Zhang, Y. Zhao, X. Feng, M. Pan, J. Zhao, W. Ji and C.-T. Au, *Catal. Sci. Technol.*, 2014, **4,** 1376-1385.

[33] J. Zhang, X. Feng, Y. Zhao, W. Ji and C.-T. Au, *J. Ind. Eng. Chem.*, 2013, **20,** 1353-1358.

[34] C. Tang, J. Pen, G. Fan, X. Li, X. Pu and W. Bai, *Catal. Commun.*, 2014, **43,** 231-234.

[35] K. Brow, R. J. Kirkpatrick and G. L. Turner, *J. Non-Cryst. Solids*, 1990, **116,** 39-45.

Chapter 4

MoO_3 Modified Calcium Pyrophosphate - Efficient Catalyst for Lactic Acid Deoxygenation

Abstract

The catalytic deoxygenation of bio derived oxygenate, lactic acid was carried out using molybdena supported catalysts. Molybdena based catalysts on different supports like γ-Al_2O_3, SiO_2 and calcium pyrophosphate were prepared by wet impregnation method. Prepared catalysts were characterized by XRD, FTIR, NH_3 TPD, and surface area analysis. The effect of different supports on deoxygenation efficiency of molybdena was studied. Acidity was observed to play a crucial role in product selectivity *i. e.* less acidic support calcium pyrophosphate with 5wt% MoO_3 showed more deoxygenation activity as compared to acidic support γ-Al_2O_3 as well as SiO_2 with same MoO_3 loading. Higher acidity led to formation of acetaldehyde as only product. Bare supports (γ-Al_2O_3, SiO_2) mainly produced acetaldehyde as a major product. To confirm the mechanism for propionic acid formation, control experiment was carried out by hydrogenating acrylic acid using MoO_3 supported on calcium pyrophosphate catalyst under optimized conditions of deoxygenation. The results confirmed formation of propionic acid by deoxygenation of lactic acid and not by hydrogenation of acrylic acid using *in situ* generated hydrogen after decarboxylation of lactic acid to acetaldehyde.

4.1 Introduction

The consumption of petroleum has increased during the 20th century due to increased demands of energy and consumer end products for unrelenting population growth. The depleting fossil fuel reservoirs are forcing the society to develop processes utilizing renewable resources for a large scale production of chemicals and fuel. In this scenario biomass is the only sustainable renewable source available which can serve as a source for both energy and carbon, for society. Also production of energy from biomass is beneficial as it generates lower greenhouse gases compared to the combustion of fossil fuels. The CO_2 released during energy conversion of biomass is used for its subsequent regrowth; hence it does not contribute to net addition of greenhouse gases.

Due to high oxygen and water content as well as low carbon density, biomass has a low energy density compared to fossil fuels. This also results in its increased transportation costs. To increase energy and reduce transportation cost of biomass, several technologies are available; (1) gasification produces syngas (CO and H_2), which can be converted to alkanes by Fischer-Tropsch reactions; (2) fast pyrolysis produces bio-oil, where biomass is heated to 450-550 °C in absence of oxygen, with a short contact time and (3) during liquefaction, biomass is heated at higher pressure and lower temperatures (250-325 °C).[1] Bio-oils or pyrolysis oils have lower sulfur and nitrogen content but larger amount of oxygen than crude oil. Bio-oils contain more acids and water than heavy fuel oil, which causes lower energy density and corrosion problems. The high water and oxygen content of bio-oils causes a lower calorific value (15-19 MJ/kJ) compared to petroleum based oil (40 MJ/kJ), and can polymerize and condensate upon exposure to oxygen and UV light leading to transportation and storage problems. Also its properties like high viscosity, nonvolatility, corrosiveness, immiscibility with fossil fuels and thermal instability makes it incompatible with fossil fuels. Hence removal of oxygen is essential for upgrading in bio-oil.

For bio-oil upgradation, there are several methods available like, deoxygenation, hydrodeoxygenation (HDO) to remove oxygen, cracking, zeolite upgrading and forming of emulsion with diesel fuel.[2] Consequently, bio oil can be upgraded using different deoxygenation techniques such as dehydration, hydrogenolysis, hydrogenation, decarbonylation, decarboxylation and HDO. These processes include catalyzed reactions; however the water and the acidity of bio oil may lead to the catalyst deactivation. Catalytic cracking is another cheap technique compared to hydro-treatment where the O_2-rich

compounds are converted to other compounds but here the catalyst gets deactivated due to coke formation and the quality of the bio-oil is low as well. Decarbonylation/decarboxylation method showed production of oxides of carbon with reduced consumption of hydrogen as compared to HDO reactions. The loss of one carbon atom per mole of hydrocarbons, in the form of CO or CO_2, can lead to the reduction in the yield of upgradeable product. In HDO process, oxygen is removed as water which needs additional hydrogen and the consumption of high quantity of hydrogen adds to the cost of the final fuel. Hence high degree of oxygen removal, while minimizing hydrogen consumption is crucial for HDO catalyst. There are several set of catalysts available for HDO reaction such as, precious metal catalysts (such as Pd, Pt, Rh, and Ru) and non-precious metal catalysts (such as Ni and Cu).[3] These are active for hydrogenation/hydrogenolysis reactions. Drawbacks of these processes are requirement of high hydrogen pressure, saturation of all double bonds, and rapid catalyst deactivation due to coke formation and water poisoning.

Recently, molybdenum based catalysts have been explored for HDO processes for lower oxygenates such as acrolein, acetaldehyde and bio oils *etc*. For propanal and 1-propanol, Mo (110) showed highly selective deoxygenation pathway toward C-O/C=O bond scission to produce propene, while bimetallic surfaces such as Ni/Mo(110) and Co/Mo(110) showed higher activity for C-C and C-H bond scission.[4] The MoO_3 treated with hydrogen at 623K has shown high activity for dehydration of 2-propanol to propene at 398K.[5] Conversion of acrolein to propene on MoO_3 in presence of hydrogen was studied by Moberg *et al.*[6] Surface hydroxyl groups formed by interaction of hydrogen on MoO_3 surface are important for both oxygen vacancy formation and generating Brønsted acid sites. The reaction rate was controlled by protonation of the C-1 carbon of chemisorbed acrolein. Similarly oxygen vacancy formation on MoO_3 was studied by Mei *et al.*[7] for deoxygenation of acetaldehyde. Results showed the feasibility of deoxygenation of CH_3CHO to ethylene (C_2H_4) on the reduced MoO_3 (010) surface. The MoO_3 catalyst is selective for HDO of biomass derived oxygenates such as linear ketones and cyclic ethers to olefins and cyclic ketones respectively and phenolics to aromatics at low H_2 pressure.[8] Mo-based catalysts supported by different carbon materials, such as reduced graphene oxide, activated charcoal, graphite, and fullerenes were screened for HDO of maize oil. Molybdenum carbide supported on reduced graphene oxide showed highest yield (90.32%) at 700 °C.[9] Selective deoxygenation of aldehyde and alcohols such as propanal, 1-propanol, furfural and furfuryl alcohol without cleaving the C-C

bond was carried out on molybdenum carbide (Mo_2C) prepared over Mo (110) surface.[10] The HDO of guaiacol (2-methoxyphenol) has been studied over alumina, SBA-15 and silica-supported molybdenum nitride catalysts at 300 °C and 5 MPa of hydrogen pressure. The alumina supported catalysts showed higher activity compared to the SBA-15 and silica-supported catalysts.[11] Along with deoxygenation molybdenum has shown reduction of the substrate at different oxidation state, $Mo^{\delta+}$ ($0 \leq \delta < 4$) species showed activity for hydrogenation of alkadienes and alkenes.[12] Nagai *et al.*[13] have shown Mo species with lower oxidation state to have higher activity for carbazole hydrogenation than Mo species with higher oxidation state. Molybdenum ions in 5 wt% MoO_3/TiO_2 with an oxidation state of +2 are the most active species for benzene hydrogenation reaction.[14] Both Mo metal and Mo^{2+} are active for benzene hydrogenation as shown by Yamada *et al.*[15]

Lactic acid is selected in present work as the model oxygenate molecule to investigate the potential HDO reaction using the MoO_3 based catalyst, as it contains both C-O and C-C bonds. Lactic acid is a versatile precursor for different end products, simply by changing catalysts and reaction conditions. Lactic acid conversion on molybdenum-based heteropolyacids, such as phosphomolybdic acid and vanadium-substituted phosphomolybdic acids, showed mainly decarboxylation reaction leading to acetaldehyde, CO_2 and H_2 as products.[16] The formed H_2 is utilized in the production of lactic acid deoxygenated product i.e. propionic acid.

Precious metal based catalyst, such as $PtH(PEt_3)_3$ convert lactic acid to propionic acid (50% yield) at a moderate temperature of 250 °C in water at low pH.[17] Gunter *et al.*[18] have shown propanoic acid as the dominant product in lactic acid dehydration reaction on molybdenum based catalyst. A large quantity of CO_2 was produced over Na_2MoO_4. In this system molybdenum is already in its highest oxidation state (VI) and is not expected to be an effective reducing agent. Propanoic acid yield of 64% at 99% lactic acid conversion at 350 °C and 1 atm was achieved by Velenyi and Dolhyj[19] using a mixed metal oxide catalyst $Mo_5Cu_4SnO_x$ on a silica-alumina support. Thermal decomposition of alkali lactate to propionate and acetate has been observed in post reaction FTIR spectroscopy for sodium salts.[20] Katryniok *et al.*[16] used silica supported heteropoly acids (HPAs) for lactic acid reaction at 275 °C in a fixed bed gas phase reactor. The catalysts based on silicotungstic and phosphotungstic acids were significantly more active, with conversions exceeding 90%, whereas catalysts prepared from phosphomolybdic acid and vanado-phosphomolybdic acids

showed comparatively low conversions of lactic acid (i.e., 70 and 60%, respectively). But formation of propanoic acid was observed, with 3% yield over the phosphomolybdic acid and 8% over the vanado-phosphomolybdic acid, whereas the silicotungstic and phosphotungstic acids exclusively showed the formation of acetaldehyde. The analysis of the gaseous products revealed that decarboxylation of lactic acid to be more prominent over the molybdenum-based HPAs. De-oxygenation of lactic acid to propionic acid was reported using homogeneous molybdenum based catalysts.[21] Lactic acid can be converted to propionic acid by two pathways, by deoxygenation of lactic acid and by reduction of lactic acid through acrylic acid.

In the previous chapters calcium pyrophosphates (CP) has shown to be highly efficient catalyst for lactic acid dehydration.[22] In this chapter, MoO_3 supported on γ-Al_2O_3, SiO_2, CP were prepared by wet impregnation method. The deoxygenation activity of supported MoO_3 catalysts was investigated for lactic acid without using external H_2 source. Effect of different supports on deoxygenation activity was studied herein. The technical challenge is to design a catalyst or catalytic process that combines decarboxylation (CO_2 rejection) and HDO (H_2O elimination) while minimizing hydrogen consumption in order to improve bio-oil stability.

4.2 Experimental Section

4.2.1 Materials

Calcium nitrate, di-ammonium hydrogen phosphate, ammonia solution and ammonium heptamolybdate were obtained from Thomas Baker chemicals India Ltd., ES-40 was obtained from Chemplast, Chennai, CAS registry no. 18945-71-7 and commercially available bohemite (AlOOH) was used as a precursor of γ-Al_2O_3. Lactic acid (89%) is used from our CSIR-National Chemical Laboratory (CSIR-NCL) Pune pilot plant which is obtained from sugarcane fermentation process (process developed by CSIR-NCL). The chemicals were used without further purification.

4.2.2 Catalyst preparation method

4.2.2a Support preparation

Calcium pyrophosphate (CP) catalyst was prepared by the co-precipitation method. Calcium nitrate (38.9 g), diammonium hydrogen phosphate (14.5 g) solutions of desired

concentration were prepared in deionized water (125 mL each). The 5% ammonium hydroxide solution was added in both the solutions till pH is 8. Calcium nitrate solution was added to diammonium hydrogen phosphate solution, drop wise with constant stirring. A thick white precipitate was formed, was aged for 12 h then filtered, washed with deionized water and dried in an oven at 120 ºC overnight. The dried calcium phosphate was calcined at 600 ºC for 4 h.

Gamma alumina (γ-Al_2O_3) was prepared by calcining boehmite at 500 °C for 5 h.

Silica was prepared from ES-40 by sol-gel method. ES-40 (52 g) was added to dry IPA (30 g); to this mixture ammonium hydroxide solution (25% aqueous) in IPA was slowly added with constant stirring. Obtained gel was air dried and calcined at 500 °C for 5 h.

4.2.2b MoO_3 supported catalyst preparation using wet impregnation method

To slurry of different supports (CP, γ-Al_2O_3, SiO_2) in distilled water (100 mL), ammonium heptamolybdate dissolved in water was added drop wise with constant stirring. The resultant slurry was dried by evaporating the water on hot plate then in oven at 120 °C for 12 h. The dried catalyst was calcined at 600 ºC (4 h) for CP and at 500 ºC (5 h) for γ-Al_2O_3, SiO_2 supports.

4.2.3. Catalyst characterization

The X-ray diffraction analysis was carried out using a Rigaku X-ray diffractometer (Model DMAX IIIVC) equipped with a Ni filtered Cu Kα radiation (λ = 1.5406 Å, 30 kV, 15 mA). The data was collected in the 2θ range 20-80° with a step size of 0.02° and scan rate of 4°/min.

FTIR measurements were carried out using Shimadzu 8300 as KBr pellet in the range of 4000-400 cm^{-1} region with 4 cm^{-1} resolution averaged over 100 scans.

BET surface area of the calcined samples was determined using NOVA 1200 Quanta chrome instrument. Prior to N_2 adsorption, the sample was evacuated at 250 °C. The specific surface area was determined according to the BET equation.

Temperature programmed desorption of ammonia (NH_3-TPD) was carried out using a Micromeritics Autocue 2910. For TPD measurement ~0.1 g catalyst sample was used.

Sample was dehydrated at 500 °C for 1 h in 50 mL min^{-1} helium flow and then cooled to 50 °C. Probe gas 5% NH_3 in helium was then adsorbed for 1 h in 50 mL min^{-1} flow. The temperature was raised up to 600 °C at a rate of 10 °C min^{-1} in 30 mL min^{-1} helium flow.

4.2.4 Catalyst activity test

Vapor phase lactic acid deoxygenation was carried out using a quartz fixed bed down flow reactor (id-11 mm) at atmospheric pressure. Reactor was charged with catalyst (particle size 20-40 mesh) in the middle section with quartz wool packed in both the ends. Porcelain beads were placed above the catalyst bed in order to preheat the feed. Before catalytic evaluation, the catalyst was preheated at required reaction temperature for 30 minute under flow of nitrogen (15 mL min^{-1}). The reaction temperature was measured using a thermocouple inserted in the catalyst bed. Lactic acid of required concentration (typically 50% w/w in water) was pumped in to the preheating zone of reactor using peristaltic pump and nitrogen gas as carrier. The reaction products were collected in a cold trap at 8 °C. The reaction mixture was analysed using gas chromatograph (Perkin Elmer) equipped with a FFAP capillary column and FID detector. The GC was calibrated by external standard method. The formation of CO and CO_2 was confirmed by GC, with molecular sieve 5A and porapack Q column respectively using TCD detector.

Hydrogenation of acrylic acid was carried using 5% MoO_3/CP (4 g) under vapor phase condition using 2% H_2 in He (40 mL min^{-1}) at 375 °C with 5% acrylic acid solution in water. The reaction mixture was analyzed using gas chromatograph (Perkin Elmer) equipped with a FFAP capillary column and FID detector.

4.3 Result and Discussion

4.3.1 The powder X-ray diffraction (XRD)

The XRD pattern (Fig. 4.1a) of CP showed the crystalline nature with diffraction peaks at 26.7, 27.7, 28.9, 29.3, 30.69 and 32.37º, confirming the structure to be β calcium pyrophosphate (JCPDS-33-0297).[22] The powder XRD patterns of 5 wt% Mo loaded CP showed the retention of β CP support structure along with peaks at 2θ=12.83, 23.34, 25.7, 27.37º, corresponding to α- MoO_3 species.[23]

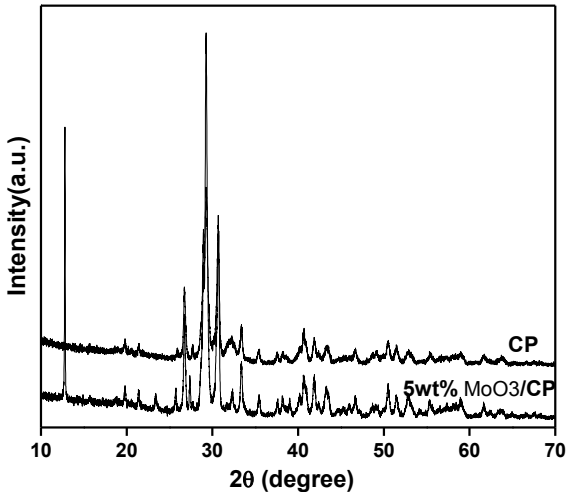

Fig.4.1a The powder X-ray diffraction (XRD) patterns of synthesized MoO_3 loaded CP catalysts.

The XRD pattern of alumina (Fig. 4.1b) confirmed the presence of γ-alumina phase (10-0425 JCPDS).[24] In powder XRD pattern of 5 wt% Mo loaded γ-Al_2O_3, peaks corresponding to molybdena phase were not observed; hence molybdena could be highly dispersed on support. The structure of γ-Al_2O_3 support was retained in MoO_3 loaded catalyst.

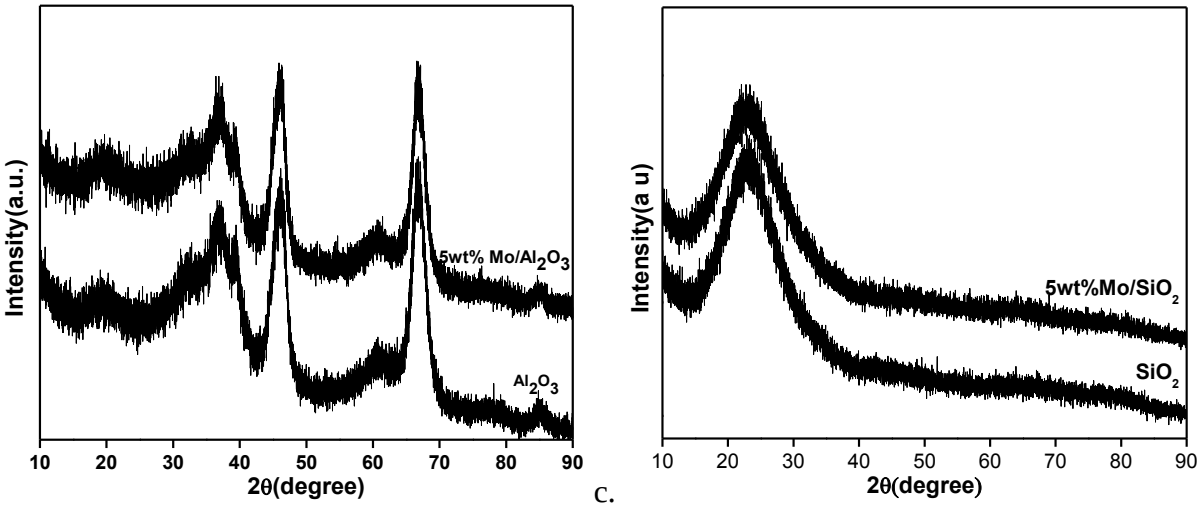

c.

Fig.4.1b, c The powder X-ray diffraction (XRD) patterns of synthesized MoO_3 loaded a) alumina b) silica catalysts.

The XRD pattern (Fig. 4.1c) of SiO_2 showed the amorphous nature with diffraction hump around 24º.[23] The XRD pattern of 5 wt% Mo loaded SiO_2 showed only retention of support structure with absence of peaks corresponding to molybdena phase, therefore it can be concluded that molybdena was highly dispersed on support.

4.3.2 FTIR spectroscopic studies

Catalyst structure was further studied by FTIR spectroscopy. Typical pyrophosphate stretching and bending vibrations were observed for CP at 1215-941 and 723 cm^{-1} respectively as shown in Fig. 4.2a. Bands at 613-494 cm^{-1} were assigned to phosphate bending vibrations.[22] With retention of pyrophosphate structure, no additional peaks corresponding to MoO_3 were observed in 5 wt% Mo loaded CP. The IR spectrum of MoO_3 loaded Al_2O_3 sample (Fig. 4.2b), presents a wide unresolved pattern extending from 435 to 920 cm^{-1} with maximum absorbance around 540 and 880 cm^{-1}. This unresolved wide structure is typical of a complex and disordered crystallographic structure. The two wide structures at 540 and 880 cm^{-1} were assigned to AlO_6 and AlO_4 stretching respectively. Hydroxyl group presence was confirmed by the hump at 3439 cm^{-1} assigned to Al-OH.[24] No additional peaks corresponding to MoO_3 were observed for 5 wt% MoO_3 loaded Al_2O_3. The IR spectrum of MoO_3 loaded SiO_2 (Fig. 4.2c, d) showed the main peak characteristic of Keggin structures at 913 and 956 cm^{-1}. These bands were assigned to the vibrations of the terminal Mo-O-Si and Mo=O bonds, respectively. The band at 756 cm^{-1} assigned to Mo-O-Mo vibrations was absent. Broad band at 1099 cm^{-1} confirmed the presence of Si-O-Si bond in SiO_2.[23]

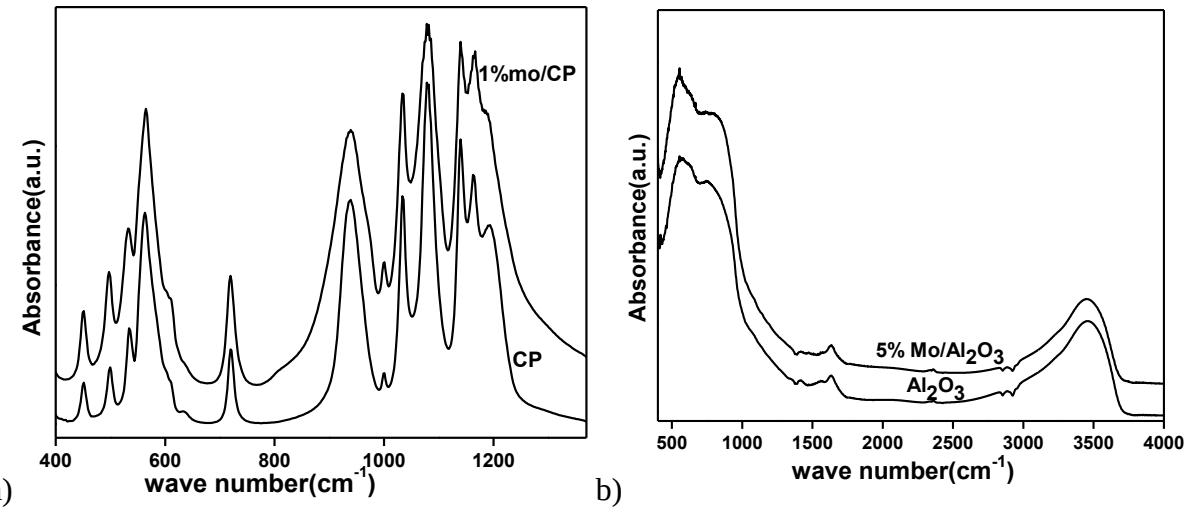

a) b)

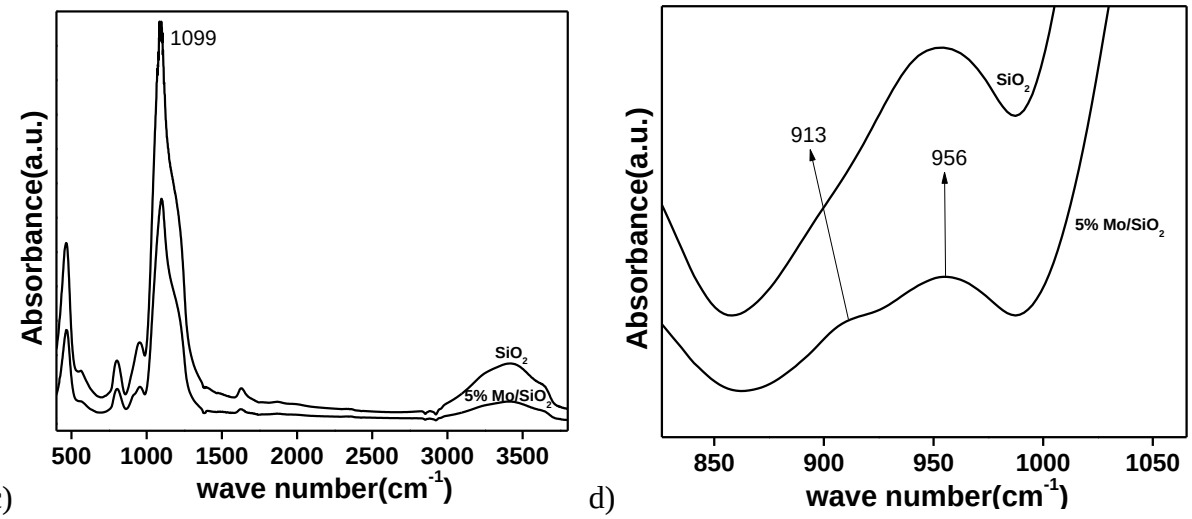

Fig. 4.2 FTIR spectra of a) MoO_3 loaded CP catalysts, b) MoO_3 loaded alumina catalysts and c, d) MoO_3 loaded silica catalysts.

4.3.3 Temperature programmed desorption studies

The acid properties of the catalysts were evaluated by temperatures programmed desorption (TPD) of NH_3 and the results are shown in Table 4.1. For MoO_3 supported on CP showed less acidity as compared to γ-Al_2O_3, and SiO_2 supports. Acidity of MoO_3 loaded CP and bare CP was comparable with no considerable difference but in case of bare γ-Al_2O_3, SiO_2, with MoO_3 loading, significant increase in acidity was observed. This difference may be due to the nature of MoO_x species formed on different supports.

Table 4.1 Textural characterization, acidity of synthesized catalysts

Entry	**Catalyst**	**Acidity mmoles / g**	**Surface Area, m^2/g**
1	CP	0.071	33
2	5 wt% Mo/CP	0.067	28
3	SiO_2	0.21	392
4	5 wt% Mo/ SiO_2	0.546	292
5	γ-Al_2O_3	0.429	237
6	5 wt% Mo/γ-Al_2O_3	0.588	182

4.3.4 Surface area analysis

The surface areas of all catalysts determined using the BET method are shown in Table 4.1. The surface area of SiO_2 support was higher compared to other supports. The surface area for SiO_2 was 392 m^2/g, which decreased after introduction of MoO_3. The decrease in surface area is attributed to the blockage of pores of SiO_2 by the deposition of molybdena species. Similarly for γ-Al_2O_3 there was significant decrease in surface area upon MoO_3 loading due to blockage of pores from 237 to 182 m^2/g. On the other hand there is only marginal decrease in surface area of CP catalysts after MoO_3 loading. It has been shown previously that the addition of tungsten or nickel on calcium phosphate does not change the surface area significantly.[25] The surface area decreased for all supports upon MoO_3 loading. This indicates the uniform distribution of MoO_3 on SiO_2 and γ-Al_2O_3 surface as seen in XRD studies.

4.4 Catalytic Activity

The synthesized catalysts were tested for vapour phase deoxygenation of lactic acid and the results are shown in Table 4.2. The reaction was carried out using fixed bed down flow reactor using 50% lactic acid at 375 °C with WHSV 3 h^{-1}. All the prepared catalysts have shown 100% conversion of lactic acid at 375 °C under identical reaction conditions except 5wt% MoO_3/CP (89%). On the other hand the product selectivity was different in case of different supports, indicating that the structure of the catalysts has significant influence on the catalytic activity.The CP catalyst has mainly shown dehydration product acrylic acid and acetaldehyde as previously seen in chapter 3. The other supports such as γ-Al_2O_3, SiO_2 have shown maximum selectivity for acetaldehyde by decarbonylation with small amount of acetic acid. Here for all supports, acetaldehyde is formed by the decarbonylation of lactic acid giving CO and H_2O as a gaseous products as confirmed by the tail gas analysis. MoO_3 loading on γ-Al_2O_3 and SiO_2, decreased the selectivity for acetaldehyde with marginal increase in selectivity for propionic acid. The MoO_3 loaded CP, showed increase in the propionic acid selectivity from 3% to 26% with decrease in the acrylic acid selectivity from 55% to only 3%. This indicates that MoO_3 triggered H_2 generation which in turn deoxygenated lactic acid to propionic acid.[16] The gas analysis showed an increase in CO_2 concentration confirming decarboxylation generating hydrogen along with acetaldehyde for MoO_3 loaded catalysts. Due to the volatile nature of the acetaldehyde the mass balance was low for the reaction where maximum selectivity for acetaldehyde was obtained. Bare support

CP has shown 90% mass balance and rest of the catalysts have shown 80-85 % mass balance. Here the amount for CO and CO_2 were calculated from the selectivity's of acetaldehyde and propionic acid. When all supports were compared, CP upon MoO_3 loading has shown maximum selectivity for propionic acid. This indicated that MoO_3 on less acidic support favours more H_2 formation compared to other supports, leading to more deoxygenated product.

In the present studies MoO_3 loaded CP catalyst has shown better deoxygenation activity with water as a solvent, with 50% concentration. Here no external hydrogen source was provided for HDO. The formed hydrogen in decarboxylation pathway was utilized for deoxygenation. Both water and the acidity of reactant feed did not cause catalyst deactivation as well as no formation of methanation products. Hence the active catalyst can be explored further for deoxygenation of bio oil without external hydrogen source.

Table 4.2: Reaction results of deoxygenation of lactic acid to propionic acid using different catalysts

Sl. No	Catalyst	Conv. (%)	Selectivity (%)				
			Acetaldehyde	Propionic acid	Acrylic acid	Acetic acid	Other products[#]
1	CP	100	30	2	55	--	13
2	5% Mo/CP	89	64	26	3	--	7
3	γ-Al_2O_3	100	80	--	1	9	10
4	5% Mo/ γ-Al_2O_3	100	78	4	1	3	14
5	SiO_2	100	90	2	--	5	3
6	5% Mo/SiO_2	100	80	12	--	3	5

Reaction conditions: Temperature- 375 °C, LA concentration-50 wt% in water, WHSV- 3 h^{-1}, N_2 flow-25 mL/min. [#] polylactates, 2,3 pentanedione.

4.4.1 Hydrogenation of acrylic acid

Propionic acid could be obtained from lactic acid through two pathways as shown in scheme 4.1, either through an intermediate acrylic acid by further hydrogenation or through direct lactic acid deoxygenation. To confirm which pathway was operating for present

catalytic system, hydrogenation of acrylic acid was carried out using external H_2 source. Hydrogenation of acrylic acid (5% in water) was carried out with 5% MoO_3/CP under vapor phase conditions at 375 °C using external H_2 source (5% H_2 in He). Reaction showed only 4% acrylic acid conversion with 1% selectivity for propionic acid with acetic acid and acetaldehyde as byproducts. From these experimental results we ruled out the second pathway for propionic acid formation from lactic acid via acrylic acid intermediate.

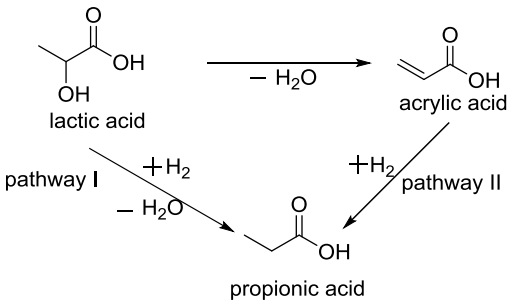

Scheme 4.1 General schematic for lactic acid conversion to propionic acid.

MoO_3 supported on CP showed higher selectivity for propionic acid (26%) compared to γ-Al_2O_3 and SiO_2. Impregnation of MoO_3, on these supports introduces deoxygenation of lactic acid to propionic acid using H_2 which is formed *in situ* due to decarboxylation of lactic acid to acetaldehyde. In previous work we have shown CP as an efficient catalyst for lactic acid dehydration to acrylic acid and acetaldehyde as only by-product occurring through decarbonylation. Lactic acid conversion on bare supports like silica, alumina has been studied before in the literature. Lactic acid conversion on silica-alumina (93% Al_2O_3 : 7% SiO_2) at 350 °C, has shown mainly decarbonylation to acetaldehyde.[26] Zhai *et al.* [27] have shown formation of acetaldehyde through decarboxylation of lactic acid using phosphomolybdic acid, ferric sulphate. When aluminium phosphate and aluminium sulfate $Al_2(SO_4)_3$ were utilized for lactic acid conversion, acetaldehyde was the major product occurring through decarbonylation pathway. When dehydration of methyl lactate was carried out on SiO_2 support at 380 °C, it showed acetaldehyde as a major product occurring mainly through decarbonylation pathway.[28] In literature when alumina and silica based catalysts were screened for lactic acid conversion, acetaldehyde was the major product occurring through decarbonylation. Katryniok *et al.*[16] used silica supported heteropoly acids (HPAs) as catalysts at 275 °C in a fixed bed gas phase reactor for lactic acid reaction. Tungsten based HPAs have shown acetaldehyde as a major product through decarbonylation, whereas molybdena based

HPAs showed acetaldehyde formation through decarboxylation, giving reduction of lactic acid to propionic acid using hydrogen co-produced with CO_2. In present work by introducing molybdena on CP, Al_2O_3, SiO_2, decarboxylation of lactic acid became prominent, which leads to the formation of CO_2 and H_2. Upon MoO_3 loading decarboxylation pathway was favored and the formed H_2 was used to form propionic acid.

4.4.2 Activation of H_2 by catalyst and subsequent hydrodeoxygenation of lactic acid

Conversion of lactic acid to propionic acid can occur through deoxygenation of lactic acid using formed H_2 in decarboxylation of lactic acid. The direct hydrogenation of acrylic acid using 5% MoO_3/CP, results ruled out the pathway II as shown in scheme 4.1. As the propionic acid is not forming through acrylic acid, it is confirmed that it is occurring through deoxygenation of lactic acid. MoO_3 species present in the catalysts are assisting the deoxygenation of lactic acid. Recently there are few reports on use of molybdena based catalysts for deoxygenation of alcohols, acrolein, acetaldehyde and bio oils *etc*.

An important feature of the MoO_3 catalyst is selective cleavage of C-O bonds without cleaving C-C bonds *i. e.* the main reaction products contain the same number of carbon atoms as that of the parent reactant. The average bond dissociation energies decrease in order of R=O> Mo=O > Ar-OH > Ar-OR > R-OH > R-OR.[8] Hence, direct C=O bond cleavage is thermodynamically unfavorable as the energy gained from the Mo=O bond formation is less than the energy required for breaking the C=O bond, and also the average bond enthalpy for C=O (at 298 K) is lower than C-O (358 kJ/mol).[29] Therefore in present work the deoxygenation of lactic acid is occurring at -COH than at -COOH, hence C-O bond breaking and the Mo-O bond forming will lead to a positive net energy gain, suggesting that the HDO process is energetically favorable. The important key features of HDO catalyst to be active are, lattice oxygen defects and the relative strength of M-O vs C-O bonds, the structural stability of metal oxides undergoing significant reduction, hydrogen bronze formation; and the relative rate of substrate reactivity and catalyst regeneration. For HDO, if the surface metal-oxygen bond is stronger, then to create surface vacancies for adsorption of the substrate is difficult, but if the metal-oxygen bond is too weak, then for metal to abstract oxygen from the molecule is difficult.[30] There are three different oxygen sites available on the perfect α-MoO_3(010) surface, i.e., the single bonded terminal oxygen (Ot), the asymmetric bicoordinated bridging oxygen (Ob), and the symmetric tricoordinated bridging oxygen (Os). Adsorption of single atomic H at the stoichiometric O-terminated MoO_3 (010) surface forms a

surface hydroxyl. Formation of the HOt group is energetically more favorable than the HOb and HOs.[7] Hydrogen activation by oxo-molybdenum (IV) compounds was studied by Reis *et al.*[31] As the H_2 molecule approaches metal octahedral coordination sphere, H-H bond is very long (1.099 A˚) in the resulted transition state, while the O-H and Mo-H bonds are partially formed (1.197 and 1.950A˚), and is heptacoordinate, displaying a very distorted coordination environment. In H_2 bronze formation, H_2 reacts with MoO_3 and forms H_2MoO_3, which eliminates water and forms oxygen vacancy and abstract oxygen from substrate. With this background mechanism for lactic acid deoxygenation reaction on 5wt% Mo/CP can be proposed as follows:

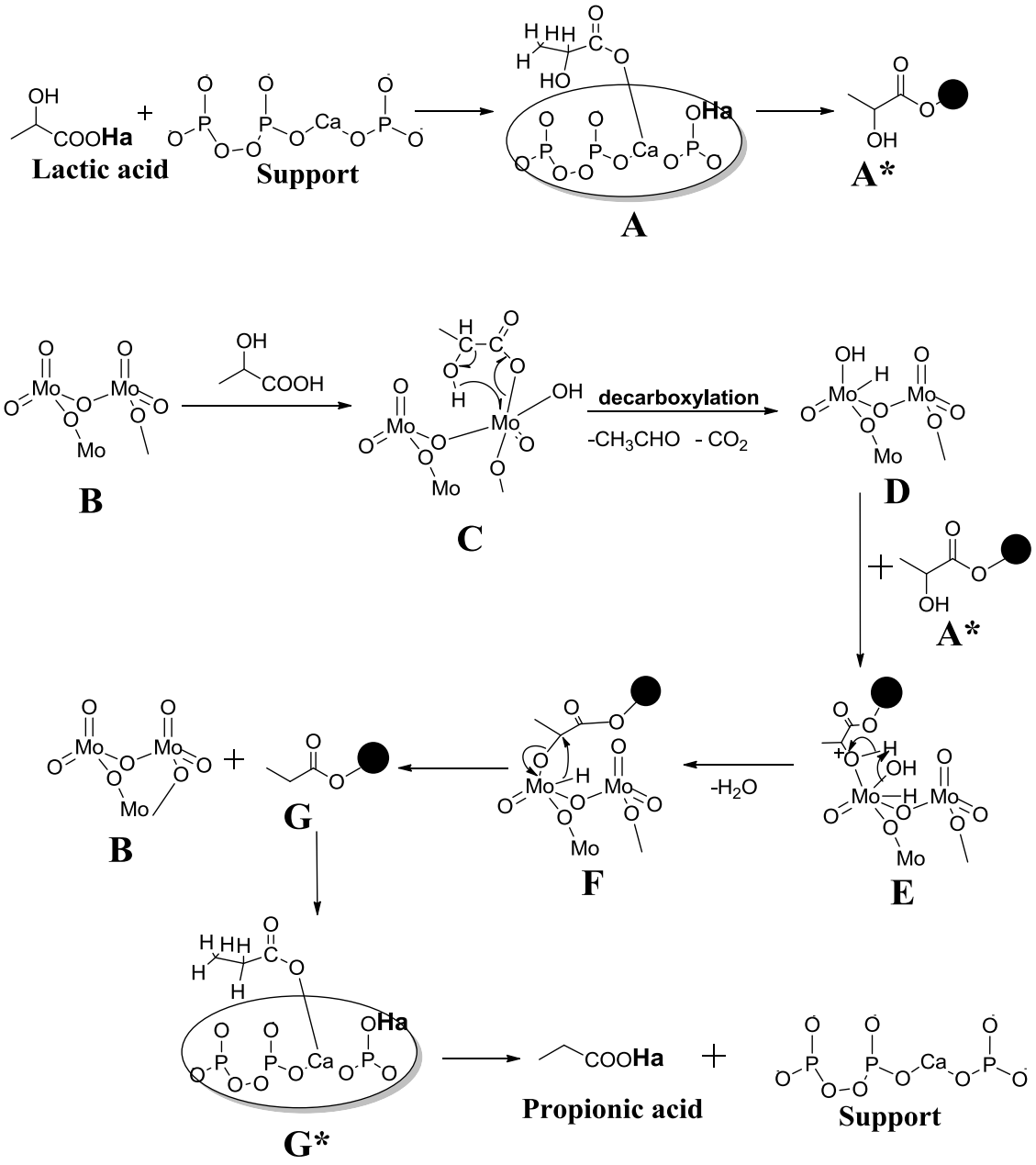

Scheme 4.2 Proposed mechanisms for lactic acid deoxygenation on MoO_3/CP.

As shown in chapter 3, the CP catalyst forms calcium lactate with free lactic acid confirmed by *in situ* FTIR studies. In the present catalytic system, lactic acid reacts with CP and forms calcium lactate A as shown in scheme 4.2. Here phosphate oxygen abstracts proton from carboxylic group of lactic acid and calcium present in the support forms Ca-OOC- bond with lactate group. Further A was represented by A* showing support as a bullet. The remaining free lactic acid which has not formed calcium lactate reacts with MoO_3 (B) and forms molybdenum complex C. Molybdena oxygen abstracts carboxylic proton (-COOH) of lactic acid to give Mo-OH bond and molybdenum forms Mo-OOC- bond with lactate (Mo-lactate). The molybdenum in C abstracts hydride from hydroxyl group of lactic acid and simultaneously decarboxylates activated lactic acid to acetaldehyde and CO_2. By eliminating acetaldehyde and CO_2, C forms molybdenum hydrido hydroxyl complex D. The hydroxyl group of calcium lactate formed by the reaction of lactic acid with support CP (A*), reacts with the H_2 activated MoO_3 (D), and forms complex E. Here in complex E, molybdenum is hepta co-ordinated. Subsequently, hydroxyl group attached to molybdenum abstracts proton from lactic acid and gets eliminated as water. The elimination of water creates oxygen vacancy on molybdenum (F) which can be fulfilled by taking oxygen from lactic acid hydroxyl group. The formed transition state F, abstracts oxygen from the substrate lactic acid and donate hydride to the lactic acid. This step leads to the formation of calcium propionate, G and gives back molybdena species B. Further propionate group abstracts proton from P-OHa (G*) and forms propionic acid as a product giving support back. In case of calcium pyrophosphate, part of lactic acid carboxyl group is protected by Ca of CP, reducing decarbonylation/decarboxylation to acetaldehyde. Upon loading MoO_3 on CP, decarboxylation becomes feasible as compared to decarbonylation. The formed Ca-lactate utilizes hydrogen, formed through decarboxylation, and shows deoxygenation product propionic acid (26%). Whereas for SiO_2, Al_2O_3, no such protection of carboxylic group of lactic acid was possible, hence major selectivity for decarboxylation/decarbonylation product was obtained with less selectivity for deoxygenation product propionic acid. With increase in the acidity of the catalyst, the decarbonylation/decarboxylation of lactic acid occurred predominantly compared to other pathways. The selectivity trend for propionic acid was in agreement with acidity of catalysts, 5wt% Mo/CP > 5wt% Mo/SiO_2 > 5wt% Mo/γ-Al_2O_3.

4.5 Conclusions

MoO_3 supported on calcium pyrophosphate (CP), was active for lactic acid deoxygenation. Upon MoO_3 loading acetaldehyde formation was through decarboxylation of lactic acid generating hydrogen. *In situ* generated molybdenum hydrido hydroxyl species by lactic acid decarboxylation reaction might be deoxygenationg lactic acid to propionic acid. Acidic bare supports γ-Al_2O_3, SiO_2 mainly showed acetaldehyde formation, whereas weakly acidic calcium pyrophosphate support showed acrylic acid as a major product. Highest propionic acid selectivity was observed on 5 wt% MoO_3/CP. Hence we conclude that molybdena supported on weakly acidic support is required to achieve better activity for deoxygenation.

4.6 References

[1] a) G. Huber and A. Corma, *Angewandte Chemie*, 2007, **46**, 7184-7201, b) D. Elliot, *Energy and Fuels*, 2007, **21**, 1792-1815.

[2] G. Huber, S. Iborra and A. Corma, *Chem. Rev*. 2006, **106**, 4044-4098.

[3] (a) R. C. Runnebaum, T. Nimmanwudipong, D. E. Block and B. C. Gates, *Catal. Sci. Technol*., 2012, **2,** 113-118, (b) S. Sitthisa and D. E. Resasco, *Catal. Lett*., 2011, **141,** 784- 791, (c) S. Sitthisa, T. Pham, T. Prasomsri, T. Sooknoi, R. G. Mallinson and D. E. Resasco, *J. Catal*., 2011, **280**, 17-27.

[4] MyatNoeZin Myint and J. G. Chen, *ACS Catal*. 2015, **5**, 256-263.

[5] T. Matsuda, Y. Hirata, H. Sakagami and N. Takahashi, *Chem. Let.*, 1997, 1261-1262.

[6] D. R. Moberg, T. J. Thibodeau, F. G. Amar and B. G. Frederick, *J. Phys. Chem. C.*, 2010, **114**, 13782-13795.

[7] D. Mei, A. M. Karim, and Y. Wang, *J. Phys. Chem. C,*, 2011, **115**, 8155-8164.

[8] T. Prasomsri, T. Nimmanwudipong and Y. Roman-Leshkov, *Energy Environ. Sci.*, 2013, **6**, 1732-1738.

[9] Y. Qin, L. He, J. Duan, P. Chen, H. Lou, X. Zheng, and H. Hong, *Chem. Cat. Chem*., 2014, **6**, 2698-2705.

[10] K. Xiong, W. Yu, and J. G. Chen, *Appl. Surf. Sci.* 2014, **323**, 88-95.

[11] I. T. Ghampson, C. Sepulveda, R. Garcia, J. L. Garcia Fierro, N. Escalona, and W. J. DeSisto, *Applied Catalysis A: Gen.* 2012, **435-436,** 51-60.

[12] Yuanzhi Li, Y. Fan, and G. Luo, *Ind. Eng. Chem. Res.* 2004, **43,** 1334-1339.

[13] M. Nagai, Y. Goto, A. Miyata, M. Kiyoshi, K. Hada, K. Oshikawa, and S. Omi, *J. Catal.* 1999, **182**, 292-301.

[14] R. B. Quincy, M. Houalla, A. Proctor, and D. M. Hercules *J. Phys. Chem.* 1990, **94**, 1520-1526.

[15] M. Yamada, J. Yasumaru, M. Houalla, and D. M. Hercule, *J. Phys. Chem.* 1991, **95**, 7037-7042.

[16] B. Katryniok, S. Paul and F. Dumeignil, *Green Chem.*, 2010, **12**, 1910-1913.

[17] B. Odell, G. Earlam, and D.J. Cole-Hamilton, *J. Organomet. Chem.* 1985, **290,** 241-248.

[18] G.C. Gunter, R.H. Langford, J.E. Jackson, and D.J. Miller, *Ind. Eng. Chem. Res.*,1995, **34**, 974-980.

[19] Preparation of aliphatic carboxylic acids and aldehydes by upgrading alpha-

hydroxycarboxylic acids, l. j. velenyi, Lyndhurst, and s. r. dolhyj, **US Patent 4,663,479.**

[20] M. S. Tam, G. C. Gunter, R. Craciun, D. J. Miller, and J. E. Jackson, *Ind. Eng. Chem. Res.* 1997, **36,** 3505-3512.

[21] T. J. Korstanje, H. Kleijn, Johann T. B. H. Jastrzebski and Robertus J. M. Klein Gebbink, *Green Chem.*, 2013, **15**, 982-989.

[22] V. C. Ghantani, M. K. Dongare and S. B. Umbarkar, *RSC Adv.*, 2014, **4**, 33319-33326

[23] T. V. Kotbagi, A. V. Biradar, S. B. Umbarkar, M. K. Dongare *Chem. Cat. Chem.* 2013, **5,** 1531 – 1537.

[24] A. Boumaza, L. Favaro, J. Ledion, G. Sattonnay, J. B. Brubach, P. Berthet, A. M. Huntz, P. Roy, and R. Tetot, *J. Sol. State Chem.*, 2009, **182,** 1171-1176.

[25] a) D. Stosic, S. Bennici, S. Sirotin, C. Calais, Jean-Luc Couturier, Jean-Luc Dubois, Arnaud Travert, Aline Aurouxa, *App. Catal. A: Gen.* 2012**, 447- 448,** 124-134; b)Z. Boukha, M. Kacimi, M. Fernando R. Pereira, J. L. Faria, Jose Luıs Figueiredo, and M. Ziyad, *App. Catal. A: Gen.* 2007, **317**, 299-309.

[26] G. C. Gunter, D. J. Miller and J. E. Jackson, *J. Catal*., 1994, **148,** 252-260.

[27] a) Z. Zhai, X. Li, C. Tang, J. Peng, N. Jiang, W. Bai, H. Gao and Y. Liao, *Ind. Eng. Chem. Res*, 2014, **53**, 10318–10327; b) C. Tang, J. Peng, X. Li, Z. Zhai, W. Bai, N. Jiang, H. Gao and Y. Liao**,** *Green Chem.***,** 2015, **17**, 1159-1166.

[28] Z. Zhang, Y. Qu, S. Wang, and J. Wang, *Ind. Eng. Chem. Res.* 2009**, 48**, 9083-9089.

[29] L. Pauling, *The Nature of the Chemical Bond*; Cornell University Press: Ithaca, NY, 1960.

[30] D. R. Moberg, T. J. Thibodeau, F. G. Amar, and B. G. Frederick, *J. Phys. Chem. C*, 2010, **114**, 13782-13795.

[31] P. M. Reis, P. J. Costa, C. C. Romao, J. A. Fernandes, M. J. Calhorda and B. Royo, *Dalton Trans.*, 2008, **13**, 1727-1733.

Chapter 5

Summary of the Thesis

Abstract:

This chapter delivers the overall summary of the outcomes and highlights the new observations.

Biomass is the only sustainable renewable source available for energy and carbon based chemicals. Consumption of carbohydrates as chemical raw material in refinery will eliminate several capital-intensive, oxidative processes used in the petroleum industry. Carbohydrates provide a sustainable route to stereo- and regiochemically pure products such as alcohols, carboxylic acids, and esters thus reducing the dependence on expensive catalysts that are currently required to install selective chemical functionality in petrochemicals. The three main aspects necessary for a biomass economy are: (1) growth of the biomass feedstock, (2) biomass conversion into a fuel, and (3) fuel utilization. Wide variety of products can be formed from biomass depending on the different treatments applied. Thermochemical processing such as pyrolysis of biomass produces pyrolysis oil which is upgraded to chemicals, by hydrodeoxygenation. Bio-based feedstock lactic acid derived plastics have replaced petrochemicals based ones due to their biological compatibility and hydrolytic degradation. Hence lactic acid was added among top 30 value-added chemicals. It is commercially produced from sugar by fermentation. Commercially 20-90% lactic acid solution is available, but due to the esterification tendency, a 90 wt% solution in equilibrium only contains 66% free lactic acid, while rest 24% is encountered in the dimer form. Lactic acid can also be produced chemically from bio based feedstock such as cellulose, rice husk, glycerol *etc*. It can be converted efficiently to various valuable chemicals. Various transformations of lactic showed two major reaction pathways, dehydration and esterification. Dehydration leads to acrylic acid, which has tremendous applications in the synthesis of super adsorbent polymers. Different phosphate based heterogeneous catalysts have been tested previously for lactic acid dehydration. However, a few drawbacks were observed in these reactions (catalysts) such as lower selectivity to acrylic acid, use of very less WHSV, low lactic acid concentration, deactivation of catalyst and more number of side products. Hence it is essential to explore some new catalyst formulation for further development. Thorough details of different forms of calcium phosphate were discussed in this work. Depending on the different Ca/P ratio, different forms of calcium phosphates are available. The scope and objective of the present thesis work is highlighted in chapter 1.

Lactic acid dehydration to acrylic acid is acid catalyzed reaction. Moderate acidity is required to get more selectivity for acrylic acid since strong acid catalysts led to the formation of

acetaldehyde. Hydroxyapatites (HAP's) which have mild acidity were prepared by co-precipitation method. The HAP's with different Ca/P ratio were obtained by adjusting different pH of a precursor solution. Though synthesised catalysts have different Ca/P ratio, the detail characterisation showed stoichiometric structure of HAP. Non stoichiometric HAP with Ca/P ratio of 1.3 (HAP-3) showed highest activity. HAP-3 has showed 100% conversion of lactic acid and 60% selectivity towards acrylic acid at 375 °C for a 50% (w/w) aqueous solution of lactic acid. As the acidity of the catalysts was increased, the selectivity for acrylic acid increased. The highest activity has been correlated to the synergistic effect of higher acid site density and weak basic site density of HAP-3. High per pass yield was obtained by using high lactic acid concentration (50%) with very high WHSV 3 h^{-1}. Catalyst life time studies showed the HAP-3 catalyst is stable up to 300 h under optimized reaction conditions. The only side product acetaldehyde, was formed by the decarbonylation and not by decarboxylation of lactic acid. This was confirmed by the gas chromatography analysis. Formation of Ca-lactate is crucial for acrylic acid selectivity, which protects carboxylic group of lactic acid and avoids decarbonylation as shown by *in situ* FTIR studies. The proposed mechanism based on *in situ* FTIR studies showed that formation of phosphate ester with hydroxyl group of lactic acid, led to the dehydration of lactic acid. While, the formation of phosphate ester with carboxylic group of lactic acid led to the decarbonylation of lactic acid.

Calcium pyrophosphate's (CP) which is another class of calcium phosphate were screened for lactic acid dehydration. The CP catalysts again with different Ca/P ratio were prepared by co-precipitation method. The CP catalysts with different Ca/P ratio were obtained by using different sodium phosphates at different pH along with calcium and phosphorous precursor solution. The pH of different precursors affected the final Ca/P ratio in final catalyst. Though synthesised catalysts have different Ca/P ratio, the detail characterization revealed the formation of pyrophosphate structure for prepared series of catalysts. Non stoichiometric CP with Ca/P ratio of 0.76 (CP-3) showed highest activity. There was100% conversion of lactic acid and 78% selectivity towards acrylic acid at 375 °C for a 50% (w/w) aqueous solution of lactic acid on CP-3. The highest activity has been correlated to the synergistic effect of higher acid site density and weak basic site density of CP-3. Formation of higher quantity of Ca-lactate was crucial for

acrylic acid selectivity as shown by *in situ* FTIR studies. *In situ* FTIR showed the formation of Ca-lactate for lower Ca/P ratio, which was also, supported by ^{31}P MAS NMR analysis of all CP catalysts.

Biomass after pyrolysis contains more oxygenated products which lowers its energy density compared to fossil fuels. It has large amount of oxygen with lower sulfur and nitrogen content than crude oil. The high water and oxygen content of pyrolysis oil leads to lower calorific value (15-19 MJ/kJ) compared to petroleum based oil (40 MJ/kJ). It can polymerize and condense upon exposure to air and UV light leading to problems of storage and transportation. Also due to high viscosity, non-volatility, corrosiveness, immiscibility with fossil fuels and thermal instability of pyrolysis oil make it incompatible with fossil fuels. Hence removal of oxygen is essential for upgrading in bio-oil. Upgradation of pyrolysis oil is carried out by hydrodeoxygenation. Here, in this work lactic acid was considered as a model substrate for hydrodeoxygenation reaction. The catalytic deoxygenation of lactic acid was carried out using molybdenum supported catalysts. The 5wt% MoO_3 on CP showed higher activity for deoxygenation of lactic acid at 375 °C for a 50% (wt/wt) aqueous solution of lactic acid. The oxygen vacancy on Mo (VI) created by the hydrogen bronze formation eliminates hydrogen as water. The hydrogen formed during decarboxylation of lactic acid to acetaldehyde created oxygen vacancy on molybdenum. This vacancy was filled by the abstraction of oxygen from -OH group of lactic acid, leading to deoxygenated product. Results of hydrogenation of acrylic acid proved that propionic acid was formed by deoxygenation of lactic acid. This catalyst can be further explored for deoxygenation of various bio-derived oxygenated for further upgradation to fuels.

This thesis work provides pathways for lactic acid valorization to acrylic acid by dehydration with very high productivity on lab scale. The thesis also provides new catalytic system for direct deoxygenation of bio-derived materials with lactic acid as model oxygenates for possible future deoxygenation of renewable raw material to fuel grade chemicals.

List of Publications

1. **Catalytic Dehydration of Lactic Acid to Acrylic Acid Using Calcium Hydroxyapatite Catalysts**, V. C. Ghantani, S. M. Lomate, M. K. Dongare, S. B. Umbarkar, **Green Chem**., **2013**, 15, 1211-1217, citation- 41.

2. **Nonstoichiometric Calcium Pyrophosphate: Highly Efficient and Selective Catalyst for Dehydration of Lactic Acid to Acrylic Acid,** V. C. Ghantani, M. K. Dongare, S. B. Umbarkar, **RSC Adv.,** 2014, 4, 33319-33326, citation-4.

3. **MoO_3 doped calcium pyrophosphate – Efficient catalyst for lactic acid deoxygenation,** V. C. Ghantani, M. K. Dongare, S. B. Umbarkar, manuscript writing in process.

Conferences

1. Photo catalytic degradation of different dyes with Titanium-wonder Gel, **CATSYMP**, February 2012 (NIIST- Thiruvanthapuram).

2. Oral presentation on 'Valorization of Bio-derived Lactic acid to acrylic acid and other products' in **Catalysis for Sustainable and Environmental Chemistry** July 2012, Lille University, FRANCE.

3. Dehydration of Bio-derived Lactic acid to acrylic acid. **CATSYMP**-February 2013, IICT Hyderabad.

4. Oral presentation on 'Dehydration of Lactic acid to acrylic acid and other products' on **Catalysis for Sustainable and Environmental Chemistry**, October 2014, NCL, PUNE.

Workshops

1. INDUS CAP‟ workshop on Industrial catalysis and catalytic processes, 2012.

2. "Catalysis for Sustainable Development" July 2013 at NCL Pune.

Erratum